

①

NAVAL POSTGRADUATE SCHOOL
Monterey, California

AD-A280 669



THESIS

DTIC
ELECTE
JUN 28 1994
S B D

**MAST-ANTENNA SURVIVABILITY:
STRUCTURAL DYNAMIC DESIGN ANALYSIS
BY COMPONENT MODE SYNTHESIS**

by

Lynn James Petersen

March, 1994

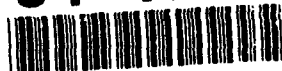
Thesis Advisor:

J.H.Gordis

Approved for public release; distribution is unlimited.

DTIC QUALITY INSPECTED 2

94-19699



94 6 28 052

Unclassified

Security Classification of this page

REPORT DOCUMENTATION PAGE

1a Report Security Classification: Unclassified			1b Restrictive Markings		
2a Security Classification Authority			3 Distribution/Availability of Report		
2b Declassification/Downgrading Schedule			Approved for public release; distribution is unlimited.		
4 Performing Organization Report Number(s)			5 Monitoring Organization Report Number(s)		
6a Name of Performing Organization Naval Postgraduate School		6b Office Symbol 34	7a Name of Monitoring Organization Naval Postgraduate School		
6c Address (city, state, and ZIP code) Monterey CA 93943-5000			7b Address (city, state, and ZIP code) Monterey CA 93943-5000		
8a Name of Funding/Sponsoring Organization NAVAL SEA SYSTEMS COMMAND		8b Office Symbol 06K213	9 Procurement Instrument Identification Number		
Address (city, state, and ZIP Code) WASHINGTON, D.C. 20362-5105			10 Source of Funding Numbers		
			Program Element No	Project No	Task No
			Work Unit Accession No		
11 Title (include security classification) MAST-ANTENNA SURVIVABILITY: STRUCTURAL DYNAMIC DESIGN ANALYSIS BY COMPONENT MODE SYNTHESIS					
12 Personal Author(s) Lynn J. Petersen					
13a Type of Report Master's Thesis		13b Time Covered From To	14 Date of Report (year, month, day) MARCH 1994		15 Page Count 169
16 Supplementary Notation The views expressed in this thesis are those of the author and do not reflect the official policy or position of the Department of Defense or the U.S. Government.					
17 Cosati Codes			18 Subject Terms (continue on reverse if necessary and identify by block number)		
Field	Group	Subgroup	MAST-ANTENNA SURVIVABILITY:STRUCTURAL DYNAMIC DESIGN ANALYSIS BY COMPONENT MODE SYNTHESIS		
19 Abstract (continue on reverse if necessary and identify by block number)					
<p>The structural survivability of shipboard mast/antenna systems subjected to underwater explosion can be "designed in," through the determination of the structural dynamics of the mast/antenna system. This thesis details the specialized application of accurate and efficient analytic methods for the structural dynamic design analysis of shipboard mast/antenna systems. Investigated herein are a class of substructuring methods, generally referred to as component mode synthesis, which provide for the rapid calculation of dynamic response of the mast/antenna structural system to weapons effects. Additionally, the methods also provide for the simulation of live fire testing. The methods allow the individual antenna and the mast to each be independently modeled, arbitrarily combined, and combined system dynamic response rapidly calculated to determine the structural survivability of a proposed mast/antenna configuration. This rapid and "modular" component-based analysis capability is specifically tailored for interactive computer-aided design analysis of shipboard mast/antenna systems.</p>					
20 Distribution/Availability of Abstract _x_ unclassified/unlimited __ same as report __ DTIC users			21 Abstract Security Classification Unclassified		
22a Name of Responsible Individual J.H. Gordis			22b Telephone (include Area Code) 408-656-2566		22c Office Symbol ME/Go

DD FORM 1473,84 MAR

83 APR edition may be used until exhausted

All other editions are obsolete

security classification of this page

Unclassified

Approved for public release; distribution is unlimited.

**MAST-ANTENNA SURVIVABILITY:
STRUCTURAL DYNAMIC DESIGN ANALYSIS
BY COMPONENT MODE SYNTHESIS**

by

**Lynn J. Petersen
Lieutenant, United States Navy
B.S., United States Naval Academy, 1986**

**Submitted in partial fulfillment
of the requirements for the degree of**

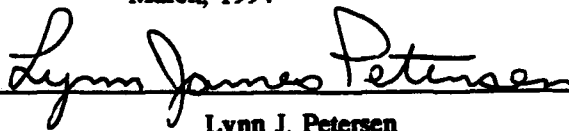
MASTER OF SCIENCE IN MECHANICAL ENGINEERING

from the

NAVAL POSTGRADUATE SCHOOL

March, 1994

Author:


Lynn J. Petersen

Approved by:


Joshua H. Gordis, Thesis Advisor


Matthew D. Kelleher, Chairman

Department of Mechanical Engineering

ABSTRACT

The structural survivability of shipboard mast/antenna systems subjected to underwater explosion can be "designed in," through the determination of the structural dynamics of the mast/antenna system. This thesis details the specialized application of accurate and efficient analytic methods for the structural dynamic design analysis of shipboard mast/antenna systems. Investigated herein are a class of substructuring methods, generally referred to as component mode synthesis methods, which provide for the rapid calculation of dynamic response of the mast/antenna structural system to weapons effects. Additionally, the methods also provide for the simulation of live fire testing. The methods allow the individual antennae and the mast each to be independently modeled, arbitrarily combined, and the combined system dynamic response rapidly calculated to determine the structural survivability of a proposed mast/antenna configuration. This rapid and "modular" component-based analysis capability is specifically tailored for interactive computer-aided design analysis of shipboard mast/antenna systems.

Accession For	
NTIS GRA&I	<input checked="checked" type="checkbox"/>
DTIC TAB	<input type="checkbox"/>
Unannounced	<input type="checkbox"/>
Justification	
By _____	
Distribution/	
Availability Codes	
Dist	Avail and/or Special
A-1	

TABLE OF CONTENTS

I. INTRODUCTION.....	1
A. BACKGROUND.....	3
B. OVERVIEW OF THE SUBSTRUCTURE APPROACH TO THE DESIGN ANALYSIS OF MAST/ANTENNA SYSTEMS.....	4
II. FORMULATION OF FINITE ELEMENT MODEL AND GENERAL COMPONENT COUPLING PROCEDURES.....	8
A. FINITE ELEMENT FORMULATION.....	9
B. GENERAL COMPONENT COUPLING PROCEDURES.....	10
1. Free Interface Normal Modes.....	11
2. Fixed Interface Normal Modes.....	12
3. Static Constraint Modes.....	13
4. Rigid Body Modes.....	14
5. Residual Flexibility Modes.....	18
C. BRIEF HISTORICAL REVIEW.....	20
III. COMPONENT MODE SYNTHESIS FORMULATIONS.....	22
A. CRAIG-BAMPTON FORMULATION.....	22
B. CRAIG-CHANG AND MACNEAL RESIDUAL FLEXIBILITY FORMULATIONS.....	33
IV. NUMERICAL VERIFICATION.....	44

A. NATURAL FREQUENCY CALCULATION AND COMPARISON OF A FIXED-FIXED CANTILEVERED BEAM FOR PURPOSES OF FINITE ELEMENT AND COMPONENT MODE SYNTHESIS CODE VALIDATION.....	45
B. NATURAL FREQUENCY CALCULATION AND COMPARISON OF MAST AND ANTENNA SYSTEM MODEL.....	52
V. BASE EXCITATION FORMULATION.....	59
A. BASE EXCITATION FROM PRESCRIBED ACCELERATION.....	60
1. Tip Deflection Calculation.....	68
2. Moment And Shear Calculation.....	74
B. BASE EXCITATION FROM PRESCRIBED DISPLACEMENT.....	80
1. Tip Deflection Calculation.....	81
2. Moment And Shear Calculation.....	84
VI. CONCLUSIONS AND RECOMMENDATIONS.....	88
APPENDIX A	91
APPENDIX B.....	98
APPENDIX C.....	105
APPENDIX D.....	116
APPENDIX E.....	126
APPENDIX F.....	129
APPENDIX G.....	132
APPENDIX H.....	137
LIST OF REFERENCES.....	153
INITIAL DISTRIBUTION LIST.....	154

LIST OF TABLES

TABLE 1: COUPLED SYSTEM NATURAL FREQUENCY COMPARISON (FIXED-FIXED BEAM)	47
TABLE 2: COUPLED SYSTEM NATURAL FREQUENCY COMPARISON (FIXED-FIXED BEAM)	48
TABLE 3: COUPLED SYSTEM NATURAL FREQUENCY COMPARISON (FIXED-FIXED BEAM)	49
TABLE 4: COUPLED SYSTEM NATURAL FREQUENCY COMPARISON (FIXED-FIXED BEAM)	50
TABLE 5: COUPLED SYSTEM NATURAL FREQUENCY COMPARISON (MAST/ANTENNA MODEL)	55
TABLE 6: COUPLED SYSTEM NATURAL FREQUENCY COMPARISON (MAST/ANTENNA MODEL)	56
TABLE 7: COUPLED SYSTEM NATURAL FREQUENCY COMPARISON (MAST/ANTENNA MODEL)	57

LIST OF FIGURES

Figure 1.	The Coupled & Uncoupled Mast and Antenna Systems	32
Figure 2.	Two Cantilevered Beam Substructures	45
Figure 3.	Comparison of CMS Methods With Frequency (Hz) Error of ≤ 0.1 Percent for "Fixed-Fixed" Beam System	51
Figure 4.	Comparison of CMS Methods With Frequency (Hz) Error of ≤ 0.1 Percent for Mast/Antenna System	58
Figure 5.	The Coupled Mast and Antenna Subjected to Base Excitation at 8.95 Hz	70
Figure 6.	Percent Error in Antenna Tip Deflection Plotted Versus the Percent of Available Mast Modes Retained. (Forcing Frequency: 8.95 Hz)	72
Figure 7.	Percent Error in Antenna Tip Deflection Plotted Versus the Percent of Available Antenna Modes Retained. (Forcing Frequency: 8.95 Hz)	72
Figure 8.	Percent Error in Antenna Tip Deflection Plotted Versus the Percent of Available Mast Modes Retained. (Forcing Frequency: 219 Hz)	73
Figure 9.	Percent Error in Antenna Tip Deflection Plotted Versus the Percent of Available Mast Modes Retained. (Forcing Frequency: 219 Hz)	73
Figure 10.	Percent Error in Shear at Mast and Antenna Connection Plotted Versus the Percent of Available Mast Modes Retained. (Forcing Frequency: 8.95 Hz).....	76
Figure 11.	Percent Error in Moment at Mast and Antenna Connection Plotted Versus the Percent of Available Mast Modes Retained. (Forcing Frequency: 8.95 Hz)	76
Figure 12.	Percent Error in Shear at Mast and Antenna Connection Plotted Versus the Percent of Available Antenna Modes Retained. (Forcing Frequency: 8.95 Hz)	77

Figure 13. Percent Error in Moment at Mast and Antenna Connection Plotted Versus the Percent of Available Antenna Modes Retained. (Forcing Frequency: 8.95 Hz)	77
Figure 14. Percent Error in Shear at Mast and Antenna Connection Plotted Versus the Percent of Available Mast Modes Retained. (Forcing Frequency: 219 Hz)	78
Figure 15. Percent Error in Moment at Mast and Antenna Connection Plotted Versus the Percent of Available Mast Modes Retained. (Forcing Frequency: 219 Hz)	78
Figure 16. Percent Error in Shear at Mast and Antenna Connection Plotted Versus the Percent of Available Antenna Modes Retained. (Forcing Frequency: 219 Hz)	79
Figure 17. Percent Error in Moment at Mast and Antenna Connection Plotted Versus the Percent of Available Antenna Modes Retained. (Forcing Frequency: 219 Hz)	79
Figure 18. Percent Error in Antenna Tip Deflection Plotted Versus the Percent of Available Mast Modes Retained. (Forcing Frequency: 47.26 Hz)	83
Figure 19. Percent Error in Antenna Tip Deflection Plotted Versus the Percent of Available Antenna Modes Retained. (Forcing Frequency: 47.26 Hz)	83
Figure 20. Percent Error in Shear at Mast and Antenna Connection Plotted Versus the Percent of Available Mast Modes Retained. (Forcing Frequency: 47.26 Hz)	86
Figure 21. Percent Error in Moment at Mast and Antenna Connection Plotted Versus the Percent of Available Mast Modes Retained. (Forcing Frequency: 47.26 Hz)	86
Figure 22. Percent Error in Shear at Mast and Antenna Connection Plotted Versus the Percent of Available Antenna Modes Retained. (Forcing Frequency: 47.26 Hz)	87
Figure 23. Percent Error in Moment at Mast and Antenna Connection Plotted Versus the Percent of Available Antenna Modes Retained. (Forcing Frequency: 47.26 Hz)	87

LIST OF SYMBOLS AND ABBREVIATIONS

A. SYMBOLS

\int	Integral
$[]$	Matrix
$[]^T$	Transpose of a matrix
$[]^{-1}$	Inverse of a matrix
$\{\}$	Column vector
$\{\}^T$	Row vector
A	Coefficient of a sinusoidal amplitude
B	Coefficient of a sinusoidal amplitude
c	Constant of integration
d	Constant of integration
t	Time
$\{F\}$	Vector of forces in the physical coordinate system
$\{F\}$	Vector of point forces/moments on the coupled system in the modal coordinate system
$\{F_i\}$	Vector of interface point forces/moments in the physical coordinate system
$\{F_o\}$	Vector of internal point forces/moments in the physical coordinate system
$[G]$	Flexibility matrix

$[I]$	Identity matrix
$[K], [M]$	Stiffness and mass matrices
$\{p\}$	Vector of generalized coordinates
$\{\dot{p}\}$	Vector of velocities in the generalized coordinate system
$\{\ddot{p}\}$	Vector of accelerations in the generalized coordinate system
$\{q\}$	Vector of displacements in the modal coordinate system
$\{\dot{q}\}$	Vector of velocities in the modal coordinate system
$\{\ddot{q}\}$	Vector of accelerations in the modal coordinate system
$[R]$	Matrix of reactions
$[T]$	Transformation matrix used to reduce component mass and stiffness matrices
$\{v\}$	Linearly independent vector
$\{\tilde{v}\}$	Linearly independent and orthogonal vector
$\{x\}$	Vector of absolute displacements in the physical coordinate system
$\{\dot{x}\}$	Vector of velocities in the physical coordinate system
$\{\ddot{x}\}$	Vector of accelerations in the physical coordinate system
$[\Lambda]$	Diagonal matrix of natural circular frequencies squared $(\text{rad/sec})^2$
α, β, γ	Scalar used in Gram-Schmidt Formulation used to extract components of a linearly independent vector which lies in the vector space of another linearly independent vector
λ	Scalar representing a natural circular frequency (i.e. an eigenvalue) expressed in $(\text{rad/sec})^2$

$[\Phi^C]$	Matrix of static constraint mode shapes
$[\Phi^N]$	Matrix of free interface normal modes
$\{\phi^N\}$	Vector containing a free interface normal mode
$[\Phi_F^N]$	Matrix of fixed interface normal modes
$\{\psi^N\}$	Vector containing a fixed interface normal mode
$[\Psi]$	Matrix of residual flexibility modes
$[\Psi^R]$	Matrix of rigid body modes
τ	Time constant
Ω	Forcing frequency (rad/sec)
ω	Natural frequency (rad/sec)

B. SUBSCRIPTS / SUPERSSCRIPTS & OVERSTRIKES

1	substructure 1
2	substructure 2
B	base coordinates
C	static constraint modes
D	deleted
d	linearly dependent
F	fixed interface
I	interface coordinates
K	kept
l	linearly independent
N	normal modes

O	internal coordinates
R	rigid body modes
r	reduced
rf	residual flexibility
s	system
u	uncoupled
\dot{x}	first derivative
\ddot{x}	second derivative

C. ACRONYMS / ABBREVIATIONS

C.C.	Computational Cost
CMS	Component Mode Synthesis
DOF	Degree of Freedom
FE	Finite Element
FEM	Finite Element Methods
FLOPS	Floating Point Operations
LFT&E	Live Fire Test and Evaluation
UNDEX	Underwater Detonation and Explosion

ACKNOWLEDGMENTS

I would like to thank Professor J.H. Gordis for his wisdom and guidance in making this thesis a very rewarding and enlightening experience. In addition, I would like to thank Professor Y.S. Shin and Mr. Mark McClean of Naval Sea Systems Command for their contributions to this study. I would like to thank my parents especially for their support in my early education and at the baccalaureate level. I cannot forget my grandmother Mary who always told me: "Get all of the education that you can, because they cannot take that away from you." Finally, I would like to thank my wife, Alena, for her patience, support and understanding, and my children, Madelyn and Robert, for their prayers; all of whom have made this thesis possible.

"I can do all things through Christ which strengtheneth me."

Philippians 4:13

I. INTRODUCTION

This thesis documents the development of analytic methods for maximizing the combat survivability of shipboard structural systems subjected to weapons effects. Survivability will be improved through the characterization of the mast/antenna system structural dynamics and the development of specialized design analysis tools for the prediction and minimization of dynamic response due to weapons effects. The objective is improved system combat survivability.

Additionally, the methods will be developed in the context of the analytical simulation of live fire test and evaluation (LFT&E) for shipboard systems. Those shipboard structural systems which undergo linear elastic dynamic response due to live fire effects can be evaluated for live fire survivability using the simulation methods to be developed, thereby eliminating the need for actual LFT&E for these systems. Alternatively, these simulations will be of benefit in the planning of actual live fire test and evaluation (LFT&E) programs. The results herein focus on shipboard mast/antenna structures. Shipboard mast/antenna systems must be designed to withstand moderate to severe shock loading induced by underwater explosion (UNDEX) of conventional or nuclear type. The UNDEX delivers devastating forces to the targets in the form of incident shock wave pressure, gas bubble oscillation, cavitation closure pulses, and various reflection wave effects. These shock-induced forces then propagate through the ship to the various systems, equipment, and

top-side structures including the mast and antennae. The response of the mast and antennae to the UNDEX shock wave is basically linear elastic and vibrational in nature. The mast and antennae tend to vibrate at their fundamental natural frequency, or at a low range of natural frequencies. The maximum amplitude of the vibration usually occurs after the shock wave passes the ship. The shock response wave form is remarkably different at various levels within the ship. In essence, the ship acts as a low pass structural filter which alters the characteristics of the propagating shock wave from one possessing high frequency components to one that contains relatively low frequency components [Ref. 1:p. 2]. Thus, the shock survivability of the mast/antenna system, which is located top-side, is a vibration problem in which relatively low frequency equipment support excitations are observed. The emphasis on design analysis relates directly to the survival of the mission critical systems on the platform. The ability of the naval vessel to carry out its mission after being subjected to an UNDEX threat depends on the survivability of these systems, and specifically the mast/antenna system. Combat survivability of new systems, such as the mast/antenna system can be "designed in" by accounting for the structural dynamics of the system during the design process. The methods developed herein focus on the structural dynamics of the mast/antenna systems, so that their combat survivability can be directly addressed in the design process. Additionally, the methods will make possible the improvement of survivability of existing systems. For example, survivability can be improved by dynamically tuning and relocating antennae based on the application of the methods to be described.

A. BACKGROUND

The dynamic response of a shipboard antenna is dependent on the dynamic interaction of the antenna with the mast during response to weapons effect. Large dynamic loads in an antenna can result if (a) the antenna is mounted on the mast at a location with large accelerations due to weapons effects, or (b) the antenna has its natural frequencies in close proximity to the excited natural frequencies of the mast. In recent years, the Navy has had frequent occurrences of shipboard antennae systems failing structurally after being subjected to shock due to weapons effects [Ref. 2]. In order to design these structural systems (i.e. mast and antennae) for minimum dynamic response and hence maximum survivability, the structural dynamic parameters which determine the dynamic response of the system must be accurately quantified. The primary structural dynamic parameters to be determined are the *modal parameters* (i.e. natural frequencies, mode shapes, modal mass and damping) of the mast and the various individual antenna. The modal parameters are required to characterize the structural dynamics of each substructure, e.g. the mast and each antenna, and hence characterize the dynamics of the combined structural system. Given an accurate coupled system analytic dynamics model, weapons-induced dynamic response can then be predicted, and system designs can be evaluated and optimized with respect to survivability. The coupled system analytic dynamics model can serve as the basis for the computer simulation of LFT&E.

B. OVERVIEW OF THE SUBSTRUCTURE APPROACH TO THE DESIGN ANALYSIS OF MAST/ANTENNA SYSTEMS

The methods described herein are directed at the automated design analysis of mast/antenna systems. The methods provide accurate estimates of the modal parameters for a mast/antenna structural system, and therefore will provide accurate estimates of the dynamic response due to weapons effects. Generally referred to as "component mode synthesis," these substructuring methods make use of independent finite element models for the mast and each antenna. In order to allow a designer to rapidly assess for survivability a large number of candidate mast/antenna system designs, the methods are computationally efficient as well as accurate. With respect to mast/antenna systems, the component mode synthesis process will allow a designer to analytically "install" the various antenna models into the mast model, and rapidly calculate coupled mast/antenna system UNDEX dynamic response. When incorporated into a computer-aided design environment, the complexities of the calculation will be transparent to the designer, and will allow the incorporation of self-checks and protection against user error and misuse. The substructure approach to mast/antenna structural dynamic analysis can be briefly outlined as follows:

- A designer either finds the dynamic characteristics of the various antennae to be installed from a "catalog" (database) of antenna modal parameters, or calculates individual antenna modal parameters from a finite element model of the antenna. The modal parameters of the antenna constitute the antenna dynamic model.

- The various antennae dynamic models are analytically coupled with the mast model, and the dynamic response of the coupled mast/antenna system due to weapons effects is calculated. If unacceptable dynamic response levels are calculated, the various antennae models can be rapidly repositioned on the mast, or exchanged with other antennae, and the new dynamic response calculated.

This scheme has several significant advantages for the automated design analysis of mast/antenna systems. The primary advantages include:

- The ability of these methods to treat the mast and antennae as "substructures," and arbitrarily and repeatedly combine them for the rapid calculation of dynamic response will make possible the evaluation of a greater number of mast/antenna configurations, and hence will greatly facilitate the determination of an optimal configuration with respect to combat survivability.
- The various masts and antennae are fabricated by various independent contractors. The component mode synthesis method allows the separate modeling of the mast and antennae, and therefore naturally preserves the independence of the contractors.
- The formulations to be described are modal, and therefore can function equally well with analytically derived modal parameters, or with modal parameters identified in a vibration test.

The analytic methods for the generation of the coupled mast/antenna model are the focus of this work. To be evaluated in this report are several component mode methods for substructure synthesis: the Craig-Bampton method and two residual flexibility

formulations. The methods are specialized for the mast/antenna analysis problem, and their relative merits compared in the context of combat survivability. The methods are based on the modal representation of components; that is, rather than representing a structure using the mass and stiffness matrices generated in a finite element model, these methods employ various classes of "mode shapes" to represent the substructures or components. For example, the familiar normal modes of vibration are one class of mode shape used.

The computational efficiency of these methods, which is critical to their effectiveness in a computer aided design environment, comes from their ability to accurately describe a component with a minimum number of mode shapes. The sections of this report which follow will describe the above mentioned synthesis formulations, and demonstrate their relative accuracy and efficiency in the calculation of the dynamic response of a small yet representative mast/antenna model, subjected to a variety of applied harmonic forces as well as deck accelerations and displacements. The model used, which includes a mast and a single antenna, is of a small size compared with that required to represent an actual mast/antenna structures. However, the model has all the features necessary to allow the assessment and critical analysis of the component mode synthesis methods.

Specifically, the three synthesis methods will each be used in the following analyses:

(1) Calculation of mast/antenna coupled system modal parameters: This is the fundamental assessment of a method's accuracy. Prior to performing the synthesis, modal parameters are calculated for the antenna model and the mast model. The appropriate component representation is generated and the mast/antenna system is synthesized. The

coupled system natural frequencies are calculated and are compared with the natural frequencies calculated using a standard finite element procedure. The standard finite element procedure means the assembly of a single model representing the total mast/antenna system. A comparison of floating point operations (FLOPS) accumulated in all cases is also provided. This comparison will demonstrate the computational advantage of the synthesis methods, an advantage critical to the development of an automated design analysis system.

Using the synthesized mast/antenna model, the following analyses are presented:

(2) Calculation of antenna peak displacement due to harmonic forcing: A simple harmonic forcing function is applied to the mast and the peak displacement of the antenna free end ("tip") is calculated, again using all three component mode synthesis methods, as well as using a standard finite element procedure.

(3) Calculation of mast/antenna interface internal stresses due to harmonic forcing: A simple harmonic forcing function is applied to the mast and the bending moment and shear loads in the mast/antenna connection are calculated. Note that these internal loads are directly proportional to stress, and hence are the critical quantities which must be calculated in order to assess structural survivability. These calculations are repeated for all three synthesis formulations, as well as for the standard finite element procedure.

II. FORMULATION OF FINITE ELEMENT MODEL AND GENERAL COMPONENT COUPLING PROCEDURES

The theory presented herein is taken directly and exclusively from reference [12].

As discussed in the Introduction, the finite element (FE) procedure will be employed to generate mathematical models of the components (substructures) involved, namely the mast and the antenna. The FE procedure produces stiffness, mass, and less commonly, damping matrices which represent the structural dynamics of each component. In order to faithfully capture the geometric and material complexities of these components, the finite element discretization must necessarily involve many degrees-of-freedom (DOF), and hence the above mentioned system matrices can be quite large. The time and cost associated with the extraction of the modal parameters (natural frequencies, mode shapes, and modal mass) from these large matrices precludes the performance of the repeated design analyses required to arrive at an optimal design. The component mode synthesis methods bypass the repeated extraction of the modal parameters for a complete mast/antenna system by directly using the modal parameters calculated for each component. The calculation for the component "modes" is performed once for each component, and the total system dynamics are synthesized using the various sets of modes so calculated. The synthesis methods not only provide very accurate predictions of dynamic response, but also provide a substantial decrease in the time required to compute dynamic response, hence allowing the performance of additional design analysis iterations.

A. FINITE ELEMENT FORMULATION

Although FE modeling typically involves the full range of element types available (e.g. beam, plate, shell), for purposes of this thesis the antenna and the mast will each be modeled using beam elements only. This model, although simple, is all that is necessary to investigate the various component coupling procedures. All methods presented herein are applicable to any structural model, and the results and conclusions presented are directly applicable to the analysis of structural systems of any complexity.

Traditionally, the mast and antennae are modeled together as a system. Alternatively, the mast and antennae can be modeled separately. By modeling the mast and antennae separately, several benefits arise:

- Masts and antennae are generally fabricated by different defense contractors. Therefore, modeling the mast and antennae separately would best preserve this independence.
- Modeling the mast and antennae separately would permit the development of a single data file containing only mast design specifications, and several separate data files containing antennae design specifications, one datafile for each antennae. With this modular, component-based approach comes the flexibility of exchanging antennae and/or changing antennae placement. This allows the rapid assessment of many mast and antennae configurations for dynamic response characteristics.

By modeling the mast and antennae separately, the computational efficiency increases as compared to modeling the mast and antennae together. This computational advantage is

due to the fact that the cost associated with the calculation of the modal parameters for a single structural model is proportional to the cube of the number of DOF of the model [Ref. 3: p. 231]. The calculations performed herein demonstrate this comparison between a total mast/antenna model and a model derived from the synthesis of mast and antenna substructure models. The benefit is associated not just with the calculation of the modal parameters, but also with the calculation of dynamic response to assess UNDEX survivability.

B. GENERAL COMPONENT COUPLING PROCEDURES

The term "component mode synthesis" refers to the manner in which each substructure is mathematically represented prior to coupling, and is based on a truncated modal expansion. This representation is most familiar in the context of the calculation of dynamic response. Here, the dynamic response of a structure can be written as a linear combination of the mode shapes calculated for the structure. If the frequency range of excitation is contained in the frequency range of the calculated modes, then the dynamic response calculated using the modes will be of acceptable accuracy. Of course, the question of how many modes to retain is non-trivial and problem specific. However, the computational efficiency of a modal approach to structural dynamics including the component mode synthesis methods to be presented, comes from the retention of a number of modes which constitute a mathematical model much smaller than the original mass and stiffness matrices from which the modes were calculated.

Component mode synthesis makes use of several types of vibrational mode shapes, distinguished by the boundary conditions imposed on the substructure prior to the calculation of these mode shapes. In addition to these vibration mode shapes, the various component mode synthesis methods require additional types of mode shapes to be calculated and included with the vibrational modes. Therefore, the term "component mode synthesis" (CMS) is a suitable name: a single structure is synthesized from separate substructures and each substructure is mathematically represented by an appropriate set of mode shapes, calculated from the finite element model of each substructure. The following are definitions of the various types of mode shapes that are used in the component mode synthesis formulations investigated herein.

1. Free Interface Normal Modes

The free interface normal modes are the modes of the component when unrestrained at all interface DOF. From the **LIST OF SYMBOLS AND ABBREVIATIONS**, the interface coordinates are denoted by the subscript "I" and the internal coordinates are denoted by the subscript "O". The interface coordinates are the coordinates where the substructures are coupled. The internal coordinates are all coordinates that are not interface coordinates. Free interface normal modes are calculated by solving the following eigenvalue problem:

$$[K - \lambda \cdot M]\{\phi^N\} = \{0\} \quad (1)$$

The stiffness and mass matrices in Eq. (1) are partitioned as follows:

$$[K] = \begin{bmatrix} K_{oo} & K_{oi} \\ K_{io} & K_{ii} \end{bmatrix} \quad [M] = \begin{bmatrix} M_{oo} & M_{oi} \\ M_{io} & M_{ii} \end{bmatrix}$$

The number of equations defined by Eq. (1) is equal to the number of rows or columns in the mass and stiffness matrices. The number of columns or rows in $[K]$ or $[M]$ equals the number of DOF of the component in physical coordinates.

2. Fixed Interface Normal Modes

The fixed interface normal modes are the modes of the component restrained at its interface DOF. The fixed interface normal modes have the following form:

$$[\Phi_F^N] = \begin{bmatrix} \Psi^N \\ 0 \end{bmatrix}$$

The upper partition of the fixed interface normal modes, or $\{\psi^N\}$, is obtained from the solution to the following eigenvalue problem:

$$[K_{oo} - \lambda \cdot M_{oo}] \{\psi^N\} = \{0\} \quad (2)$$

In words, the matrix of fixed interface normal modes is a partitioned matrix consisting of the matrix of mode shapes obtained in the solution to Eq. (2) in the upper partition, and a matrix of zeros in the lower partition. The zeros imply zero displacement at the interface. The number of rows in the matrix of zeros is equal to the number of

interface coordinates, while the number of columns is equal to the number of internal coordinates of the substructure.

Both the upper partition of the fixed interface normal modes and free interface normal modes are unity modal mass normalized such that the following property is satisfied:

$$[\Psi^N]^T [M_{oo}] [\Psi^N] = [I] \quad (3)$$

$$[\Phi^N]^T [M] [\Phi^N] = [I] \quad (4)$$

3. Static Constraint Modes

Static constraint modes are calculated by enforcing a unit deflection on each interface DOF while holding all other DOF restrained. Calculating the resulting displacements of the internal coordinates defines the static constraint modes. Thus, the set of static constraint modes is defined by the equation:

$$\begin{bmatrix} K_{oo} & K_{oi} \\ K_{io} & K_{ii} \end{bmatrix} \begin{bmatrix} \Psi_{oi} \\ I_{ii} \end{bmatrix} = \begin{bmatrix} 0_{oi} \\ R_{ii} \end{bmatrix} \quad (5)$$

where $[R_{ii}]$ is the matrix of "reactions" at the interface or "I" coordinates.

From the top row partition:

$$[\Psi_{oi}] = [-K_{oo}^{-1} K_{oi}] \quad (6)$$

If it can be assumed that no external forces or inertial forces are applied to the internal DOF, as in a static's problem, the matrix of static constraint mode shapes, or $[\Phi^c]$, are represented by the following equation:

$$[\Phi^c] = \begin{bmatrix} \Psi_{oi} \\ I_n \end{bmatrix} = \begin{bmatrix} -K_{oo}^{-1} K_{oi} \\ I_n \end{bmatrix} \quad (7)$$

where $[\Phi^c]$ is the static constraint mode matrix.

4. Rigid Body Modes

Rigid body modes are possessed by systems that are not restrained. Rigid body modes have zero frequency. They can be solved for using Eq. (2). They can also be solved for in the same way that static constraint modes are solved, provided that the number of coordinates retained is equal to the number of rigid body modes. The eigensolver in MATLABTM, the software that was used in the examples in Chapters IV and V, is ineffective in producing rigid body modes using Eq. (2). The rigid body modes and associated frequencies as calculated by MATLAB using Eq. (2) possess a complex part. Therefore, rigid body modes can be obtained using Eq. (5). However, it was determined when applying the property in Eq. (4), the orthogonality property, that the rigid body modes are linearly independent but not orthogonal with respect to the mass matrix. To produce orthogonal mode shapes from a set of mode shapes that are linearly independent a theory from linear algebra, the Gram-Schmidt theory [Ref 4: p. 165], was invoked. The Gram-Schmidt theory will now be presented.

Given three linearly independent vectors $\{v_1\}$, $\{v_2\}$ & $\{v_3\}$ (three vectors are selected because there are three rigid body modes. In general, six vectors would need to be made orthogonal corresponding to six rigid body modes) that three linearly independent and orthogonal vectors, $\{\tilde{v}_1\}$, $\{\tilde{v}_2\}$ & $\{\tilde{v}_3\}$ can be obtained as follows:

Let $\{\tilde{v}_1\} = \{v_1\}$.

Find a vector $\{\tilde{v}_2\}$ such that the following orthogonality property is satisfied

$$\{\tilde{v}_2\}^T [M] \{\tilde{v}_1\} = 0 \quad (8)$$

To satisfy the requirements of Eq. (8), $\{\tilde{v}_2\}$ will be defined by:

$$\{\tilde{v}_2\} = \{v_2\} - \alpha \{\tilde{v}_1\} \quad (9)$$

where α is a scalar that is used to extract the components of $\{\tilde{v}_1\}$ that lie in the vector space of $\{v_2\}$.

Substituting Eq. (9) into Eq. (8) the following relation is obtained:

$$\{v_2 - \alpha \cdot \tilde{v}_1\}^T [M] \{\tilde{v}_1\} = 0 \quad (10)$$

Expanding Eq. (10), the following relation is obtained:

$$\{v_2\}^T [M] \{\tilde{v}_1\} - \alpha \{\tilde{v}_1\}^T [M] \{\tilde{v}_1\} = 0 \quad (11)$$

From Eq. (11) α is obtained as follows:

$$\alpha = \frac{\{\mathbf{v}_2\}^T [\mathbf{M}] \{\tilde{\mathbf{v}}_1\}}{\{\tilde{\mathbf{v}}_1\}^T [\mathbf{M}] \{\mathbf{v}_1\}} \quad (12)$$

By substituting Eq. (12) into Eq. (9), the second linearly independent and orthogonal vector $\{\tilde{\mathbf{v}}_2\}$ is obtained.

Now there are two linearly independent and orthogonal vectors with respect to the mass matrix. A third linearly independent and orthogonal vector will now be determined.

Using the same formulation as above, a vector $\{\tilde{\mathbf{v}}_3\}$ is defined as follows:

$$\{\tilde{\mathbf{v}}_3\} = \{\mathbf{v}_3\} - \beta \{\tilde{\mathbf{v}}_2\} - \gamma \{\tilde{\mathbf{v}}_1\} \quad (13)$$

where β and γ are scalars that are used to extract the components of $\{\tilde{\mathbf{v}}_1\}$ and $\{\tilde{\mathbf{v}}_2\}$ respectively that lie in the vector space of $\{\mathbf{v}_3\}$.

Using the properties of orthogonality the following relations must be satisfied:

$$\{\tilde{\mathbf{v}}_3\}^T [\mathbf{M}] \{\tilde{\mathbf{v}}_1\} = 0 \quad (14)$$

$$\{\tilde{\mathbf{v}}_3\}^T [\mathbf{M}] \{\tilde{\mathbf{v}}_2\} = 0 \quad (15)$$

Substituting Eq.(13) into both Eq.(14) and Eq.(15) the following relations are obtained:

$$\{v_3 - \beta \tilde{v}_2 - \gamma \tilde{v}_1\}^T [M] \{\tilde{v}_1\} = 0 \quad (16)$$

$$\{v_3 - \beta \tilde{v}_2 - \gamma \tilde{v}_1\}^T [M] \{\tilde{v}_2\} = 0 \quad (17)$$

By expanding Eq.(16) and Eq.(17), the following relations are obtained:

$$\{v_3\}^T [M] \{\tilde{v}_1\} = \beta \{\tilde{v}_2\}^T [M] \{\tilde{v}_1\} + \gamma \{\tilde{v}_1\}^T [M] \{\tilde{v}_1\} \quad (18)$$

$$\{v_3\}^T [M] \{\tilde{v}_2\} = \beta \{\tilde{v}_2\}^T [M] \{\tilde{v}_2\} + \gamma \{\tilde{v}_1\}^T [M] \{\tilde{v}_2\} \quad (19)$$

Solving Eq.(18) and Eq.(19) simultaneously the following expressions are obtained for β and γ :

$$\beta = \frac{\{\tilde{v}_1\}^T [M] \{\tilde{v}_2\} \{v_3\}^T [M] \{\tilde{v}_1\} - \{\tilde{v}_1\}^T [M] \{\tilde{v}_1\} \{v_3\}^T [M] \{\tilde{v}_2\}}{\{\tilde{v}_2\}^T [M] \{\tilde{v}_1\} \{\tilde{v}_1\}^T [M] \{\tilde{v}_2\} - \{\tilde{v}_2\}^T [M] \{\tilde{v}_2\} \{\tilde{v}_1\}^T [M] \{\tilde{v}_1\}} \quad (20)$$

$$\gamma = \frac{-\{\tilde{v}_2\}^T [M] \{\tilde{v}_2\} \{v_3\}^T [M] \{\tilde{v}_1\} + \{\tilde{v}_2\}^T [M] \{\tilde{v}_1\} \{v_3\}^T [M] \{\tilde{v}_2\}}{\{\tilde{v}_2\}^T [M] \{\tilde{v}_1\} \{\tilde{v}_1\}^T [M] \{\tilde{v}_2\} - \{\tilde{v}_2\}^T [M] \{\tilde{v}_2\} \{\tilde{v}_1\}^T [M] \{\tilde{v}_1\}} \quad (21)$$

Substituting Eq. (20) and Eq. (21) into Eq. (13), the third linear independent and orthogonal vector $\{\tilde{v}_3\}$ is obtained.

Therefore, rigid body modes will be solved for using Eq. (5) and the Gram-Schmidt procedure derived above.

5. Residual Flexibility Modes

Before defining "residual" flexibility, the concept of flexibility must first be defined. The flexibility of a restrained structure (i.e. a structure whose stiffness matrix is of full rank) is the inverse of the stiffness of the structure. By inverting the stiffness matrix, one obtains the flexibility matrix as follows:

$$[G] = [K]^{-1} \quad (22)$$

Equation (22) can also be written as follows:

$$[G] = [\Phi^N] [\Lambda_N]^{-1} [\Phi^N]^T \quad (23)$$

The residual flexibility matrix is obtained from the flexibility matrix, the kept free interface normal modes, and the inverse of the natural frequencies as follows:

$$[G^r] = [G] - [\Phi_k^N] [\Lambda_k]^{-1} [\Phi_k^N]^T = [\Phi_D^N] [\Lambda_D]^{-1} [\Phi_D^N]^T \quad (24)$$

The residual flexibility modes are the portion of the exact static flexibility shapes that are not represented by a set of retained modes. Residual flexibility modes require the knowledge of other modes that are retained in the model and are dependent upon the retained modes. There are two ways to calculate the residual flexibility modes.

1) If the structure is grounded, such as the mast, then the stiffness matrix is full rank and invertible. By post-multiplying Eq. (24) by $\begin{bmatrix} 0_{OI} \\ I_R \end{bmatrix}$ one obtains the residual flexibility modes for restrained substructures.

$$[\Psi] = [G^r] \cdot \begin{bmatrix} \bar{0}_{oi} \\ I_{ii} \end{bmatrix} \quad (25)$$

2) However, If the component is not grounded before assembly, such as an antenna, then an inertia relief solution must be calculated to determine the flexibility matrix as follows:

$$[G] = [I - \Psi^R \Psi^{R^T} M]^T \cdot [K^*] \cdot [I - \Psi^R \Psi^{R^T} M] \quad (26)$$

where Ψ^R are the rigid body modes of the structure.

$[K^*]$ is formed by inverting the restrained or internal partition of the stiffness matrix in the following way:

$$[K^*] = \begin{bmatrix} \bar{0} & 0 \\ 0 & K_{oo}^{-1} \end{bmatrix} \quad (27)$$

This "new" $[G]$ or flexibility matrix is free of rigid body modes. The Craig-Chang formulation, which will be presented in Chapter III uses free-interface normal modes and residual flexibility modes. The residual flexibility modes of unrestrained substructures are obtained from the neglected or deleted free interface normal modes just like they were obtained from a substructure that is restrained. The only difference is that the flexibility matrix obtained in Eq. (26) is used. Residual flexibility modes are calculated by computing the static flexibility and subtracting the flexibility due to the retained modes. The residual

flexibility modes are obtained from the flexibility matrix in Eq. (26) in the same way that they were obtained in Eq. (25):

$$[\Psi] = [G^r] \cdot \begin{bmatrix} \bar{0}_{OI} \\ I_{II} \end{bmatrix} \quad (28)$$

It is noteworthy to state that by performing the operation in Eq. (25) and Eq. (28) that the "OI" and "II" partitions of the residual flexibility matrix are extracted to form the residual flexibility modes.

C. BRIEF HISTORICAL REVIEW

The following is a brief historical background in the development of component mode synthesis:

- [1965] In his paper, *Dynamic Analysis of Structural Systems by Component Modes*, Hurty developed the first substructure coupling method. His technique involved fixed interface normal modes, rigid-body modes, and static constraint modes. [Ref. 5]
- [1967] Bamford first introduced the concept of flexibility modes in his paper *A Modal Combination Program for Dynamic Analysis of Structures*. [Ref. 6]
- [1968] In *Coupling of Substructures for Dynamic Analysis*, [Ref. 7] Craig & Bampton extended Hurty's concepts by showing that rigid-body modes did not need to be separated from static constraint modes, but could be calculated using

the same procedure. The Craig-Bampton procedure is one of the techniques used in this study.

- [1969] Goldman, in his paper *Vibration Analysis of Dynamic Partitioning* [Ref. 8] and Hou, in his paper *Review of Modal Synthesis Techniques and a New Approach*, [Ref. 9] first introduced the use of free-interface normal modes.
- [1971] MacNeal used both free-interface normal modes and residual flexibility modes to couple substructures. He also suggested the use of statically derived modes in describing substructure motion. These methods were introduced in his paper *A Hybrid Method of Component Mode Synthesis*. [Ref. 10] The MacNeal method is another technique that will be analyzed in this study.
- [1977] In his Doctoral Dissertation, *A General Procedure for Substructure Coupling in Dynamic Analysis*, [Ref. 11] Chang, under the guidance of Craig, showed how both free-interface normal modes and residual flexibility modes could be employed to couple substructures. The Craig/Chang procedure is the third and final substructure coupling technique to be examined in this study.

Now that the mode descriptions have been defined, and a brief history of when the various methods of CMS were developed, the three methods to be examined in this study can now be derived. It is the intent of Chapter III to describe the three CMS techniques and how the various mode shapes are employed to synthesize substructures into a system.

III. COMPONENT MODE SYNTHESIS FORMULATIONS

The theory presented herein is taken directly and exclusively from references [11 and 12].

A. CRAIG-BAMPTON FORMULATION

There are three substructure coupling procedures that serve as potential candidates to be used in the mast/antenna synthesis. The Craig-Bampton formulation, the Craig-Chang residual flexibility method, and the MacNeal residual flexibility method. In this section, the Craig-Bampton formulation will be presented, while in Section B the Craig-Chang and MacNeal residual flexibility methods will be presented together because of the similarities in the methods.

The Craig-Bampton reduction procedure uses a combination of static constraint modes and fixed interface normal modes to reduce the component model. Both the static constraint modes and the fixed interface normal modes are obtained from the finite element substructure models. This combined set of mode shapes will be used to transform the original large order substructure mass and stiffness matrices down to a significantly smaller size, a size equal to the number of mode shapes included in the transformation matrix. The transformation matrix $[T_1]$, for the Craig-Bampton formulation, contains the shape functions as its columns as follows:

$$\begin{Bmatrix} x_o \\ x_i \end{Bmatrix} = \begin{bmatrix} \Psi^N & -K_{oo}^{-1}K_{oi} \\ 0 & I \end{bmatrix} \begin{Bmatrix} p_o \\ p_i \end{Bmatrix} = [T_1] \begin{Bmatrix} p_o \\ p_i \end{Bmatrix} \quad (29)$$

This transformation matrix is obtained for each substructure in the system. The size of the static constraint mode partition of the transformation matrix is always fixed because the number of columns corresponds to the number of interface degrees of freedom. However, the size of the fixed interface normal mode partition is not held constant. The number of columns can range as low as one column if only one fixed interface normal mode is retained, or as high "m" columns where "m" is the total number of internal degrees of freedom. The size of the transformation matrix depends upon how many modes are required to accurately represent the physical dynamic response of the system when subjected to a forced input. Retaining fewer modes than the total possible modes available is referred to as "modal truncation," and provides the computational efficiency of the method. Retaining fewer modes than the total amount of modes available means fewer calculations required in conducting the dynamic analysis. On the other hand, if the number of modes retained are not sufficient to accurately determine the dynamic response, then the benefits of reduced compute times do not outweigh the magnitude of error obtained in the analysis. Therefore, while the benefits of modal truncation are important in shortening compute times, they are not as important as obtaining accurate results. In terms of computational efficiency, large benefits can be achieved using this method if only the lower range of frequencies is of interest. This method is applicable to the mast which is subjected to typically low forcing frequencies. By retaining a few of each of the component modes, an accurate assessment of the dynamic response of the mast and

antenna is obtained. The examples contained in Chapters IV and V demonstrate how by retaining just a few modes of each substructure, accurate results are achieved.

By pre-multiplying the respective mass and stiffness matrices by the transpose of the transformation matrix and then post multiplying the mass and stiffness matrices by the transformation matrix, the reduced component model is obtained as follows:

$$[K_r] = \begin{bmatrix} \Psi^N & -K_{oo}^{-1}K_{oi} \\ 0_{jo} & I_{ii} \end{bmatrix}^T \begin{bmatrix} K_{oo} & K_{oi} \\ K_{jo} & K_{ii} \end{bmatrix} \begin{bmatrix} \Psi^N & -K_{oo}^{-1}K_{oi} \\ 0_{jo} & I_{ii} \end{bmatrix} = \begin{bmatrix} K_r^1 & K_r^2 \\ K_r^{2^T} & K_r^3 \end{bmatrix} \quad (30a)$$

$$[M_r] = \begin{bmatrix} \Psi^N & -K_{oo}^{-1}K_{oi} \\ 0_{jo} & I_{ii} \end{bmatrix}^T \begin{bmatrix} M_{oo} & M_{oi} \\ M_{jo} & M_{ii} \end{bmatrix} \begin{bmatrix} \Psi^N & -K_{oo}^{-1}K_{oi} \\ 0_{jo} & I_{ii} \end{bmatrix} = \begin{bmatrix} M_r^1 & M_r^2 \\ M_r^{2^T} & M_r^3 \end{bmatrix} \quad (30b)$$

Carrying out the operations in Eq.(30a,b) and simplifying, the partitions of the reduced mass and stiffness matrices are expressed as follows:

$$K_r^1 = [\Lambda_{kk}]$$

$$K_r^2 = K_r^{2^T} = [0]$$

$$K_r^3 = [K_{ii} - K_{jo}K_{oo}^{-1}K_{oi}]$$

$$M_r^1 = [I_{kk}]$$

$$M_r^2 = M_r^{2^T} = [\Psi^N (M_{oo} (-K_{oo}^{-1}K_{oi}) + M_{oi})]$$

$$M_r^3 = [(-K_{oo}^{-1}K_{oi})^T (M_{oo} (-K_{oo}^{-1}K_{oi}) + M_{oi}) + M_{jo} (-K_{oo}^{-1}K_{oi}) + M_{ii}]$$

The term "reduced", designated by the subscript "r", means that the resulting mass and stiffness matrices, $[K_r]$ & $[M_r]$, are of smaller dimension than the original matrix. Although this transformation matrix reduces the size of the component model, it does not assemble the individual substructure models. There is a second transformation matrix that synthesizes the substructures to produce the total system by enforcing compatibility and equilibrium of interface coordinates and interface forces as follows:

$$\{x_i^1\} = \{x_i^2\} \quad (31a)$$

$$\{F_i^1\} = -\{F_i^2\} \quad (31b)$$

The compatibility of interface coordinates denoted by Eq. (31a) implies that the displacement at the interface of structure 1 equals the displacement at the interface of structure 2. Likewise, the equilibrium of interface forces denoted by Eq. (31b) implies that the sum of the forces at the interface are equal but acting in opposite directions.

The generalized coordinates employed in many CMS methods can be identified with the interface DOF and the interior DOF. In order to synthesize two substructures into a system, a linear transformation that maps the set of linearly independent coordinates, p_1 , into the set of generalized coordinates "p" is defined as follows:

$$\{p\} = [T_2] \{p_1\} \quad (32)$$

Additionally, the compatibility equation, Eq. (31a) can be written in terms of the generalized coordinates "p" and combined to form a matrix compatibility equation of the form:

$$[C]\{p\}=\{0\} \quad (33)$$

Let the vector of generalized coordinates be partitioned into linearly independent and linearly dependent coordinates, and partition the compatibility matrix accordingly. Equation (33) can now be written as follows:

$$\begin{bmatrix} C_{dd} & C_{di} \end{bmatrix} \begin{Bmatrix} p_d \\ p_i \end{Bmatrix} = \{0\} \quad (34)$$

where subscript "d" and subscript "i" represent linear dependence and linear independence respectively. The C_{dd} partition of the compatibility matrix is a nonsingular square matrix. Expanding Eq. (34), the dependent coordinates can be written in terms of the independent coordinates as follows:

$$\{p_d\} = [-C_{dd}^{-1}C_{di}]\{p_i\} \quad (35)$$

Using Eq. (35), the vector of generalized coordinates can now be given by:

$$\begin{Bmatrix} p_d \\ p_i \end{Bmatrix} = \begin{bmatrix} -C_{dd}^{-1}C_{di} \\ I_n \end{bmatrix} \{p_i\} \quad (36)$$

By satisfying Eq. (32), $[T_2]$ can be written as follows:

$$[T_2] = \begin{bmatrix} -C_{dd}^{-1} C_{di} \\ I_n \end{bmatrix} \quad (37)$$

This transformation matrix is employed to couple the uncoupled mass and stiffness matrices. [Ref. 12:p. 472] The coupling procedure for the Craig-Bampton formulation will now be derived. Let

$$p^1 = \begin{Bmatrix} p_o^1 \\ p_i^1 \end{Bmatrix}, \quad p^2 = \begin{Bmatrix} p_o^2 \\ p_i^2 \end{Bmatrix} \quad (38a,b)$$

where p_o represents the generalized internal coordinates and p_i represents the generalized interface coordinates respectively. Additionally, superscript "1" refers to substructure 1 and superscript "2" refers to substructure 2.

Define p_i^2 as the set of dependent coordinates, and let the set of linearly independent coordinates be expressed as follows:

$$\{p_i\} = \begin{Bmatrix} p_o^1 \\ p_i^1 \\ p_o^2 \end{Bmatrix} \quad (39)$$

Rewriting the compatibility equation in terms of the generalized coordinates, Eq. (31a), and using the relation in Eq. (38a,b) the following is obtained:

$$\{p_i^1\} - \{p_i^2\} = \{0\} \quad (40)$$

Noting that the set of dependent coordinates are designated by p_1^2 and using Eq. (33), Eq. (40) can be written as follows:

$$[-I] \begin{Bmatrix} [0] & [I] & [0] \end{Bmatrix} \begin{Bmatrix} p_1^2 \\ p_o^1 \\ p_1^1 \\ p_o^2 \end{Bmatrix} \quad (41)$$

Using Eq. (34),

$$[C_{dd}] = [-I], \quad [C_{d1}] = \begin{bmatrix} [0] & [I] & [0] \end{bmatrix} \quad (42)$$

From Eq. (42) and using Eq. (37), the second transformation matrix is obtained as follows:

$$[T_2] = \begin{bmatrix} -C_{dd}^{-1}C_{d1} \\ I_n \end{bmatrix} = \begin{bmatrix} [0] & [I] & [0] \\ [I] & [0] & [0] \\ [0] & [I] & [0] \\ [0] & [0] & [I] \end{bmatrix} \quad (43)$$

In order to be consistent with the partitioning of the mass and stiffness matrices, the second transformation matrix can be rewritten as follows:

$$[T_2] = \begin{bmatrix} [I] & [0] & [0] \\ [0] & [I] & [0] \\ [0] & [0] & [I] \\ [0] & [I] & [0] \end{bmatrix} \quad (44)$$

Equation (33) is now satisfied as follows:

$$\begin{Bmatrix} p_o^1 \\ p_i^1 \\ p_o^2 \\ p_i^2 \end{Bmatrix} = \begin{bmatrix} [I] & [0] & [0] \\ [0] & [I] & [0] \\ [0] & [0] & [I] \\ [0] & [I] & [0] \end{bmatrix} \begin{Bmatrix} p_o^1 \\ p_i^1 \\ p_o^2 \\ p_i^2 \end{Bmatrix} \quad (45)$$

The system model is obtained from an uncoupled mass and stiffness matrix. These uncoupled mass and stiffness matrices are themselves formed from the reduced mass and stiffness matrices from each substructure as follows:

$$[M_u] = \begin{bmatrix} M_r^1 & 0 \\ 0 & M_r^2 \end{bmatrix} \quad [K_u] = \begin{bmatrix} K_r^1 & 0 \\ 0 & K_r^2 \end{bmatrix} \quad (46a,b)$$

where the subscript "u" denotes "uncoupled."

The coupled system mass and stiffness matrices are obtained by pre-multiplying the uncoupled mass and stiffness matrices in Eq. (46a,b) by the transpose of the transformation matrix in Eq. (45) and then post-multiplying the uncoupled mass and stiffness matrices by the transformation matrix.

$$[M_s] = [T_2]^T [M_u] [T_2] \quad [K_s] = [T_2]^T [K_u] [T_2] \quad (47a,b)$$

where the subscript "s" denotes "system."

Carrying out the operations in Eq. (47a,b) the resulting coupled system mass and stiffness matrices are given by:

$$[M_s] = \begin{bmatrix} M_{KK}^1 & 0 & M_{KI}^1 \\ 0 & M_{KK}^2 & M_{KI}^2 \\ M_{IK}^1 & M_{IK}^2 & M_{II} \end{bmatrix} \quad [K_s] = \begin{bmatrix} K_{KK}^1 & 0 & 0 \\ 0 & K_{KK}^2 & 0 \\ 0 & 0 & K_{II} \end{bmatrix} \quad (48a,b)$$

The respective partitions of the system mass and stiffness matrices are expressed as follows:

$$\begin{aligned} M_{KK}^1 &= [I_{KK}^1] \\ M_{KK}^2 &= [I_{KK}^2] \\ M_{KI}^1 &= M_{IK}^{1T} = [\Psi^{N1T} (M_{OO}^1 (-K_{OO}^{-1} K_{OI})^1 + M_{OI}^1)] \\ M_{KI}^2 &= M_{IK}^{2T} = [\Psi^{N2T} (M_{OO}^2 (-K_{OO}^{-1} K_{OI})^2 + M_{OI}^2)] \\ M_{II} &= [(-K_{OO}^{-1} K_{OI})^{1T} (M_{OO}^1 (-K_{OO}^{-1} K_{OI})^1 + M_{OI}^1) + M_{IO}^1 (-K_{OO}^{-1} K_{OI})^1 + M_{II}^1 + \dots \\ &\quad (-K_{OO}^{-1} K_{OI})^{2T} (M_{OO}^2 (-K_{OO}^{-1} K_{OI})^2 + M_{OI}^2) + M_{IO}^2 (-K_{OO}^{-1} K_{OI})^2 + M_{II}^2] \\ K_{KK}^1 &= [\Lambda_{KK}^1] \\ K_{KK}^2 &= [\Lambda_{KK}^2] \\ K_{II} &= [K_{II}^1 - K_{IO}^1 K_{OO}^{-1} K_{OI}^1 + K_{II}^2 - K_{IO}^2 K_{OO}^{-1} K_{OI}^2] \end{aligned}$$

There are a number of advantages to the Craig-Bampton component mode representation. The first, which is especially beneficial to the analysis of the mast/antenna system, is that the reduced DOF system contain the interface DOF explicitly. This makes it very easy to couple mast and antenna substructures. In the figure on page 32 is an

illustration of the mast/antenna system used for the examples in this thesis. Along the length of the cross bar are various node positions. These node positions serve to connect the beams that represent the cross bar, and can also serve as nodes to connect antenna to the crossbar. By specifying different "connection coordinates" (i.e. the "I" coordinates), and with separate mast and antenna data files contained in the library, the engineer can quickly couple various antennae with the mast and rapidly determine the dynamic response.

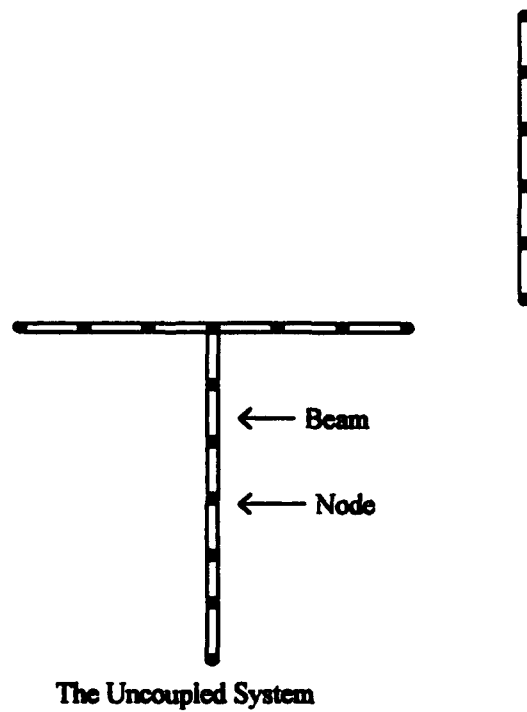
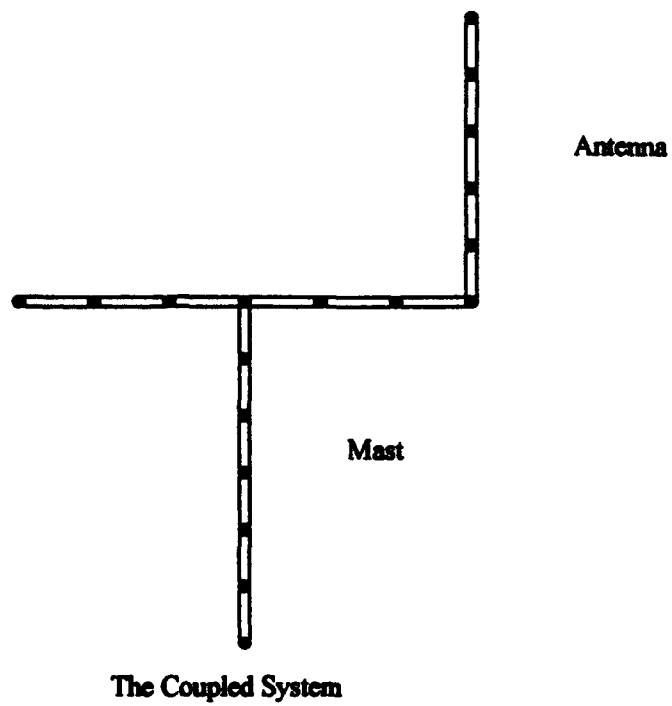


Figure 1: The Coupled & Uncoupled Mast and Antenna Systems

Should the location of the antenna placement not be suitable, the engineer can specify a new set of interface coordinates along the cross bar, plug in the antenna at the new location, and rapidly calculate a system from which a new dynamic response can be calculated.

Because of these advantages, and because the Craig-Bampton component mode representation tends to result in accurate system frequencies, as will be shown, this is a widely used method. Additionally, the NASTRAN superelement scheme uses the Craig-Bampton component mode representation with minor extensions as a solution path to the dynamic response problem.

B. CRAIG-CHANG AND MACNEAL RESIDUAL FLEXIBILITY FORMULATIONS

The Craig-Chang and MacNeal residual flexibility formulations will now be discussed. Due to the similiarity in the methods, the Craig-Chang procedure will be presented first, and the modification of this method to produce the final system of equations of the MacNeal method will be discussed subsequently. While the Craig-Bampton representation uses a combination of static constraint modes and fixed interface normal modes, the Craig-Chang residual flexibility formulation combines free interface normal modes with residual flexibility modes; thus the name: residual flexibility method. The transformation matrix which is used to reduce the component mass and stiffness matrices contains columns of the retained or kept free interface normal modes and residual flexibility modes.

The transformation matrix, or $[T_1]$, is shown as follows:

$$\begin{Bmatrix} x_o \\ x_i \end{Bmatrix} = \begin{bmatrix} \Phi_{OK}^N & \Psi_{OD} \\ \Phi_{IK}^N & \Psi_{ID} \end{bmatrix} \begin{Bmatrix} p_o \\ p_i \end{Bmatrix} = [T_1] \begin{Bmatrix} p_o \\ p_i \end{Bmatrix} \quad (49)$$

In the same way that the Craig-Bampton components were reduced, so to are the Craig-Chane components reduced except now using the transformation matrix of Eq. (49). The reduced mass and stiffness matrices are obtained as follows:

$$[M_r] = \begin{bmatrix} \Phi_{OK}^N & \Psi_{OD} \\ \Phi_{IK}^N & \Psi_{ID} \end{bmatrix}^T \begin{bmatrix} M_{OO} & M_{OI} \\ M_{IO} & M_{II} \end{bmatrix} \begin{bmatrix} \Phi_{OK}^N & \Psi_{OD} \\ \Phi_{IK}^N & \Psi_{ID} \end{bmatrix} = \begin{bmatrix} M_r^1 & M_r^2 \\ M_r^{2^T} & M_r^3 \end{bmatrix} \quad (50a)$$

$$[K_r] = \begin{bmatrix} \Phi_{OK}^N & \Psi_{OD} \\ \Phi_{IK}^N & \Psi_{ID} \end{bmatrix}^T \begin{bmatrix} K_{OO} & K_{OI} \\ K_{IO} & K_{II} \end{bmatrix} \begin{bmatrix} \Phi_{OK}^N & \Psi_{OD} \\ \Phi_{IK}^N & \Psi_{ID} \end{bmatrix} = \begin{bmatrix} K_r^1 & K_r^2 \\ K_r^{2^T} & K_r^3 \end{bmatrix} \quad (50b)$$

Carrying out the operations of Eq.(50a,b) the following is obtained for the respective partitions of the reduced mass and stiffness matrices:

$$M_r^1 = [I_{KK}]$$

$$M_r^2 = M_r^{2^T} = [0_{KD}]$$

$$M_r^3 = [\Psi_{ID}]^T [M_{II} \Psi_{ID}] = [\Phi_{ID}^N] [\Lambda_{DD}]^T [\Lambda_{DD}]^T [\Phi_{ID}^N]^T$$

$$K_r^1 = [\Lambda_{KK}]$$

$$K_r^2 = K_r^{2^T} = [0_{KD}]$$

$$K_r^3 = [\Psi_{ID}]^T [K_{II} \Psi_{ID}] = [\Phi_{ID}^N] [\Lambda_{DD}]^T [\Phi_{ID}^N]^T$$

Again, each component has its own transformation matrix. A reduction in component matrix size is achieved by retaining less than the total number of free interface normal modes. The number of residual flexibility mode shapes is fixed, and equals the number of interface degrees of freedom.

It is not readily apparent how the lower right hand partition of the reduced mass and stiffness matrices are obtained. In Chapter II, the flexibility matrix was obtained by inverting the stiffness matrix for a fully restrained substructure. If the substructure was not restrained, then the flexibility matrix was obtained by performing an inertia relief solution. However, it was also shown that the flexibility matrix could be obtained by the following equation:

$$[G] = [\Phi^N] [\Lambda_N]^{-1} [\Phi^N]^T \quad (23)$$

Additionally, the residual flexibility matrix was defined by the following equation:

$$[G^r] = [G] - [\Phi_K^N] [\Lambda_K]^{-1} [\Phi_K^N]^T = [\Phi_D^N] [\Lambda_D]^{-1} [\Phi_D^N]^T \quad (24)$$

The residual flexibility modes were obtained by post multiplying Eq. (24) by $\begin{bmatrix} 0_{OI} \\ I_{II} \end{bmatrix}$. This operation extracts the "OI" and "II" partitions of the residual flexibility matrix. Additionally, the residual flexibility modes were obtained from the free interface normal modes in the following way:

$$[\Psi] = [\Phi_D^N] [\Lambda_D]^{-1} [\Phi_D^N]^T \begin{bmatrix} 0_{OI} \\ I_{II} \end{bmatrix} \quad (51)$$

Using the relation between the residual flexibility modes and the deleted free interface normal modes in Eq. (51), the lower right partitions of the reduced mass and stiffness matrices will now be derived.

$$M_r^3 = [\Psi_{DI}] [M_{II}] [\Psi_{ID}] = [\Phi_{ID}^N] [\Lambda_{DI}]^{-1} [\Phi_{ID}^N]^T [M_{II}] [\Phi_{ID}^N] [\Lambda_{DI}]^{-1} [\Phi_{ID}^N]^T \quad (52)$$

Using the properties of orthogonality:

$$[\Phi_{ID}^N]^T [M_{II}] [\Phi_{ID}^N] = [I_{DD}] \quad (53)$$

Substituting Eq. (53) into Eq. (52) the lower right partition of the reduced mass matrix is obtained as follows:

$$M_r^3 = [\Phi_{ID}^N] [\Lambda_{DD}]^{-1} [\Lambda_{DD}]^{-1} [\Phi_{ID}^N]^T \quad (54)$$

Likewise for the stiffness matrix, using Eq. (52) and the relationship between residual flexibility modes and the deleted free interface normal modes, the following equation is obtained:

$$K_r^3 = [\Psi_{DI}] [K_{II}] [\Psi_{ID}] = [\Phi_{ID}^N] [\Lambda_{DI}]^{-1} [\Phi_{ID}^N]^T [K_{II}] [\Phi_{ID}^N] [\Lambda_{DI}]^{-1} [\Phi_{ID}^N]^T \quad (55)$$

Because the free interface normal modes are unity modal mass normalized, the following is obtained:

$$[\Phi_{ID}^N]^T [K_{II}] [\Phi_{ID}^N] = [\Lambda_{DD}] \quad (56)$$

Substituting Eq. (56) into Eq. (55), the lower right partition of the reduced stiffness matrix is obtained as follows:

$$K_r^3 = [\Phi_{ID}^N] [\Lambda_{DD}]^{-1} [\Phi_{ID}^N]^T \quad (57)$$

Just like the Craig-Bampton formulation, each of the substructures have their own transformation matrix. The purpose of this transformation matrix is to reduce the respective component models before synthesis into the system model. This transformation matrix does not synthesize the substructures. Another transformation matrix is employed to synthesize the substructures. As in the Craig-Bampton formulation, this second transformation matrix results from satisfying compatibility and equilibrium equations:

$$\{x_i^1\} = \{x_i^2\} \quad (58a)$$

$$\{F_i^1\} = -\{F_i^2\} \quad (58b)$$

Unlike the Craig-Bampton component mode representation where the static constraint modes are independent of the fixed interface normal modes, the residual flexibility modes are dependent upon the free interface normal modes, and a simple boolean matrix will not synthesize the substructures. This second transformation matrix, or $[T_2]$, will now be derived.

The component equation of motion in terms of the physical coordinates is given by

$$[M]\{\ddot{x}\} + [K]\{x\} = \{F\} \quad (59)$$

Transforming Eq. (59) to component generalized coordinates by letting

$$\{x\} = [T_1] \{p\} \quad (60)$$

the following uncoupled equations are obtained:

$$[M_{KK}] \{\ddot{p}_K\} + [K_{KK}] \{p_K\} = [\Phi_K^N]^T \{F\} \quad (61a)$$

$$[M_{DD}] \{\ddot{p}_D\} + [K_{DD}] \{p_D\} = [\Psi_D]^T \{F\} \quad (61b)$$

where $[M_{KK}]$, $[K_{KK}]$, $[M_{DD}]$ and $[K_{DD}]$ are the upper left and lower right partitions of the reduced mass and stiffness matrices respectively, or M_r^1 , K_r^1 , M_r^3 and K_r^3 partitions of the reduced mass and stiffness matrices. Equations (61a,b) are uncoupled because residual flexibility modes are obtained as linear combinations of the deleted free interface normal modes. The deleted free interface normal modes are orthogonal to the kept free interface normal modes. The response of the deleted generalized coordinates will now be approximated by the pseudostatic response by ignoring the acceleration of the deleted generalized coordinates as follows:

$$[K_{DD}] \{p_D\} = [\Psi_D]^T \{F\} \quad (62)$$

But it was shown that:

$$[K_{DD}] = [K_r^3] = [\Psi_D]^T [K_{II}] [\Psi_D] = [\Phi_D^N]^T [\Lambda_{DD}] [\Phi_D^N]^T \quad (63)$$

Equations (62) and (63) can be combined to give:

$$[\Phi_D^N]^T [\Lambda_{DD}]^{-1} [\Phi_D^N]^T (\{p_D\} - \{F_I\}) = \{0\} \quad (64)$$

Since the matrix product in Eq.(64) is nonsingular, the following must be true:

$$\{p_D\} = \{F_I\} \quad (65)$$

Using Eq. (65), the equilibrium equation, Eq. (58b), can now be written as follows:

$$\{p_D^1\} + \{p_D^2\} = \{0\} \quad (66)$$

From Eq. (66) and rewriting the compatibility equation, the two constraint equations are given by:

$$\{x_I^1\} - \{x_I^2\} = \{0\} \quad (58a)$$

$$\{p_D^1\} + \{p_D^2\} = \{0\} \quad (66)$$

Now let the generalized coordinates "p" and the linearly independent generalized coordinates "p_i" be arranged as follows:

$$\{p\} = \begin{Bmatrix} p_D^1 \\ p_D^2 \\ p_K^1 \\ p_K^2 \end{Bmatrix} \quad \{p_i\} = \begin{Bmatrix} p_K^1 \\ p_K^2 \end{Bmatrix} \quad (67a,b)$$

where the deleted generalized coordinates are dependent upon the kept generalized coordinates.

Combining Eqs. (58a), (66a,b) and (67a,b) with $[T_1]$, the compatibility matrix in Eq. (34) is obtained as follows:

$$[C] = [C_{dd} \mid C_{di}] = \begin{bmatrix} [\Psi_D^1] & [-\Psi_D^2] & [\Phi_{IK}^{N^1}] & [-\Phi_{IK}^{N^2}] \\ [I] & [I] & [0] & [0] \end{bmatrix} \quad (68)$$

From Eq. (37),

$$[T_2] = \begin{bmatrix} -C_{dd}^{-1} C_{di} \\ I_n \end{bmatrix} \quad (37)$$

Since $[C_{dd}]$ was defined as a non-singular square matrix, implies that $[C_{dd}]$ is invertible.

The inverse of $[C_{dd}]$ is obtained as follows:

$$[C_{dd}^{-1}] = \begin{bmatrix} [k_1] & [k_1 \Psi_D^2] \\ [-k_1] & [I - k_1 \Psi_D^2] \end{bmatrix} \quad (69)$$

where $[k_1] = [\Psi_D^1 + \Psi_D^2]^{-1}$.

Combining Eqs. (37), (68) and (69) the second transformation matrix is obtained as follows:

$$[T_2] = \begin{bmatrix} [-k_1 \Phi_{IK}^1] & [k_1 \Phi_{IK}^2] \\ [k_1 \Phi_{IK}^1] & [-k_1 \Phi_{IK}^2] \\ [I] & [0] \\ [0] & [I] \end{bmatrix} \quad (70)$$

As in the Craig-Bampton procedure, the uncoupled mass and stiffness matrices are formed from the reduced component mass and stiffness matrices.

$$[M_u] = \begin{bmatrix} M_{DD}^1 & 0 & 0 & 0 \\ 0 & M_{DD}^2 & 0 & 0 \\ 0 & 0 & I_{KK}^1 & 0 \\ 0 & 0 & 0 & I_{KK}^2 \end{bmatrix} \quad [K_u] = \begin{bmatrix} K_{DD}^1 & 0 & 0 & 0 \\ 0 & K_{DD}^2 & 0 & 0 \\ 0 & 0 & \Lambda_{KK}^1 & 0 \\ 0 & 0 & 0 & \Lambda_{KK}^2 \end{bmatrix} \quad (71a,b)$$

By pre- and post-multiplying both the uncoupled mass matrix represented by Eq. (71a) and the uncoupled stiffness matrix represented by Eq. (71b) by $[T_2]^T$ and $[T_2]$ respectively, the system equations of motion are obtained as follows:

$$[M_s] = \begin{bmatrix} M_{11} & M_{12} \\ M_{21} & M_{22} \end{bmatrix} \quad [K_s] = \begin{bmatrix} K_{11} & K_{12} \\ K_{21} & K_{22} \end{bmatrix} \quad (72a,b)$$

The partitions of the system mass and stiffness matrices represented by Eq. (72a,b) are expressed as follows:

$$\begin{aligned} M_{11} &= [I_{KK}^1 + \Phi_{IK}^{1T} m_1 \Phi_{IK}^1] & K_{11} &= [\Lambda_{KK}^1 + \Phi_{IK}^{1T} k_1 \Phi_{IK}^1] \\ M_{12} = M_{21}^T &= [-\Phi_{IK}^{1T} m_1 \Phi_{IK}^2] & K_{12} = K_{21}^T &= [-\Phi_{IK}^{1T} k_1 \Phi_{IK}^2] \\ M_{22} &= [I_{KK}^2 + \Phi_{IK}^{2T} m_1 \Phi_{IK}^2] & K_{22} &= [\Lambda_{KK}^2 + \Phi_{IK}^{2T} k_1 \Phi_{IK}^2] \end{aligned}$$

where $m_1 = k_1 (M_{DD}^1 + M_{DD}^2) k_1$. The inertia due to high order free interface normal modes is represented by "m₁." [Ref. 12:p. 491]

As stated in the beginning of this section, the MacNeal component mode representation would be presented. By neglecting the inertia due to high-order free interface normal modes, (i.e. "m₁"), one obtains the MacNeal mass and stiffness matrices [Ref 11:p. 59] as follows:

$$\begin{aligned} M_{11} &= [I_{KK}^1] & K_{11} &= [\Lambda_{KK}^1 + \Phi_{IK}^{1T} k_1 \Phi_{IK}^1] \\ M_{12} = M_{21}^T &= [0] & K_{12} = K_{21}^T &= [-\Phi_{IK}^{1T} k_1 \Phi_{IK}^2] \\ M_{22} &= [I_{KK}^2] & K_{22} &= [\Lambda_{KK}^2 + \Phi_{IK}^{2T} k_1 \Phi_{IK}^2] \end{aligned}$$

As will be demonstrated through the examples, the effect of neglecting "m₁" is important when predicting the higher frequencies. The MacNeal representation is accurate in the lower and mid frequency range, but less accurate in the higher frequency range.

Just like the Craig-Bampton component mode representation there are several advantages to both residual flexibility methods. By analyzing both the Craig-Chang and

MacNeal system mass and stiffness matrices, one can see that the final system coordinates are just the free interface normal mode coordinates from each substructure. This resulted from the operations that were conducted in forming the system mass and stiffness matrices. Additionally, since the residual flexibility modes account for the static flexibility of all modes, the methods are statically exact. The procedure is applicable to the mast and antenna problem. Since the connection coordinates are not explicitly retained, this allows the engineer to retain fewer mode shapes and still obtain accurate results. This benefit can be achieved when coupling antenna systems such as the SPS-48E radar to the mast. Unlike a whip antenna which essentially is coupled at one node, the SPS-48E radar or similar radar are connected to the mast at more than one node. Since there are multiple connection points, and the residual flexibility method does not retain the connection coordinates explicitly, a reduction in compute times result, an advantage not found in other substructure coupling procedures.

IV. NUMERICAL VERIFICATION

In Chapters I through III, the various types of vibrational mode shapes were defined and used in the derivations of the three CMS formulations that are presented in this thesis. In this chapter, some numerical convergence examples are made to compare system natural frequencies obtained by the three CMS methods presented in this thesis.

The first example is provided solely as a validation of both the FE and CMS computer codes. In his Doctoral Dissertation, Chang performed a numerical example by which two fixed-free cantilevered beams were synthesized into a fixed-fixed cantilevered beam. The beams were synthesized using the various types of CMS methods. Example 1 is a replication of that example.

In example 2, the mast and antenna substructures, illustrated in Figure 1, are synthesized into the mast and antenna system. The system is synthesized three different times using a varying amount of substructure mode shapes. The resulting natural frequencies are obtained using MATLAB'S eigensolver. A comparison is made between each of the methods and against a FE generated model of the mast and antenna system. This comparison reflects both the accuracy of the three methods in predicting the natural frequencies and the number of calculations, or floating point operations "FLOPS", that are required to synthesize the structures and perform the eigensolution.

A. NATURAL FREQUENCY CALCULATION AND COMPARISON OF A FIXED-FIXED CANTILEVERED BEAM FOR PURPOSES OF FINITE ELEMENT AND COMPONENT MODE SYNTHESIS CODE VALIDATION.

As stated in the beginning of this chapter, the purpose of this example is to validate the FE and CMS code which were written by the author. Figure 2 illustrates a fixed-fixed cantilevered beam that was synthesized from two fixed-free cantilevered beams.

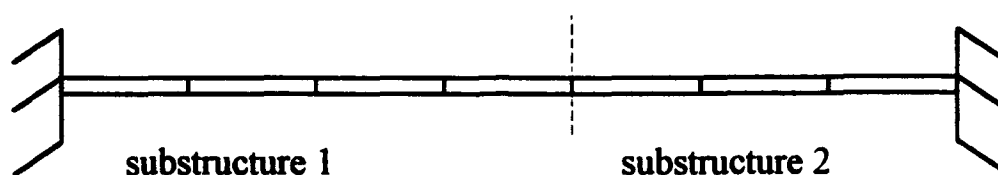


Figure 2: Two Cantilevered Beam Substructures

Each substructure has two degrees of freedom at each node; one translational and one rotational. The first substructure is represented by 4 beam elements corresponding to 8 DOF, while the second substructure is represented by 3 beam elements corresponding to 6 DOF. After synthesis, the system has a total of 12 DOF. As in Chang's example, each method was run using a total of 4, 6, 8 and 10 DOF, or 33, 50, 67, and 83% of all available modes. The results contained in Tables 1-4 are expressed in "Hz" and are the exact same results that are found in Tables 12-15 of the referenced example which are expressed in " $(\text{rad/sec})^2$."

In analyzing the results contained in Tables 1-4, it appears, for this case, that the Craig-Chang procedure yielded a better prediction of the natural frequencies than the

other two formulations. The results are summarized in Figure 3: Comparison of CMS methods with frequency (Hz) error of ≤ 0.1 percent for a fixed-fixed beam. In all cases, the MacNeal procedure predicted a natural frequency in excess of fifty percent error as compared to the standard finite element solution. This error in the predicted natural frequency occurred when predicting the highest mode only. In general, the MacNeal procedure predicted the lower range of natural frequencies comparatively well, but appeared to falter when predicting the higher frequency range. A possible reason for this occurrence comes as a result of neglecting the inertia of high order free interface normal modes, or " m_1 ," as delineated in Chapter III.

TABLE 1. COUPLED SYSTEM NATURAL FREQUENCY COMPARISON (FIXED-FIXED BEAM)
Percent Of Substructure 1 Modes Retained: 25%
Percent Of Substructure 2 Modes Retained: 33%

Mode No.	Standard Finite Element	Craig-Bampton		Craig-Chang		MacNeal	
	Freq. (Hz)	Freq. (Hz)	Error (%)	Freq. (Hz)	Error (%)	Freq. (Hz)	Error (%)
1	0.002298	0.002300	0.087	0.002298	0.000	0.002300	0.087
2	0.006341	0.006347	0.095	0.006341	0.000	0.006347	0.095
3	0.012468	0.013215	5.991	0.012577	0.874	0.013250	6.272
4	0.020739	0.032032	54.45	0.022526	8.617	0.032758	57.95

Notes: The column "Standard Finite Element" contains the mode frequencies for the "fixed-fixed" beam system assembled using a standard finite element approach. The corresponding mode frequency estimates for the three synthesis methods are shown in the three columns to the right. Retained mode percentages are rounded to the nearest integer for clarity.

TABLE 2. COUPLED SYSTEM NATURAL FREQUENCY COMPARISON (FIXED-FIXED BEAM)
Percent of Substructure 1 Modes Retained: 50%
Percent of Substructure 2 Modes Retained: 33%

Mode No.	Standard Finite Element	Craig-Bampton		Craig-Chang		MacNeal	
	Freq. (Hz)	Freq. (Hz)	Error (%)	Freq. (Hz)	Error (%)	Freq. (Hz)	Error (%)
1	0.002298	0.002299	0.007	0.002298	0.000	0.002299	0.007
2	0.006341	0.006342	0.016	0.006341	0.006	0.006346	0.079
3	0.012468	0.012504	0.289	0.012468	0.002	0.012481	0.104
4	0.020739	0.020803	0.309	0.020819	0.386	0.021401	3.192
5	0.031288	0.034193	9.285	0.032337	3.353	0.035307	12.85
6	0.043768	0.069842	59.57	0.048429	10.65	0.069767	59.40

Notes: The column "Standard Finite Element" contains the mode frequencies for the "fixed-fixed" beam system assembled using a standard finite element approach. The corresponding mode frequency estimates for the three synthesis methods are shown in the three columns to the right. Retained mode percentages are rounded to the nearest integer for clarity.

TABLE 3. COUPLED SYSTEM NATURAL FREQUENCY COMPARISON (FIXED-FIXED BEAM)
Percent of Substructure 1 Modes Retained: 63%
Percent of Substructure 2 Modes Retained: 50%

Mode No.	Standard Finite Element	Craig-Bampton		Craig-Chang		MacNeal	
	Freq. (Hz)	Freq. (Hz)	Error (%)	Freq. (Hz)	Error (%)	Freq. (Hz)	Error (%)
1	0.002298	0.002298	0.000	0.002298	0.000	0.002298	0.000
2	0.006341	0.006342	0.011	0.006341	0.000	0.006342	0.008
3	0.012468	0.012469	0.008	0.012468	0.000	0.012472	0.032
4	0.020739	0.020766	0.130	0.020740	0.005	0.020786	0.227
5	0.031288	0.031309	0.067	0.031289	0.003	0.031314	0.083
6	0.043768	0.044121	0.807	0.043841	0.167	0.044475	1.615
7	0.064347	0.068397	6.294	0.065791	2.244	0.069594	8.154
8	0.085189	0.111382	30.75	0.093292	9.512	0.133040	56.17

Notes: The column "Standard Finite Element" contains the mode frequencies for the "fixed-fixed" beam system assembled using a standard finite element approach. The corresponding mode frequency estimates for the three synthesis methods are shown in the three columns to the right. Retained mode percentages are rounded to the nearest integer for clarity.

TABLE 4. COUPLED SYSTEM NATURAL FREQUENCY COMPARISON (FIXED-FIXED BEAM)
Percent of Substructure 1 Modes Retained: 75%
Percent of Substructure 2 Modes Retained: 67%

Mode No.	Standard Finite Element	Craig-Bampton		Craig-Chang		MacNeal	
	Freq. (Hz)	Freq. (Hz)	Error (%)	Freq. (Hz)	Error (%)	Freq. (Hz)	Error (%)
1	0.002298	0.002298	0.000	0.002298	0.000	0.002298	0.000
2	0.006341	0.006341	0.001	0.006341	0.000	0.006341	0.002
3	0.012468	0.012468	0.001	0.012468	0.000	0.012469	0.011
4	0.020739	0.020741	0.012	0.020739	0.000	0.020749	0.053
5	0.031288	0.031290	0.006	0.031288	0.000	0.031295	0.020
6	0.043768	0.043796	0.066	0.043770	0.006	0.043916	0.339
7	0.064347	0.064462	0.178	0.064355	0.012	0.064502	0.242
8	0.085189	0.085314	0.146	0.085255	0.077	0.086228	1.219
9	0.112592	0.115092	2.221	0.113970	1.224	0.119873	6.467
10	0.147562	0.168439	14.15	0.159127	7.838	0.225772	53.00

Notes: The column "Standard Finite Element" contains the mode frequencies for the "fixed-fixed" beam system assembled using a standard finite element approach. The corresponding mode frequency estimates for the three synthesis methods are shown in the three columns to the right. Retained mode percentages are rounded to the nearest integer for clarity.

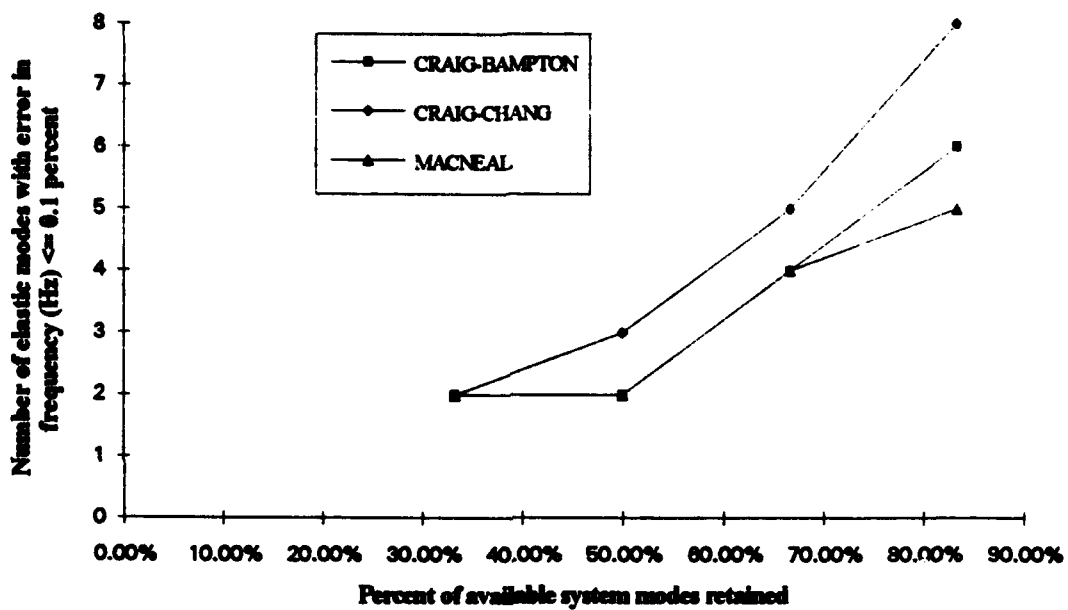


**Figure 3: Comparison of CMS Methods With Frequency (Hz)
Error of ≤ 0.1 Percent for "Fixed-Fixed" Beam System**

B. NATURAL FREQUENCY CALCULATION AND COMPARISON OF MAST AND ANTENNA SYSTEM MODEL

The purpose of the first example was to validate both the FE code and the various CMS codes. The CMS code, written in MATLAB, will accommodate the most general FE modeling. In other words, the CMS code is written independent of the type of FE modeling. Should the mast and antenna system be modeled by beam elements with 6 DOF/node, the CMS code can be applied to it without any modification.

In this section another numerical example which demonstrates the use of the three component mode synthesis procedures is presented. A "mock-up" mast and antenna system consisting of 17 elements was assembled using a standard finite element procedure and all three component mode synthesis procedures. Although the mast/antenna system that is used in the examples is modeled with just a few elements, the resulting models are large enough to allow the effects of mode truncation to be assessed. Again, it is not the intent of this report to solve a base excitation problem on a realistic mast and antenna model, but rather to demonstrate how CMS can be used when performing dynamic analyses for design purposes.

Just like the first example, this example compares natural frequency calculations for the total mast/antenna system as computed using the three CMS formulations as well as using a standard FE procedure. Tables 5-7 contain the results of this comparison. In the tables, each row contains the estimate of a mode frequency. The first column contains the mast/antenna system natural frequency estimates as calculated using the standard FE procedure, and serves as the reference value against which the CMS natural frequency

estimates are to be compared. Columns 2 through 4 contain the analogous natural frequency estimates and percent error, as calculated from the mast/antenna system model synthesized using each of the three CMS procedures. Also included in the column headings are floating point operations (FLOPS) counts which provide a measure of the number of calculations required to assemble the mast/antenna system and calculate the natural frequencies and mode shapes.

Table 1 presents the system frequency comparison where 18% of the available mast modes are retained, and 22% of the available antenna modes are retained. Table 2 repeats the calculations with 42% of the available mast modes retained and 39% of the available antenna modes retained, and Table 3 repeats the calculations with 79% of the available mast modes retained and 67% of the available antenna modes retained. Note that each subsequent table presents comparisons for an increasing number of mode frequencies due to the fact that an increase in the number of retained component modes makes possible an increase in the number of system modes which may be calculated.

Note that in the FEM model, the FLOPS count stays fixed at slightly over $2 \cdot 10^6$. This is a rather small number as the model is a small model when compared to one that a design engineer would generate for analysis of an actual mast/antenna assembly. It is noteworthy to state that in this particular model, $0.7 \cdot 10^6$ FLOPS were expended in computing the combination of fixed interface normal modes and static constraint modes using the Craig-Bampton procedure. Additionally, $0.8 \cdot 10^6$ FLOPS were expended in computing the free interface normal modes using the Craig-Chang and MacNeal

procedures. Theoretically, once the various vibrational modes have been found, they need not be calculated again. Note also that in all three models, these figures comprise a significant portion of the total FLOPS.

From Tables 5 through 7, it is seen that all three methods produce excellent frequency predictions. All three methods demonstrate sudden increases in frequency error above a certain mode. This reveals the extent to which the retained component modes accurately represent the dynamics of the synthesized mast/antenna system. In the MacNeal procedure, the percentage error exceeded 100% when calculating the highest mode. This error in predicting the highest frequency mode could possibly be attributed to neglecting the inertia due to high-order free interface normal modes. Note that by neglecting the inertia, that the accuracy in predicting natural frequencies is only effected at the last few modes.

As stated in the previous paragraph, all three methods produced excellent results in predicting natural frequencies, but with less cost in terms of number of computations as compared to the standard FE calculation. The Craig-Chang procedure in general provided the greatest number of natural frequencies with error less than or equal to 0.1% (in Hz) (see Figure 4). However, the Craig-Bampton procedure yielded the same number of frequencies with error less than or equal to 0.1% as the Craig-Chang procedure when retaining a large of number of component modes, but at a slightly more cost than the Craig-Chang procedure.

TABLE 5. COUPLED SYSTEM NATURAL FREQUENCY COMPARISON (MAST/ANTENNA MODEL)
Percent of Available Mast Modes Retained: 18%
Percent of Available Antenna Modes Retained: 22%

Mode No.	Standard Finite Element (2.05E+06 FLOPS)	Craig-Bampton (7.72E+05 FLOPS)	Craig-Chang (1.17E+06 FLOPS)	MacNeal (1.06E+06 FLOPS)
	Freq. (Hz)	Freq. (Hz)	Freq. (Hz)	Freq. (Hz)
1	6.885	6.885	6.885	6.887
2	10.396	10.398	10.396	10.398
3	13.301	13.301	13.301	13.301
4	19.102	19.104	19.102	19.102
5	47.257	47.260	47.260	47.403
6	69.884	70.040	69.893	70.155
7	83.502	83.504	83.502	83.503
8	121.024	134.053	121.372	121.441
9	122.115	184.492	143.508	238.807
10	135.967	303.331	222.630	341.199
		Error (%)	Error (%)	Error (%)
		0.002	0.000	0.019
		0.019	0.002	0.020
		0.002	0.000	0.000
		0.012	0.002	0.002
		0.007	0.007	0.309
		0.224	0.013	0.388
		0.003	0.000	0.000
		10.765	0.287	0.344
		51.080	17.518	95.559
		>100.00	63.738	>100.00

Notes: The column "Standard Finite Element" contains the mode frequencies for the mast/antenna system assembled using a standard finite element approach. The corresponding mode frequency estimates for the three synthesis methods are shown in the three columns to the right. The Floating Point Operations (FLOPS) required for each synthesis method and the finite element calculation are shown. Retained mode percentages are rounded to the nearest integer for clarity.

TABLE 6. COUPLED SYSTEM NATURAL FREQUENCY COMPARISON (MAST/ANTENNA MODEL)

Mode No.	Standard Finite Element (2.05E+06 FLOPS)	Craig-Bampton (8.63E+05 FLOPS)	Craig-Chang (1.23E+06 FLOPS)	MacNeal (1.15E+06 FLOPS)
	Freq. (Hz)	Freq. (Hz)	Freq. (Hz)	Freq. (Hz)
	Error (%)	Error (%)	Error (%)	Error (%)
1	6.885	6.885	6.885	6.885
2	10.396	10.396	10.396	10.396
3	13.301	13.301	13.301	13.301
4	19.102	19.092	19.102	19.102
5	47.257	47.257	47.257	47.260
6	69.884	69.886	69.883	69.886
7	83.502	83.503	83.502	83.502
8	121.024	121.058	121.027	121.028
9	122.115	122.197	122.118	122.119
10	135.967	135.971	135.964	136.021
--				
19	462.776	463.860	463.361	468.640
20	537.237	537.239	537.237	537.238
21	647.348	706.684	648.220	649.499
22	692.643	735.918	721.256	746.016
23	733.509	934.920	738.706	900.717
24	756.314	1256.376	1019.930	2453.914
		66.118	34.855	>100.00

Notes: The column "Standard Finite Element" contains the mode frequencies for the mast/antenna system assembled using a standard finite element approach. The corresponding mode frequency estimates for the three synthesis methods are shown in the three columns to the right. The Floating Point Operations (FLOPS) required for each synthesis method and the finite element calculation are shown. Retained mode percentages are rounded to the nearest integer for clarity. Modes 11 through 18 excluded to conserve space.

TABLE 7. COUPLED SYSTEM NATURAL FREQUENCY COMPARISON (MAST/ANTENNA MODEL)
Percent of Available Mast Modes Retained: 79%
Percent of Available Antenna Modes Retained: 67%

Mode No.	Standard Finite Element (2.05E+06 FLOPS)	Craig-Bampton (1.82E+06 FLOPS)	Craig-Chang (1.80E+06 FLOPS)	MacNeal (1.66E+06 FLOPS)
1	Freq. (Hz) 6.885	Freq. (Hz) 6.885	Freq. (Hz) 6.885	Freq. (Hz) 6.885
2	10.396	10.396	10.396	10.396
3	13.301	13.301	13.301	13.301
4	19.102	19.092	19.102	19.102
5	47.257	47.257	47.257	47.258
--				
28	977.426	978.347	977.447	978.075
29	1022.223	1022.255	1022.234	1022.294
30	1098.507	1098.592	1098.893	1108.635
31	1267.414	1267.416	1267.445	1267.854
32	1306.822	1306.373	1306.876	1307.009
33	1415.797	1418.637	1420.494	1468.806
34	1477.522	1477.863	1477.798	1499.859
35	1538.404	1539.828	1547.072	1578.170
36	1656.532	1659.662	1659.529	1684.335
37	1671.847	2009.052	1785.483	2623.856
38	1885.441	2275.957	2040.943	7736.296
				>100.00

Notes: The column "Standard Finite Element" contains the mode frequencies for the mast/antenna system assembled using a standard finite element approach. The corresponding mode frequency estimates for the three synthesis methods are shown in the three columns to the right. The Floating Point Operations (FLOPS) required for each synthesis method and the finite element calculation are shown. Retained mode percentages are rounded to the nearest integer for clarity. Modes 6 through 27 excluded to conserve space.

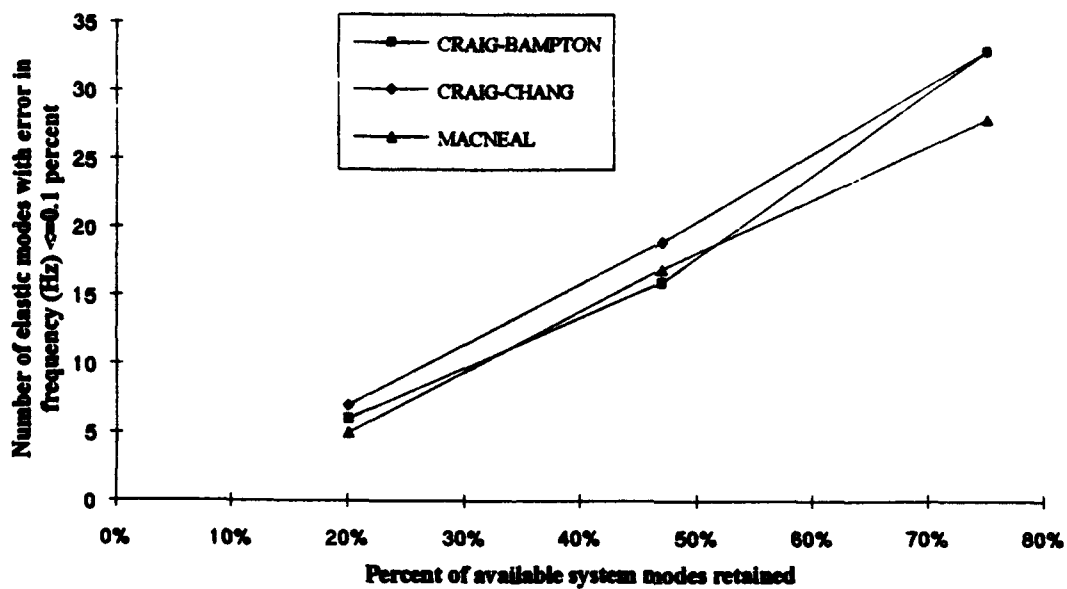


**Figure 4: Comparison of CMS Methods With Frequency (Hz)
Error of ≤ 0.1 Percent for Mast/Antenna System**

V. BASE EXCITATION FORMULATIONS

In the previous section, the natural frequencies of the mast and antenna system were calculated for increasing number of retained component modes. Natural frequencies and mode shapes are important modal parameters and are fundamental in solving for the forced response of a system. As demonstrated in the previous section, accurate natural frequencies of a system can be obtained using CMS at a cost less than that associated with standard FE modeling.

In this section, two base excitation formulations will be presented. The first formulation requires the knowledge of the acceleration of the mast base coordinates (i.e. the coordinates where the mast and ship are coupled) as a function of time. In other words, the formulation requires that the acceleration time history of the base coordinates be known. The second formulation requires the knowledge of the displacement of the base coordinates as a function of time, or the displacement time history of the base coordinates. Using both formulations, numerical convergence assessments will be made, and the benefits that CMS has to offer the mast/antenna design process will be demonstrated.

A. BASE EXCITATION FROM PRESCRIBED ACCELERATION

Once the FE program has numerically assembled the mast mass and stiffness matrices, and the acceleration of the base coordinates are specified as a function of time, the base excitation problem can be derived from the following equation of motion:

$$\begin{bmatrix} M_{OO} & M_{OB} \\ M_{BO} & M_{BB} \end{bmatrix} \begin{Bmatrix} \ddot{x}_O \\ \ddot{x}_B \end{Bmatrix} + \begin{bmatrix} K_{OO} & K_{OB} \\ K_{BO} & K_{BB} \end{bmatrix} \begin{Bmatrix} x_O \\ x_B \end{Bmatrix} = \begin{Bmatrix} F_O \\ 0 \end{Bmatrix} \quad (73)$$

where subscript "O" represents the interior coordinates, and subscript "B" represents the base coordinates.

Solving the top row of equations in Eq. (73) the following is obtained:

$$M_{OO}\ddot{x}_O + M_{OB}\ddot{x}_B + K_{OO}x_O + K_{OB}x_B = F_O \quad (74)$$

Since the acceleration of the base is prescribed, the base acceleration term will be moved to the right hand of the equals sign to obtain the following:

$$M_{OO}\ddot{x}_O + K_{OO}x_O + K_{OB}x_B = F_O - M_{OB}\ddot{x}_B \quad (75)$$

From the bottom row, the following equation is obtained:

$$M_{BO}\ddot{x}_O + M_{BB}\ddot{x}_B + K_{BO}x_B + K_{BB}x_B = 0 \quad (76)$$

From Eq. (76), the following relation is obtained for the base displacement:

$$x_B = -K_{BB}^{-1} [M_{BO}\ddot{x}_O + M_{BB}\ddot{x}_B + K_{BO}x_O] \quad (77)$$

Equation (77) is now substituted into Eq. (75), and after simplifying, the following equation of motion in terms of the interior coordinates is given by:

$$[M_{oo} - K_{ob} K_{bb}^{-1} M_{bo}] \ddot{x}_o + [K_{oo} - K_{ob} K_{bb}^{-1} K_{bo}] x_o = F_o + [K_{ob} K_{bb}^{-1} M_{bb} - M_{ob}] \ddot{x}_b \quad (78)$$

Equation (78) is the system equation of motion of the internal coordinates in terms of the prescribed base acceleration for the mast only. Since the antenna has no prescribed base acceleration, the above formulation is not applied to the FE generated mass and stiffness matrices of the antenna.

Now that both substructures have been numerically constructed, they are now ready to be synthesized into the mast and antenna system. Both the mast and antenna substructure mass and stiffness matrices and force vector are now partitioned into internal and connection coordinates as follows:

$$[M] = \begin{bmatrix} M_{oo} & M_{oi} \\ M_{io} & M_{ii} \end{bmatrix}, \quad [K] = \begin{bmatrix} K_{oo} & K_{oi} \\ K_{io} & K_{ii} \end{bmatrix}, \quad \{F\} = \begin{Bmatrix} F_o \\ F_i \end{Bmatrix}$$

where the subscript "O" and subscript "I" represent the internal and interface coordinates respectively.

Using the procedures of Chapter III, the respective substructure mass and stiffness matrices and force vectors are transformed into a "reduced" system by using the first transformation matrix as follows:

$$[M_r] = [T_i]^T [M] [T_i] \quad [K_r] = [T_i]^T [K] [T_i] \quad \{F_r\} = [T_i]^T \{F\} \quad (79 \text{ a, b, c})$$

As derived in Chapter III, the coupled mast/antenna system mass and stiffness matrices and force vectors are formed from an uncoupled system using the second transformation matrix, and is given by:

$$[M_s] = [T_2]^T [M_u] [T_2] \quad [K_s] = [T_2]^T [K_u] [T_2] \quad \{F_s\} = [T_2]^T \{F_u\} \quad (80 \text{ a, b, c})$$

where the subscripts "s" and "u" represent the coupled system and uncoupled system respectively.

The operations in Eq. (79 a, b, c) and Eq. (80 a, b, c) are applicable to each of the CMS methods using each method's respective transformation matrices, (i.e. $[T_1]$ and $[T_2]$). Now that the system force vector and system mass and stiffness matrices have been formed, the coupled system natural frequencies and mode shapes can be obtained from the following:

$$[K_s - \lambda \cdot M_s] \{\phi^N\} = \{0\} \quad (81)$$

In Chapter III it was shown how the generalized coordinates or, "p" coordinates, were obtained from a linear transformation of the physical coordinates or, "x" coordinates, using the first transformation matrix. Additionally, a set of linearly independent coordinates were obtained from the set of generalized coordinates, which consist of linearly independent and linearly dependent coordinates, using the second transformation

matrix. Therefore, the coordinates associated with Eq. (80 a, b, c) and Eq. (81) are the set of generalized linearly independent coordinates or, "p₁," as defined in Chapter III.

The set of generalized linearly independent coordinates are transformed into a set of modal coordinates by the following relation:

$$\{p_o\} = [\Phi^N] \cdot \{q_o\} \quad (82)$$

where $\{p_o\}$ represents the vector of generalized linearly independent internal coordinates, $\{q_o\}$ represents the vector of modal internal coordinates, and $[\Phi^N]$ represents the matrix of unity modal mass free interface normal modes obtained from the solution to Eq.(81).

The system equation of motion is then pre-multiplied by the transpose of the matrix of normal modes to obtain the following modal system of equations:

$$[I]\{\ddot{q}_o\} + [\Lambda]\{\dot{q}_o\} = \{F\} \quad (83)$$

where $\{\ddot{q}_o\}$ represents the vector of modal accelerations and $\{F\}$ represents the vector of modal forces.

There are "m" equations associated with the solution to Eq. (83) where "m" is equal to the number of rows or columns in either the system mass or stiffness matrice. The acceleration at the base is a prescribed harmonic input.

The base acceleration is taken as:

$$\{\ddot{x}_b\} = -\Omega^2 \{X_b\} \sin(\Omega t) \quad (84)$$

where " Ω " represents the forcing frequency expressed in rad/sec, and $\{X_b\}$ represents the vector of amplitudes of the base displacement expressed in inches. Since acceleration is prescribed at the base, and the product of mass and acceleration is consistent with the units of force, the resulting forcing function is also harmonic.

Therefore, the form of the " i_a " equation of this system of equations, (i.e. Eq. (83)), is given by:

$$\ddot{q}_{o_i} + \omega_i^2 q_{o_i} = F_i(\sin(\Omega t)) \quad (85)$$

where $\omega_i^2 = \lambda_i$ and is associated with the " i_a " natural frequency of the system.

Equation (85) can be solved using two different methods. Since Eq. (85) is an ordinary differential equation, the solution can be obtained by finding the particular solution which requires the knowledge of the initial conditions, (i.e. $\phi_i^N \cdot q_{i0}(t=0)$ and $\phi_i^N \cdot \dot{q}_{i0}(t=0)$) or the initial displacement and velocity of the system. Since there are no initial conditions on the mast and antenna prior to the shock wave meaning that the mast and antenna is motionless prior to the shock wave, a more convenient and preferred way to solve Eq. (85) is through convolution. The homogenous solution to Eq. (85) is given by:

$$q_i(t) = A_i(\cos(\omega_i t)) + B_i(\sin(\omega_i t)) \quad (86)$$

where "A_i" and "B_i" are the amplitudes of the modal displacement and are evaluated from the initial conditions.

Using convolution, the particular solution is given

$$q_i(t) = A_i(\cos(\omega_i t)) + B_i(\sin(\omega_i t)) + \int_0^t \frac{1}{\omega_i} \sin(\omega_i(t-\tau)) F_i \sin(\Omega \tau) d\tau \quad (87)$$

where "τ" is a time constant.

The integral in Eq. (87) is generally known as the convolution integral or more formally as Duhamel's integral. After solving Duhamel's integral, Eq. (87) can be rewritten as follows:

$$q_i(t) = A_i(\cos(\omega_i t)) + B_i(\sin(\omega_i t)) - \frac{F_i \Omega \sin(\omega_i t)}{\omega_i(\omega_i^2 - \Omega^2)} + \frac{F_i \sin(\Omega t)}{(\omega_i^2 - \Omega^2)} \quad (88)$$

Since there is no initial displacement or velocity, "A_i" and "B_i" are both equal to 0.

Equation (88) is then simplified as follows:

$$q_i(t) = - \frac{F_i \Omega \sin(\omega_i t)}{\omega_i(\omega_i^2 - \Omega^2)} + \frac{F_i \sin(\Omega t)}{(\omega_i^2 - \Omega^2)} \quad (89)$$

Equation (89) is solved for each of the "m" equations in the system of equations. By solving Eq. (89), the modal displacement for each coordinate is obtained as a function of time.

Since the mast was modeled as a "free-free" structure meaning that there were no restrained coordinates, the synthesis of the mast and antenna system yields a structure that is also "free-free". This means that there are some rigid body modes associated with the

eigensolution of the system of equations. Since the mast was modeled with three DOF/node, there are three rigid body modes which correspond to three natural frequencies of 0 rad/sec. Therefore, for the first three equations of Eq. (83), Eq. (89) cannot be applied in solving for the modal displacement of the first three coordinates as a function of time. Using Eq. (85) and substituting "0" for ω Eq. (85) is simplified as follows:

$$\ddot{q}_{0i}(t) = F_i \sin(\Omega t), \quad i=1:3 \quad (90)$$

Integrating Eq. (90), the following is obtained for the modal velocity as a function of time for the first three modal coordinates:

$$\dot{q}_{0i}(t) = \frac{-F_i}{\Omega} \cos(\Omega t) + c_i, \quad i=1:3 \quad (91)$$

where "c" is a constant of integration.

Integrating Eq. (91), the following is obtained for the modal displacement as a function of time for the first three modal coordinates:

$$q_{0i}(t) = \frac{-F_i}{\Omega^2} \sin(\Omega t) + c_i t + d_i, \quad i=1:3 \quad (92)$$

where "d" is a second constant of integration.

The constants of integration "c" and "d" are obtained by substituting the initial conditions into Eq. (91) and Eq. (92) and solving Eq. (91) and Eq. (92) for "c" and "d". Substituting

the initial condition of displacement into Eq. (92) the second constant of integration is obtained:

$$d_i = 0, \quad i=1:3$$

The first constant of integration, "c," is obtained in a similar manner. Substituting the velocity initial conditions in Eq. (91), the first time constant is obtained:

$$c_i = \frac{\phi_i^T F_i}{\Omega}, \quad i=1:3$$

Substituting the constants of integration into Eq.(92), the modal displacements for the first three coordinates can be obtained from the following relation:

$$q_{o_i}(t) = \frac{-F_i}{\Omega^2} \sin(\Omega t) + \frac{\phi_i^T F_i}{\Omega} t, \quad i=1:3 \quad (93)$$

Equation (93) is used to obtain the modal displacement solution as a function of time for the first three coordinates, while Eq. (89) is used to obtain the modal displacement solution as a function of time for the remainder of the set of coordinates.

Once the modal response is obtained, Eq. (82) is used to obtain the response in linearly independent generalized coordinates. By using the second transformation matrix followed in succession by the first transformation matrix in a manner similar to that of Eq. (82), the response of all of the physical coordinates that defines the system is obtained.

In what follows, the relation in Eq. (78) is used in conjunction with a standard FE model of the total mast/antenna system to perform the prescribed base acceleration dynamic analysis. This analysis serves as the reference against which the results of various CMS formulations are to be compared. To restate, in each CMS formulation, Eq. (78) is used to define the mast component model, as only the mast has prescribed base accelerations.

In the following section, two numerical examples are provided. It is the intent of the examples to:

- (1) compare the results obtained from the three CMS formulations
- (2) and demonstrate the benefits of using CMS versus standard FE modeling when solving base excitation problems.

1. Tip Deflection Calculation

On page 70 is a diagram of the mast and antenna system being subjected to base excitation. The excitation was performed at two different and arbitrarily selected frequencies. The first frequency was at 8.95 Hz. This frequency falls between mode 1 and mode 2 of the total mast/antenna system. The second frequency was between mode 9 and mode 10 at 219 Hz. The wide spread in the frequencies was intended to demonstrate that many more modes need to be retained when calculating the response to higher frequency excitation as compared with lower frequency excitations. In this example, the antenna tip deflection was calculated using the standard FE procedure and the three CMS procedures. The percent error in antenna tip deflection was plotted versus the percent of available component modes retained (see Figures 6-9). The calculations were performed twice. In

the first calculation, mast modes were truncated while retaining all of the available antenna modes, and antenna modes were truncated in the second calculation while retaining all of the available mast modes. When the mast was subjected to the forced input at the lower frequency the Craig-Bampton and Craig-Chang procedure yielded results which converged more rapidly to the exact answer than the MacNeal procedure.

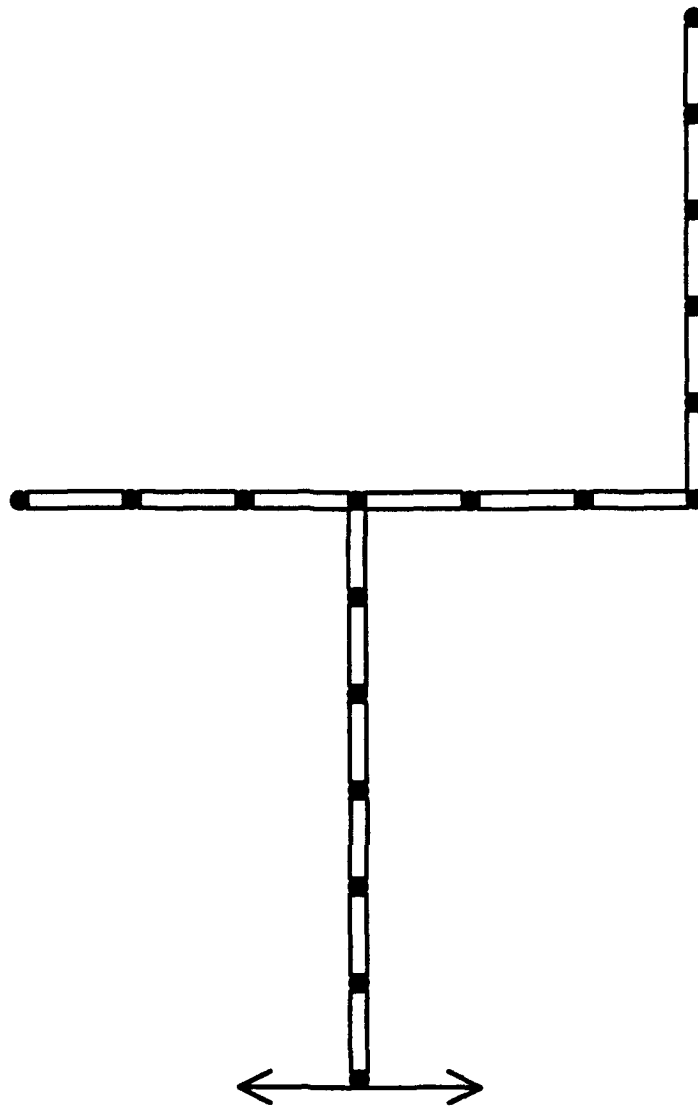


**Figure 5: The Coupled Mast and Antenna Subjected to Base
Excitation at 8.95 Hz**

Although, hard to determine from Figures 6 and 7, the Craig-Bampton procedure yielded the best results using fewer modes than the Craig-Chang procedure in both the mast truncation and antenna truncation runs. When 20% of the available mast modes were used, all three procedures predicted a tip deflection measurement that was within 0.05% of the "exact" value (the "exact" value was calculated using the standard FE procedure). This accurate assessment was obtained at a cost of 60% of the number of calculations that were required of the FE solution. The error obtained when 20% of the available mast modes were retained was significantly small. Since all of the vibrational mode shapes were obtained in this calculation (i.e. fixed interface normal modes, free interface normal modes, static constraint modes, and residual flexibility modes), future assessments which retain more mast modes would come at an even lesser cost than the initial assessment.

When the mast was subjected to the higher forcing frequency, all three methods converged more slowly as compared to the lower forcing frequency when truncating both mast modes and antenna modes (see Figures 8 and 9). Since the forcing frequency was higher, more modes needed to be retained in order to obtain accurate results. From the results of the tip deflection calculations, it appears that the combination of fixed interface normal modes and static constraint modes have led to the higher rate of convergence using the Craig-Bampton procedure. However, the results obtained using the Craig-Chang procedure compared quite well with the results obtained using the Craig Bampton method.

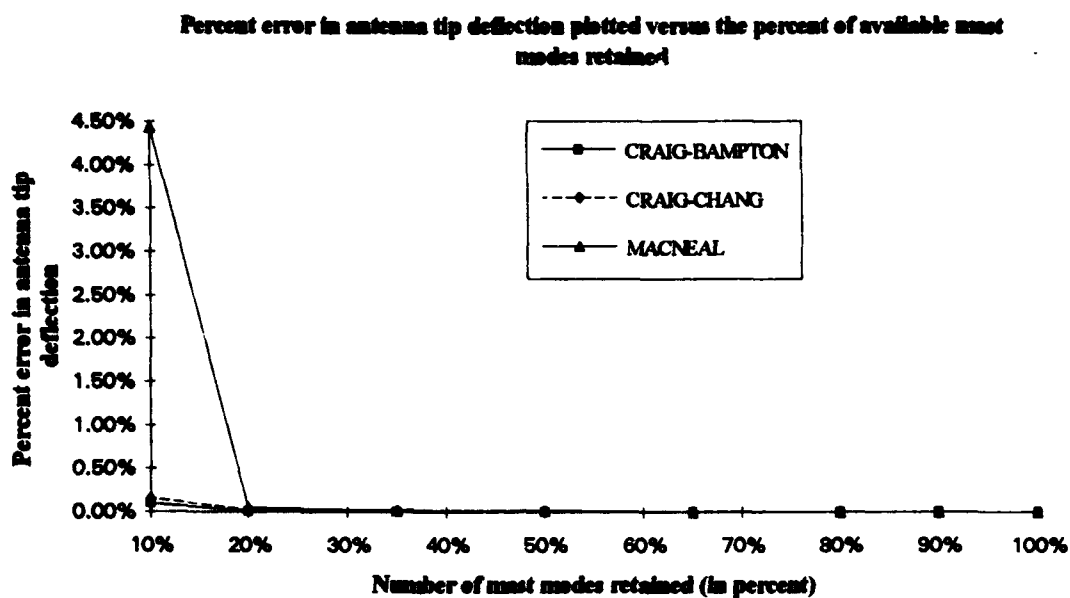


Figure 6: Percent Error in Antenna Tip Deflection Plotted Versus the Percent of Available Mast Modes Retained. (Forcing Frequency: 8.95 Hz)

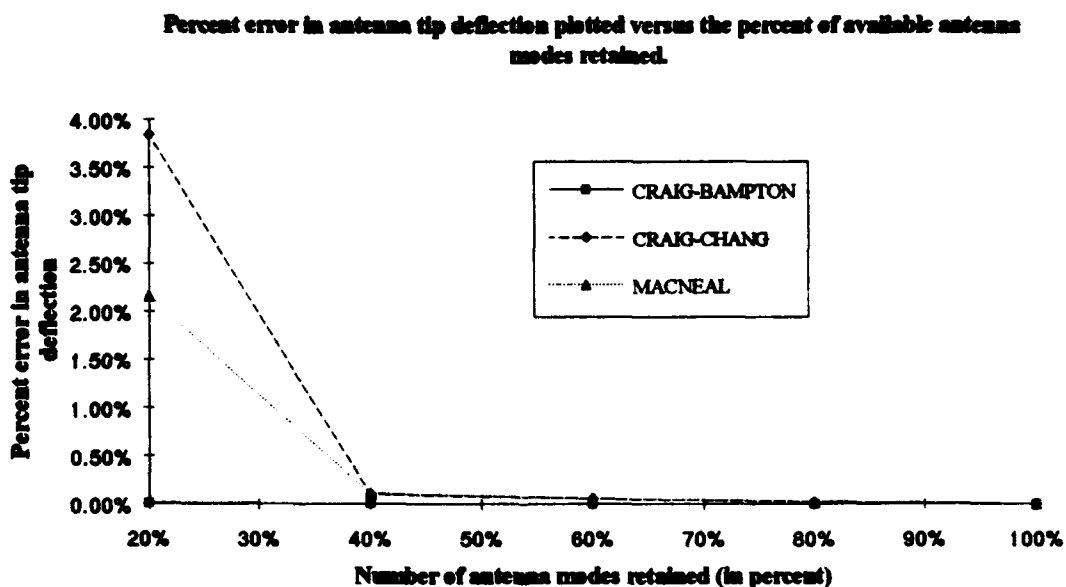


Figure 7: Percent Error in Antenna Tip Deflection Plotted Versus the Percent of Available Antenna Modes Retained. (Forcing Frequency: 8.95 Hz)

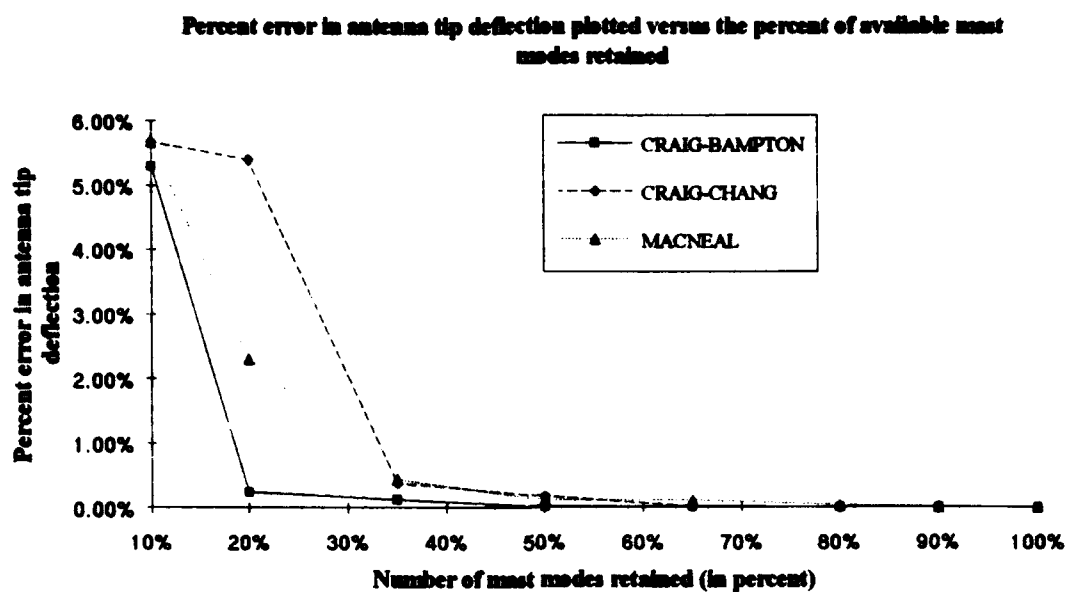


Figure 8: Percent Error in Antenna Tip Deflection Plotted Versus the Percent of Available Mast Modes Retained. (Forcing Frequency: 219 Hz)

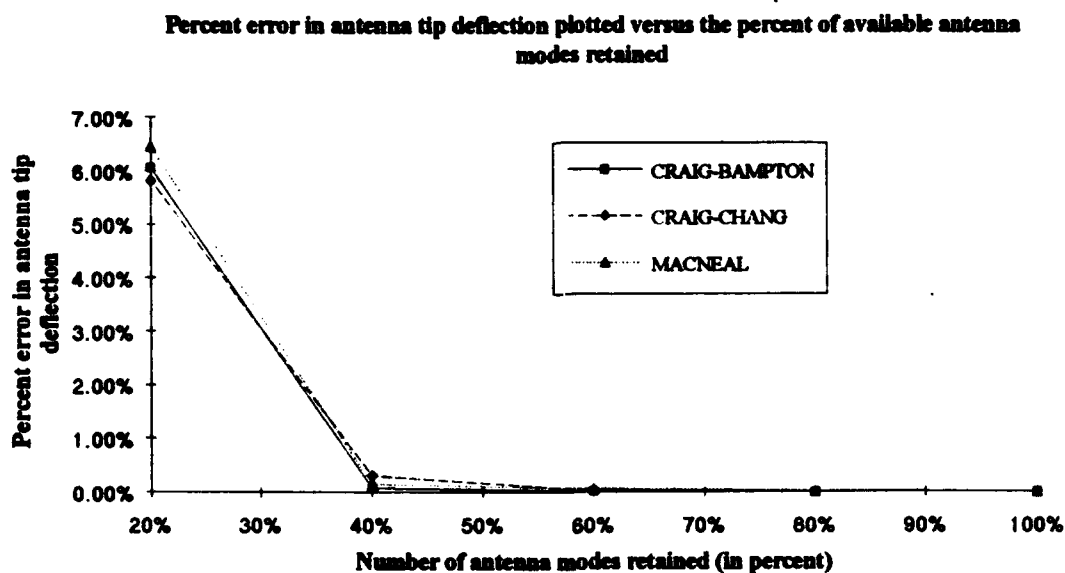


Figure 9: Percent Error in Antenna Tip Deflection Plotted Versus the Percent of Available Antenna Modes Retained. (Forcing Frequency: 219 Hz)

2. Moment and Shear Calculation

In order to assess structural survivability, accurate prediction of the internal stresses in the antenna and the antenna/mast interface must be calculated. Therefore, this section demonstrates the calculation of the internal peak dynamic bending moments and shear loads in the antenna.

The moment and shear calculations were calculated using the three CMS procedures and the results are compared in the figures. The percent error in moment and shear were plotted versus the percent of available mast modes retained and percent of available antenna modes retained. Again, the same two forcing frequencies used in the tip deflection calculation are used here in the moment and shear calculations; specifically 8.95 and 219 Hz.

The results obtained when calculating the shear and moment at the mast/antenna connection mirror the results of the tip deflection calculations (see Figures 10-17). Again, the Craig-Bampton procedure yielded results that converged more quickly to the "exact" answer (provided by standard FE calculations) than the other methods. However, the results obtained using the Craig-Chang procedure were quite similar to those obtained using the Craig-Bampton method. Despite a large initial error produced by the MacNeal method as compared to the other two methods, nearly "exact" solutions were obtained at a cost much less than using standard FE calculation procedures. If the moment and shear at the mast/antenna interface exceeded an appropriate failure criteria, the antenna can be easily relocated from the end node to another node along the cross bar by redefining the

connection coordinates of the mast. New moment and shear calculations would be made until an acceptable response obtained. Redefining the connection coordinates, synthesizing the new structure, and calculating the response is much more convenient and computationally efficient than reassembling the mast and antenna system, which would be required using standard FE procedures.

When the mast and antenna system were subjected to the forced input at the higher forcing frequency, the rate of convergence was again much slower than that which was obtained at the lower excitation frequency. However, all methods yield accurate results at a computational cost less than using the standard FE procedure with the higher forcing frequency.

Percent error in shear at mast and antenna connection plotted versus the percent of available mast modes retained

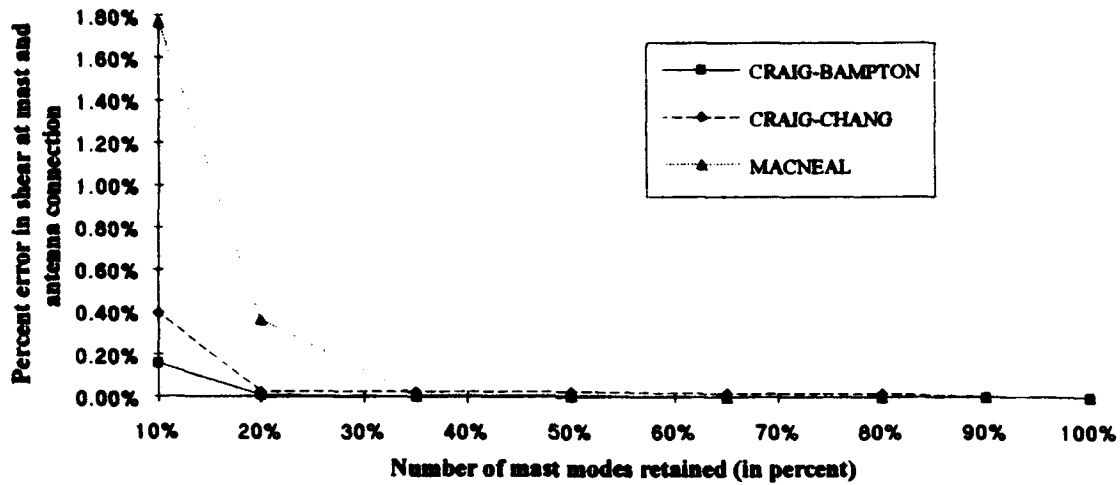


Figure 10: Percent Error in Shear at Mast and Antenna Connection Plotted Versus the Percent of Available Mast Modes Retained. (Forcing Frequency: 8.95Hz)

Percent error in moment at mast and antenna connection plotted versus the percent of available mast modes retained

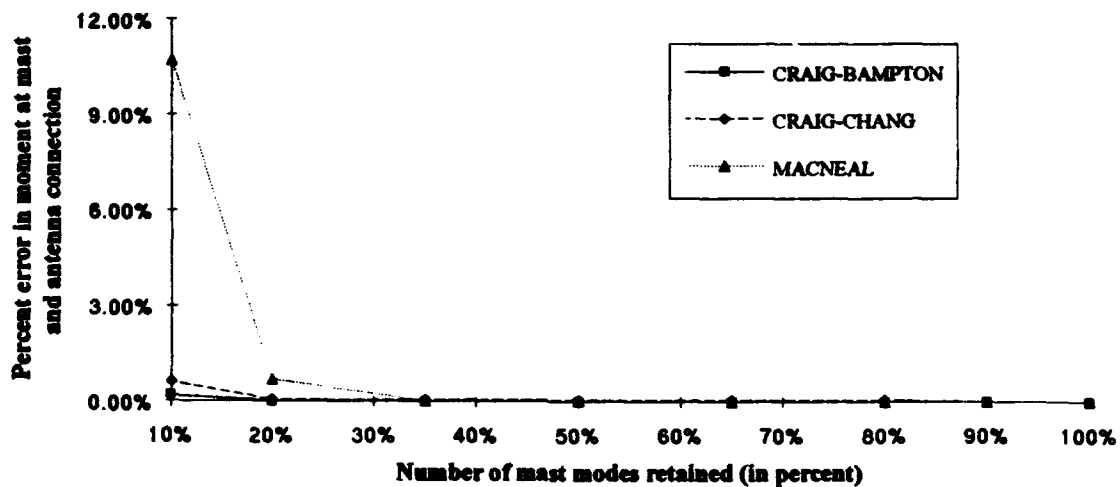


Figure 11: Percent Error in Moment at Mast and Antenna Connection Plotted Versus the Percent of Available Mast Modes Retained. (Forcing Frequency: 8.95 Hz)

Percent error in shear at mast and antenna connection plotted versus the percent of available antenna modes retained

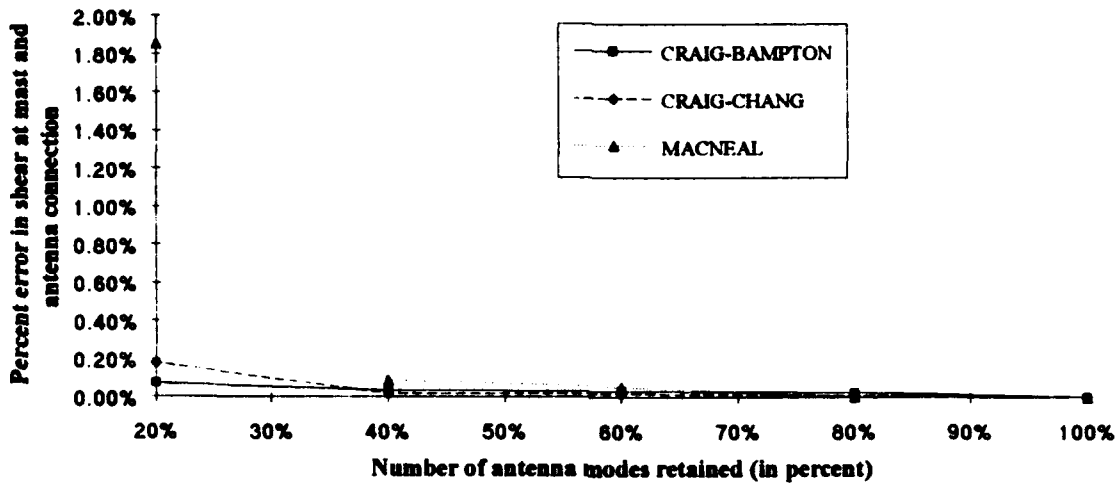


Figure 12: Percent Error in Shear at Mast and Antenna Connection Plotted Versus the Percent of Available Antenna Modes Retained. (Forcing Frequency: 8.95 Hz)

Percent error in moment at mast and antenna connection plotted versus the percent of available antenna modes retained

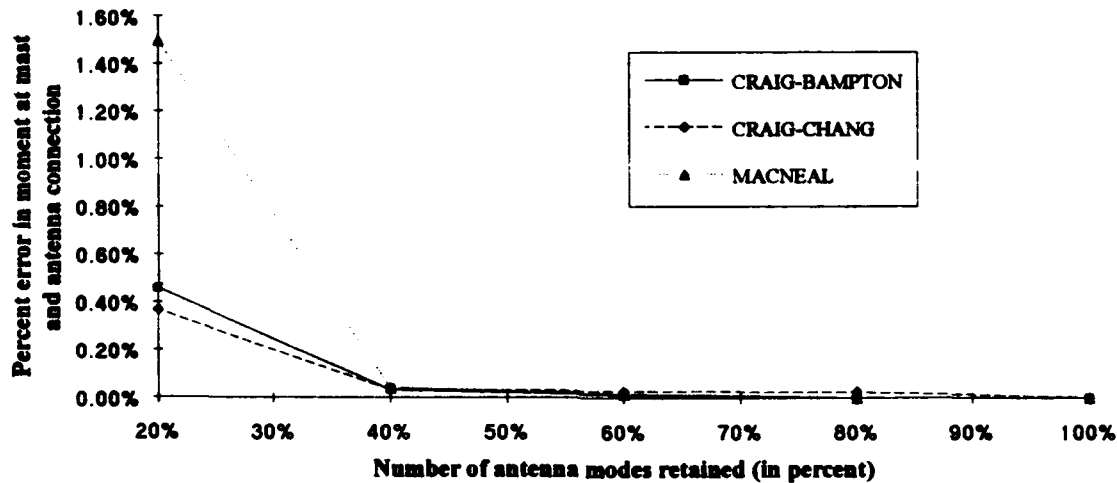


Figure 13: Percent Error in Moment at Mast and Antenna Connection Plotted Versus the Percent of Available Antenna Modes Retained. (Forcing Frequency: 8.95 Hz)

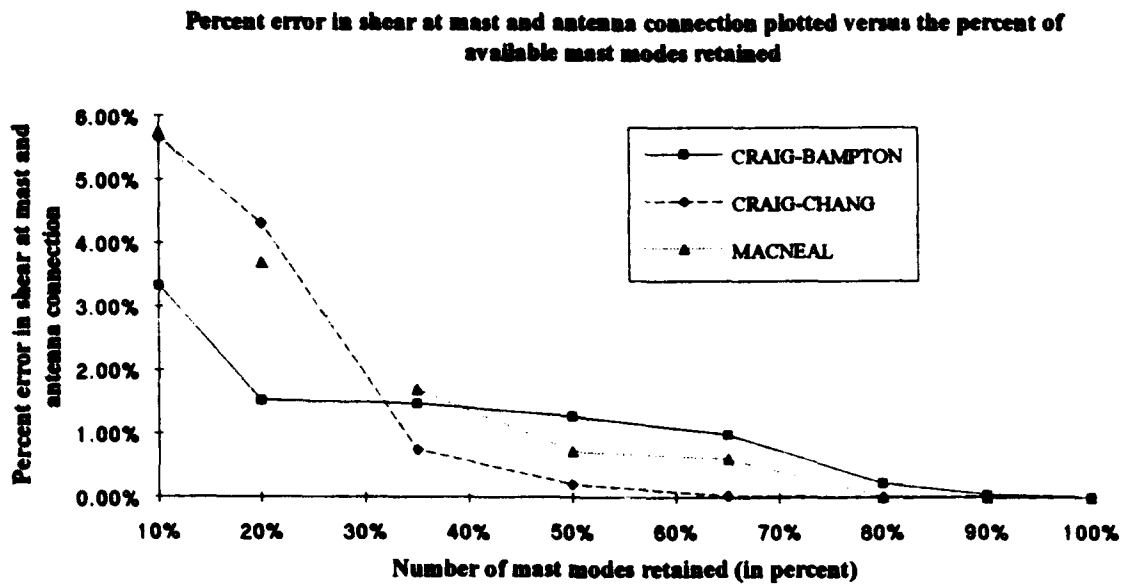


Figure 14: Percent Error in Shear at Mast and Antenna Connection Plotted Versus the Percent of Available Mast Modes Retained. (Forcing Frequency: 219 Hz)

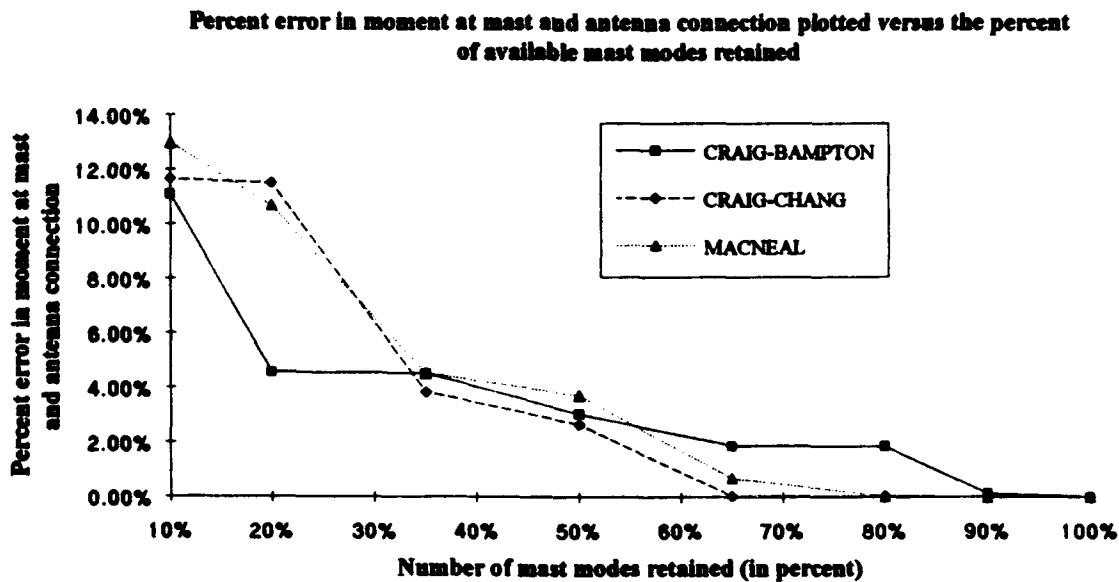


Figure 15: Percent Error in Moment at Mast and Antenna Connection Plotted Versus The Percent of Available Mast Modes Retained. (Forcing Frequency: 219 Hz)

Percent error in shear at mast and antenna connection plotted versus the percent of available antenna modes retained

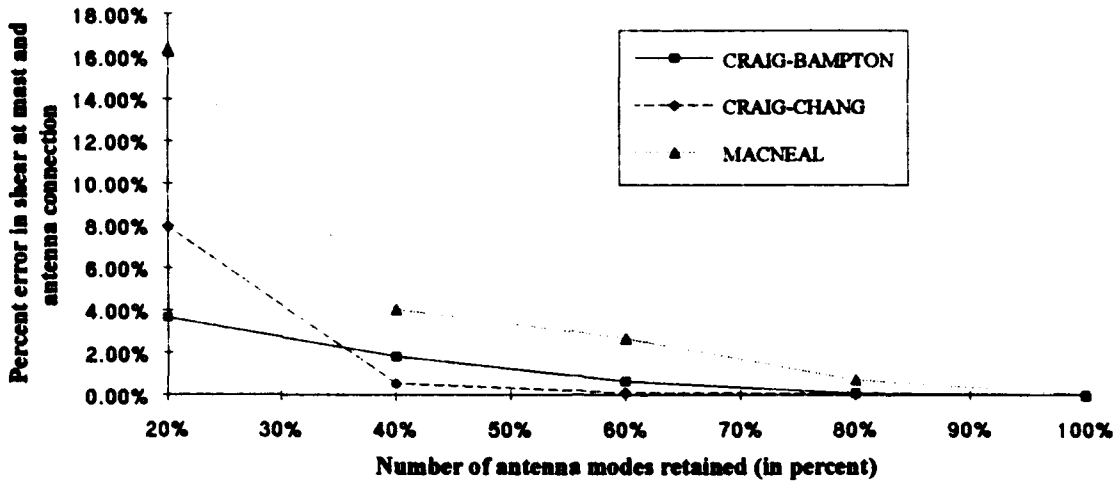


Figure 16: Percent Error in Shear at Mast and Antenna Connection Plotted Versus the Percent of Available Antenna Modes Retained. (Forcing Frequency: 219 Hz)

Percent error in moment at mast and antenna connection plotted versus the percent of available antenna modes retained

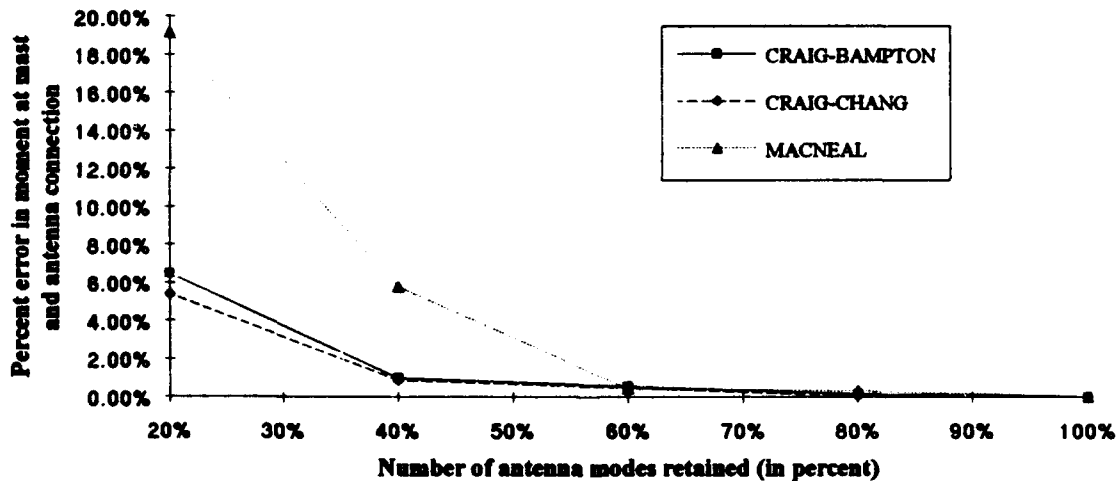


Figure 17: Percent Error in Moment at Mast and Antenna Connection Plotted Versus the Percent of Available Antenna Modes Retained. (Forcing Frequency: 219 Hz)

B. BASE EXCITATION FROM PRESCRIBED DISPLACEMENT

The following derivation is applicable to the base excitation problem, where base displacements (as opposed to base accelerations) are to be prescribed. As in the base excitation from prescribed acceleration, the derivation starts with the FEM generated mass and stiffness matrices as follows:

$$\begin{bmatrix} M_{OO} & M_{OB} \\ M_{BO} & M_{BB} \end{bmatrix} \begin{Bmatrix} \ddot{x}_O \\ \ddot{x}_B \end{Bmatrix} + \begin{bmatrix} K_{OO} & K_{OB} \\ K_{BO} & K_{BB} \end{bmatrix} \begin{Bmatrix} x_O \\ x_B \end{Bmatrix} = \begin{Bmatrix} F_O \\ 0 \end{Bmatrix} \quad (73)$$

The bottom row is expanded into the following equation:

$$M_{BO}\ddot{x}_O + M_{BB}\ddot{x}_B + K_{BO}x_O + K_{BB}x_B = 0 \quad (76)$$

From Eq. (28), the base acceleration is obtained as follows:

$$\ddot{x}_B = -M_{BB}^{-1} [M_{BO}\ddot{x}_O + K_{BO}x_O + K_{BB}x_B] \quad (94)$$

From Eq. (25), the top row is expanded to obtain:

$$M_{OO}\ddot{x}_O + M_{OB}\ddot{x}_B + K_{OO}x_O + K_{OB}x_B = F_O \quad (74)$$

Substituting Eq. (94) into Eq. (74) and simplifying, the equation of motion for the internal coordinates as a function of prescribed base displacement is obtained as follows:

$$[M_{OO} - M_{OB}M_{BB}^{-1}M_{BO}]\ddot{x}_O + [K_{OO} - M_{OB}M_{BB}^{-1}K_{BO}]x_O = F_O - [K_{OB} + M_{OB}M_{BB}^{-1}K_{BB}]x_B \quad (95)$$

Notice that the matrix that pre-multiplies the acceleration term has units of mass, and the matrix that pre-multiplies the displacement term has units of stiffness. The matrix that pre-multiplies the base displacement term has units of stiffness. Therefore, all terms of this equation of motion are dimensionally consistent with units of force.

The same modal decomposition procedures described in the base acceleration formulation apply to the base displacement formulation. Since the displacements at the base are prescribed, the base coordinates are no longer degrees of freedom. This means that there are no rigid body modes associated with the base displacement formulation. As a result, Eq. (89) is used to obtain the response of all coordinates. As in the base acceleration formulation, the time history of the base displacement is taken to be simple harmonic, and is represented by:

$$\{x_B\} = \{X_B\} \sin(\Omega t) \quad (96)$$

Numerical convergence examples are provided in the following section. Both examples are similar to the examples presented in the prescribed base acceleration problem.

1. Tip Deflection Calculation

The mast and antenna system was subjected to a base excitation where the time history of the displacement of the base coordinates was prescribed. The excitation was performed at a frequency which corresponded approximately to mode 5 (47.26 Hz) of the mast/antenna system. Since the system was modeled without damping, a frequency which corresponded exactly to a natural frequency of the system could not be prescribed. The

excitation frequency is equivalent to the mode 5 natural frequency to within 2 decimal places. As in the base acceleration problem, the frequency was arbitrarily selected. The tip deflection of the antenna was calculated and percent error in tip deflection was plotted versus percent of available component modes retained (see Figures 18 and 19). The calculations were performed twice. Mast modes were truncated in the first calculation, and antenna modes were truncated in the second calculation. All three procedures yielded accurate results in both the mast and antenna truncation tests. When the mast/antenna system was excited at mode 5, the Craig-Chang and MacNeal procedures provided very similar results for both the mast truncation and antenna truncation. As was determined in the tip deflection calculations of the base acceleration problem, the Craig-Bampton procedure yielded the best results using fewer modes than did the Craig-Chang and MacNeal procedures in both truncation tests. This again could possibly be due to the combination of fixed interface normal modes and static constraint modes providing a better representation of prescribed base displacement than the combination of free interface normal modes and residual flexibility modes. However, all three provided accurate results and at a cheaper cost than the FE model.

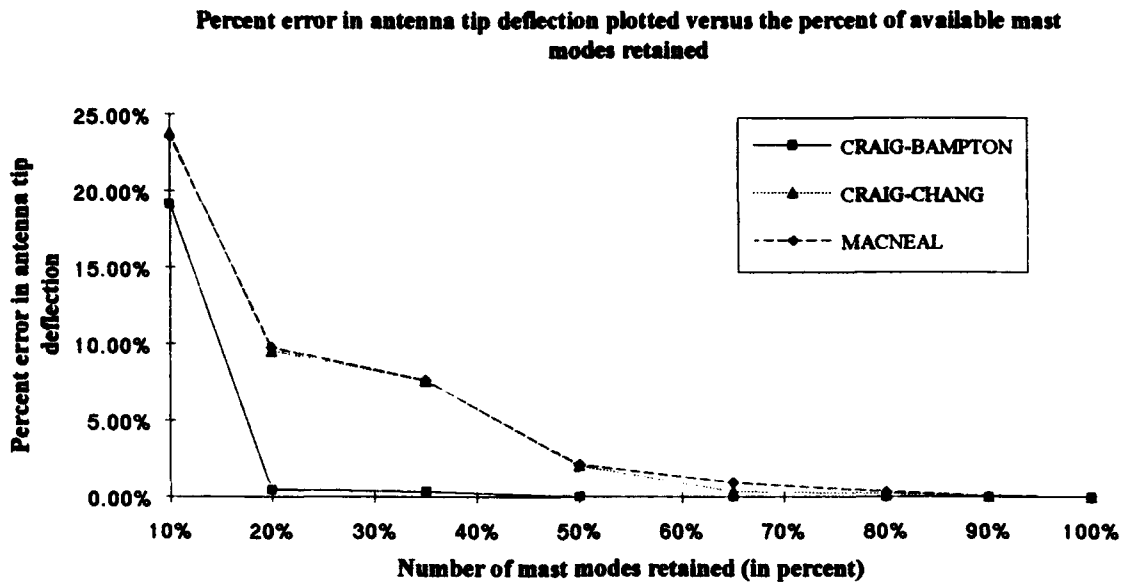


Figure 18: Percent Error in Antenna Tip Deflection Plotted Versus the Percent of Available Mast Modes Retained (Forcing Frequency: 47.26 Hz)

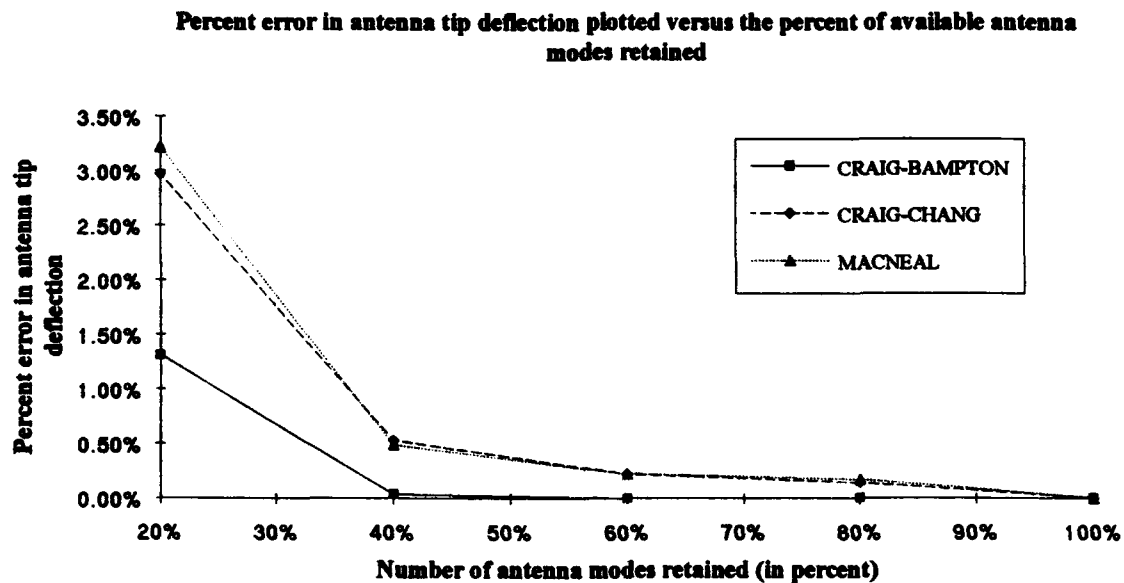


Figure 19: Percent Error in Antenna Tip Deflection Plotted Versus the Percent of Available Antenna Modes Retained. (Forcing Frequency: 47.26 Hz)

2. Moment and Shear Calculation

Percent error in shear and moment at the mast and antenna connection were plotted versus the percent of available component modes retained (see Figures 20-23). The base excitation was conducted again at 47.26 Hz. Similar results were obtained in the shear and moment calculations as were obtained in the tip deflection calculations. The Craig-Bampton procedure provided more accurate results using fewer modes than the Craig-Chang and MacNeal methods. The convergence rate of the Craig-Chang and MacNeal methods were almost identical in the mast mode truncation. When the mast was excited at mode 5, all three yielded excellent results in the antenna mode truncation analysis. However, the Craig-Bampton procedure converged more quickly than the other methods. It appears that the combination of fixed interface normal modes and static constraint modes lead to a higher rate of convergence in determining tip deflection and antenna/mast shear and moment calculations. Although all three procedures initially had a higher percentage error when truncating mast modes, than when truncating antennae modes, they all provide as accurate if not more accurate results than the antenna truncation at less cost in terms of computations. It is also noteworthy to compare the computational cost in retaining mast modes versus retaining antenna modes in predicting accurate system response. For example, in the shear calculation when the mast was excited at mode 5, the Craig-Chang procedure yielded a percentage error of 2.1% while using $1.66 \cdot 10^6$ FLOPS during the mast mode truncation test. During the antenna mode

truncation test, the Craig-Chang procedure yielded a percentage error of 2.03% using $1.89 \cdot 10^6$ FLOPS.

Since the impact of shock waves on the mast/antenna system are typically of low frequency, and as can be seen from the results of the prescribed base acceleration and base displacement examples provided, it is recommended that the Craig-Bampton component mode representation be used to synthesize the mast and antenna system

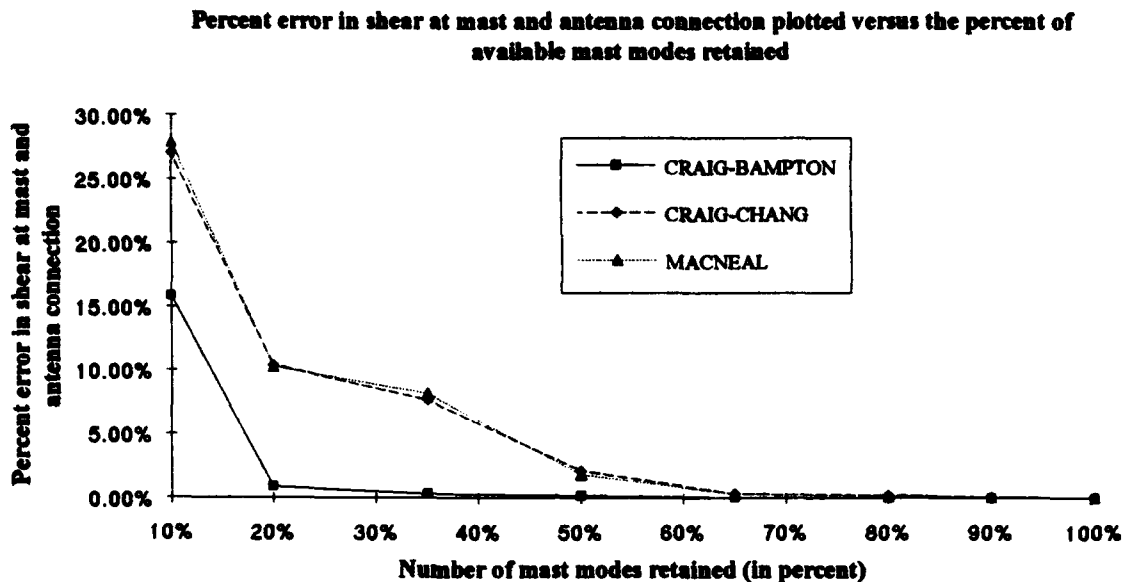


Figure 20: Percent Error in Shear at Mast and Antenna Connection Plotted Versus the Percent of Available Mast Modes Retained. (Forcing Frequency: 47.26 Hz)

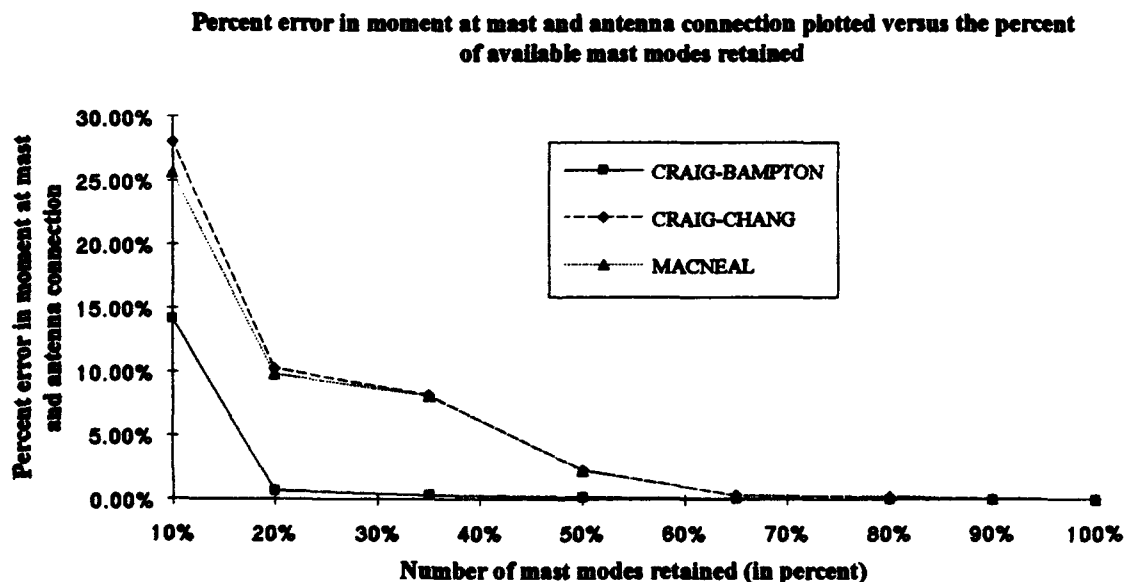


Figure 21: Percent Error in Moment at Mast and Antenna Connection Plotted Versus the Percent of Available Mast Modes Retained. (Forcing Frequency: 47.26 Hz)

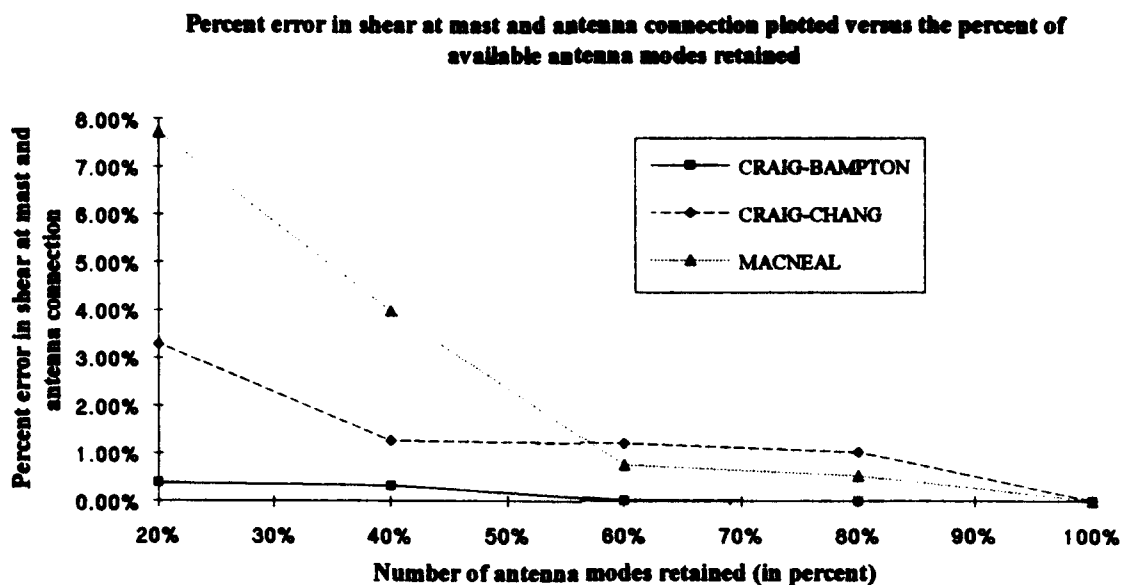


Figure 22: Percent Error in Shear at Mast and Antenna Connection Plotted Versus the Percent of Available Antenna Modes Retained. (Forcing Frequency: 47.26 Hz)

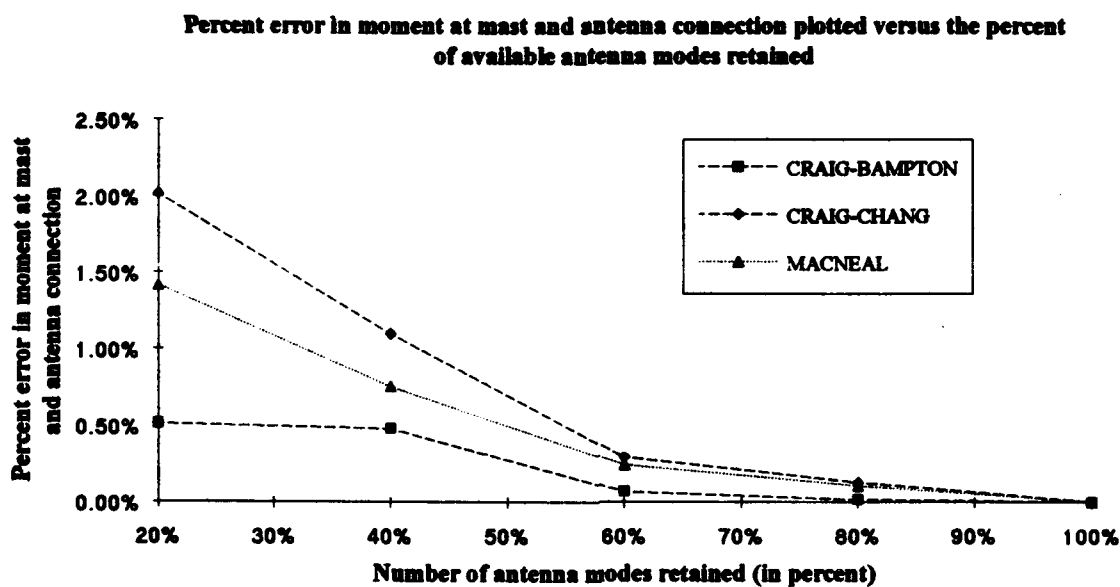


Figure 23: Percent Error in Moment at Mast and Antenna Connection Plotted Versus the Percent of Available Antenna Modes Retained. (Forcing Frequency: 47.26 Hz)

VI. CONCLUSIONS AND RECOMMENDATIONS

The survivability of shipboard combat systems equipment is paramount to the warfare fighting capability of the ship and her crew. Should a fire control radar, or any vital topside combat systems equipment fail as a result of an induced shock wave, the ship's war fighting capacity would be crippled. However, using proven structural dynamics techniques, the design engineer can design the mast/antenna system in such a manner as to minimize risk of failure.

This study has been conducted to show the progress that has been made thus far in the maximization of combat survivability of shipboard mast and antenna systems. As demonstrated in this study, the mast and antenna can be treated as *separate substructures*, and using CMS, can be assembled as a mast/antenna system, from which dynamic response to base excitation can be calculated. Treating each antenna as a substructure, allows the cataloging of the various antennae. A selected antenna can be "plugged" into various locations along the mast until a suitable dynamic response is obtained. As has been demonstrated herein, CMS along with FE modeling provides rapid and accurate results at a computational cost significantly less than standard FE modeling alone. The mast and antenna model used in this study consisted of only 17 elements which corresponds to a total of 51 degrees of freedom. Although the results that were obtained on this "small" model were accurate and computationally efficient, the same benefits can

be expected with larger models; models that will be used to represent realistic mast and antenna systems.

All three methods yield results that are accurate and more computationally efficient than standard FE modeling. However, from the results obtained, it is strongly recommended that the Craig-Bampton component mode representation be used to synthesize the mast and antenna system. Since the Craig-Bampton procedure yielded more accurate results while using fewer component modes than the other methods, the Craig-Bampton procedure is the substructure coupling formulation of choice due to good accuracy and ease of implementation. It is strongly suggested that the following recommendations be implemented when computing the dynamic response of a shipboard mast and antenna system:

- Modify the existing FE code such that the mast and antenna system can be modeled with 6 DOF/node. This type of modeling will allow for out of plane dynamic analysis. In addition to accommodating a more general analysis of the mast and antenna system, model the mast and antennae with other types of elements such as shell and plate elements in addition to the existing beam elements.
- Use CMS in conjunction with FE modeling. In particular, it is recommended that the Craig-Bampton procedure be used as the substructure coupling method. Additionally, if another software package which is tailored to FE analysis be used to conduct the dynamic analysis, the NASTRAN superelement scheme contains the

Craig-Bampton component mode representation as a solution path to dynamic analyses.

In this study it has been demonstrated that the mast and the various antennae can be modeled separately as substructures using standard FE modeling. Using component mode synthesis, the substructures can be assembled into a system and dynamic response computed accurately at a computational cost that is less than standard FE modeling alone. Implementing the above recommendations will lead to the maximization of topside combat systems equipment survivability.

APPENDIX A

```
% LT Lynn James Petersen
% Naval Postgraduate School
% Mast-Antenna Survivability: Structural Dynamic Design Analysis by Component Mode
% Synthesis
% Main Program: Progsynt.m
% This program numerically constructs a FE model of the either the "mast", the
% "antenna" as components or the mast and antenna as a system. The user specifies the
% desired configuration
% To begin the program, the user specifies the desired structure (i.e. the mast, or
% antenna, or mast/antenna system.)
```

```
p = input('enter which structure is to be assembled: enter 1 if mast/antenna,...
          enter 2 if mast, enter 3 if antenna');
if p == 1
    datdabe % data file for the mast/antenna system
elseif p==2
    data_mst % data file for the mast
```

```

else

    data_ant % data file for the antenna

end;

flops(0) % reset the FLOPS count

% A. Calculation of the number of elements, nodes, length of each element, radius of
gyration and orientation.

A1 = size(con); % "con" is the connectivity matrix

numel = A1(1); % number of elements

C1 = size(coord); % "coord" is the matrix of coordinates

nodes = C(1); % number of nodes

for i = 1:numel;

    IC = con(i,1);

    ID = con(i,2);

% determine the length of the respective beam element

l(1,i)=sqrt((coord(ID,1)-coord(IC,1))^2+(coord(ID,2)-coord(IC,2))^2);

DX(i)=coord(ID,1)-coord(IC,1);

DY(i)=coord(ID,2)-coord(IC,2);

```

% determine the orientation of the beam element

if DX(i)>= 0 & DY(i)>= 0;

theta(1,i)=acos(DX(i)/l(1,i));

elseif DX(i)<0 & DY(i)>=0;

theta(1,i)=acos(DY(i)/l(1,i))+pi/2;

elseif DX(i)<0 & DY(i)<0;

theta(1,i)=acos(abs(DX(i))/l(1,i))+pi;

else

theta(1,i)=acos(abs(DY(i))/l(1,i))+(3*pi/2);

end;

% calculate the radius of gyration

r(1,i) = sqrt(I(1,i)/A(1,i));

end;

% B. Computer truncation error minimization

% The function trig will now be called to ensure that “exact” values are sent to the

% stiffness and mass matrix function.

[c1,s1]=trig(theta,numel);

% C. Assembly of stiffness and mass matrices:

% The function "El3mk.m" will be called to assemble the elemental mass and stiffness matrices.

% The "global" mass and stiffness matrices will be assembled simultaneously

kb1 = [zeros(nodes * 3, nodes * 3)];

mb1 = [zeros(nodes * 3, nodes * 3)];

for i=1:numel;

[ke,me]=el3mk(l(i),gamma(i),I(i),E(i),r(i),c1(i),s1(i));

v=con(i,1);

w=con(i,2);

kb1(3*v-2:3*v,3*v-2:3*v) = kb1(3*v-2:3*v,3*v-2:3*v) + ke(1:3,1:3);

kb1(3*v-2:3*v,3*w-2:3*w) = kb1(3*v-2:3*v,3*w-2:3*w) + ke(1:3,4:6);

kb1(3*w-2:3*w,3*v-2:3*v) = kb1(3*w-2:3*w,3*v-2:3*v) + ke(4:6,1:3);

kb1(3*w-2:3*w,3*w-2:3*w) = kb1(3*w-2:3*w,3*w-2:3*w) + ke(4:6,4:6);

mb1(3*v-2:3*v,3*v-2:3*v) = mb1(3*v-2:3*v,3*v-2:3*v) + me(1:3,1:3);

mb1(3*v-2:3*v,3*w-2:3*w) = mb1(3*v-2:3*v,3*w-2:3*w) + me(1:3,4:6);

mb1(3*w-2:3*w,3*v-2:3*v) = mb1(3*w-2:3*w,3*v-2:3*v) + me(4:6,1:3);

mb1(3*w-2:3*w,3*w-2:3*w) = mb1(3*w-2:3*w,3*w-2:3*w) + me(4:6,4:6);

end;

% D. Boundary conditions

kb1([BC],:)= [];

kb1(:,[BC])=[];

mb1([BC],:)= [];

mb1(:,[BC])=[];

% E. Internal and base coordinates

if p == 1; % mast and antenna system

% partition the mass and stiffness matrices into base and internal coordinates

[KEX,MEX,FEX]=kmbe(kb1,mb1,INTM,BSM,XBM);

kb1=KEX;

mb1=MEX;

% convert the force vector into a product of mass * acceleration

% because of MATLAB'S inefficiency in calculating rigid body eigenvalues and

% eigenvectors (natural frequencies and mode shapes) we will make the first three natural

% frequencies 0, and calculate rigid body modes just as was done in the Craig-Chang

% formulation

P = [1 2 3];

F = [4:length(kb1)];

KEX2 = [KEX(F,F) KEX(F,P);KEX(P,F) KEX(P,P)];

MEX2= [MEX(F,F) MEX(F,P);MEX(P,F) MEX(P,P)];

```

KEX3=KEX(F,F);

KEX4=KEX(F,P);

RBMODES= [-inv(KEX3)*(KEX4)

           eye(length(P))];

% calculate the natural frequencies and mode shapes

[lamex,phiex]=fmodes(KEX2,MEX2);

for i=1:3;

    lamex(i,1)=0; % make first three natural frequencies equal to zero

end;

lamex;

omeg=sqrt(lamex)/(2*pi)

phiex(:,1:3)=RBMODES;

b2=3;

[phrb] = rigid(MEX2,phiex,b2);

% check orthogonality

phiex(:,1:3)=phrb;

tu=phiex(:,1:3)'*MEX2*phiex(:,1:3);

modstiff=phiex(:,1:3)'*KEX2*phiex(:,1:3);

flops % determine FLOPS of FE formulation and solution

save data3.mat kb1 mb1 coord con lamex phiex BS INT XB fFEX

```

```

    save data3a.mat c1 s1 l r

elseif p==2      % mast substructure

    [KEX,MEX,FEX]=kmbe(kb1,mb1,INTM,BSM,XBM);

    kb1=KEX;

    mb1=MEX;

% convert the force vector into a product of mass * acceleration

% note: this operation needs to be performed now prior to CMS

%      fl = f - (- (8.9525*2*pi)^2*FEX);  % low frequency

%      fl = f + (219.265*2*pi)^2*FEX; % high frequency

flops      % determine the flops count to assemble the mast

save data1.mat kb1 mb1 V C coord con INT O fl XBM BSM

save data1a.mat c1 s1 l r

else;

    fl=f

    flops      % determine the flops count to assemble the antenna

    save data2.mat kb1 mb1 O INT coord con f V C

    save data2a.mat c1 s1 l r

end;

```

APPENDIX B

```
% LT Lynn James Petersen
% Naval Postgraduate School
% Mast-Antenna Survivability: Structural Dynamic Design Analysis by Component
% Mode Synthesis
% Program: Cbfbx.m
% Two substructure synthesis with forcing vector and base excitation
% This program uses the Craig-Bampton method for synthesizing structures together.
% The program loads the data files into the program. Once into the program, the program
% will synthesize the structures together, and calculate the coupled natural frequency and
% free interface mode shapes
% note: this program will synthesize only two structures together
% A. The substructures will now be loaded
    load data1.mat;
    k1=kb1,m1=mb1,V1=V,C1=C,f1=f1;
    load data2.mat;
    k2=kb1,m2=mb1,V2=V,C2=C,f2=f;
flops(0) % reset the FLOPS count
```


% B. K matrix partitioning to support calculation of static constraint modes

Kvv1 = k1(V1,V1);

Kvc1 = k1(V1,C1);

Kvv2 = k2(V2,V2);

Kvc2 = k2(V2,C2);

% C. Partition stiffness and mass matrices for synthesis:

k1=[k1(V1,V1) k1(V1,C1);k1(C1,V1) k1(C1,C1)];

m1=[m1(V1,V1) m1(V1,C1);m1(C1,V1) m1(C1,C1)];

k2=[k2(V2,V2) k2(V2,C2);k2(C2,V2) k2(C2,C2)];

m2=[m2(V2,V2) m2(V2,C2);m2(C2,V2) m2(C2,C2)];

% D. Calculate static constraint modes:

Cmodes1 = [-inv(Kvv1)*Kvc1

eye(length(C1))];

Cmodes2 = [-inv(Kvv2)*Kvc2

eye(length(C2))];

% E. Calculate the fixed interface normal modes.

kfix1=k1(1:length(V1),1:length(V1));

mfix1=m1(1:length(V1),1:length(V1));

kfix2=k2(1:length(V2),1:length(V2));

mfix2=m2(1:length(V2),1:length(V2));

[lam1,Nmodes1]=fmodes(kfix1,mfix1),pause

```

% F. Note: the next command retains the desired modes and appends zeros to the
% interface coordinates:

    y = input('Enter the number of fixed interface modes that are desired to be kept')

    [Nmodes1] = [Nmodes1(:,1:y);zeros(3,y)];

% G. Obtain natural frequencies and mode shapes for the second substructure

    [lam2,Nmodes2]=fmodes(kfix2,mfix2),pause

% H. Note: the next command retains the desired modes and appends zeros to the
% interface coordinates for the second structure

    s = input('Enter number of modes desired to be retained for second structure')

    [Nmodes2] = [Nmodes2(:,1:s);zeros(3,s)];

% I. Obtain the "reduction" transformation matrix from the fixed interface normal
% modes and static constraint modes:

    [NC_MODES1] = [Nmodes1 Cmodes1];

    [NC_MODES2] = [Nmodes2 Cmodes2];

% J. Obtain the reduced mass and stiffness matrices:

    k1_red = NC_MODES1' * k1 * NC_MODES1;

    m1_red = NC_MODES1' * m1 * NC_MODES1;

    k2_red = NC_MODES2' * k2 * NC_MODES2;

    m2_red = NC_MODES2' * m2 * NC_MODES2;

    a = length(C1);

    b = length(C2);

    d = length(V1);

```

```

    e = length(V2);

    size1 = length(k1_red);

    size2 = length(k2_red);

% K. Form the uncoupled stiffness and mass matrices:

    K_uncpl = [k1_red zeros(size1,size2);zeros(size2,size1) k2_red];

    M_uncpl = [m1_red zeros(size1,size2);zeros(size2,size1) m2_red];

% L. Place the force vector in the correct form and pre multiply by the transformation
matrix:

    f1=[f1(V1,1);f1(C1,1)];

    f2=[f2(V2,1);f2(C2,1)];

    F1V = Nmodes1(1:d,1:y)*f1(1:d,1);

    F1C = Cmodes1(1:d,1:a)*f1(1:d,1) + f1(d+1:length(f1),1);

    F2V = Nmodes2(1:e,1:s)*f2(1:e,1);

    F2C = Cmodes2(1:e,1:b)*f2(1:e,1) + f2(e+1:length(f2),1);

    FCB = [ F1V;

            F2V;

            F1C+F2C];

% M. Form the coupled stiffness and mass matrices:

    K_cpl = zeros(y+s+a,y+s+a);

    g=length(K_cpl);

```

```

% structure 1: diagonal

K_cpl(1:y,1:y)=K_cpl(1:y,1:y)+K_uncpl(1:y,1:y);

% structure 2: diagonal

K_cpl(y+1:y+s,y+1:y+s)=K_cpl(y+1:y+s,y+1:y+s)+...
K_uncpl(y+a+1:y+a+s,y+a+1:y+a+s);

% structure 1&2: connection

K_cpl(y+s+1:y+s+a,y+s+1:y+s+a)=K_cpl(y+s+1:y+s+a,y+s+1:y+s+a)+...
K_uncpl(y+1:y+a,y+1:y+a)+K_uncpl(y+a+s+1:y+s+a+b,y+a+s+1:y+s+a+b);

% mass matrix

M_cpl = zeros(y+s+a,y+s+a);

h=length(M_cpl);

g=h;

% structure 1: diagonal

M_cpl(1:y,1:y)=M_cpl(1:y,1:y)+M_uncpl(1:y,1:y);

% structure 2: diagonal

M_cpl(y+1:y+s,y+1:y+s)=M_cpl(y+1:y+s,y+1:y+s)+...
M_uncpl(y+a+1:y+a+s,y+a+1:y+a+s);

% structure 1&2: diagonal

M_cpl(y+s+1:y+s+a,y+s+1:y+s+a)=M_cpl(y+s+1:y+s+a,y+s+1:y+s+a)+...
M_uncpl(y+1:y+a,y+1:y+a)+M_uncpl(y+a+s+1:y+s+a+b,y+a+s+1:y+s+a+b);

% structure 1: off diagonal partitions

M_cpl(y+s+1:y+s+a,1:y)=M_cpl(y+s+1:y+s+a,1:y)+M_uncpl(y+1:y+a,1:y);

```

```

M_cpl(1:y,y+s+1:y+s+a)=M_cpl(1:y,y+s+1:y+s+a)+M_uncpl(1:y,y+1:y+a);

% structure 2: off diagonal partitions

M_cpl(y+s+1:y+s+b,y+1:y+s)=M_cpl(y+s+1:y+s+b,y+1:y+s)+...

M_uncpl(y+a+s+1:y+a+s+b,y+a+1:y+a+s);

M_cpl(y+1:y+s,y+s+1:y+s+b)=M_cpl(y+1:y+s,y+s+1:y+s+b)+...

M_uncpl(y+a+1:y+a+s,y+a+s+1:y+a+s+b);

% N. Obtain the C-B component mode synthesized eigenvectors and eigenvalues:

[lam_cpl,phi_cpl] = fmodes(K_cpl,M_cpl);

omeg_cb=sqrt(lam_cpl)/(2*pi); % convert from (rad/sec)^2 to Hz

% P. Perform transformation to support base excitation calculation, clean up first three

% natural frequencies, and first three modes

P=[length(K_cpl)-2:length(K_cpl)];

F=[1:length(K_cpl)-3];

KEX2=[K_cpl(F,F) K_cpl(F,P); K_cpl(P,F) K_cpl(P,P)];

MEX2=[M_cpl(F,F) M_cpl(F,P); M_cpl(P,F) M_cpl(P,P)];

KEX3=K_cpl(F,F);

KEX4=K_cpl(F,P);

Rbmodes=[-inv(KEX3)*(KEX4)

eye(length(P))];

[lamex,phiex]=fmodes(KEX2,MEX2);

```

```

for i=1:3;

    lamex(i,1)=0;

end;

phiex(:,1:3)=Rbmodes;

b2=3;

[phrb]=rigid(MEX2,phiex,b2); % perform Gram-Schmidt orthogonalization

phiex(:,1:3)=phrb;

% check orthogonalization:

tu=phiex(:,1:3)*MEX2*phiex(:,1:3),pause

tk=phiex(:,1:3)*KEX2*phiex(:,1:3),pause

% redefine variables

K_cpl=KEX2;

M_cpl=MEX2;

lam_cpl=lamex;

phi_cpl=phiex;

flops          % determine the FLOPS

save data10.mat K_cpl M_cpl FCB a b d e y s NC_MODES1 NC_MODES2

               lam_cpl phi_cpl

```

APPENDIX C

```
% LT Lynn James Petersen
% Naval Postgraduate School
% Mast-Antenna Survivability: Structural Dynamic Design Analysis by Component Mode
% Synthesis
% Program: Ccfrb2.m
% This program is written in accordance with the Craig-Chang Residual Flexibility
% method. The program loads two data files containing information from a FE
% generated substructure. This information includes: a) the mass and stiffness matrices b)
% listing of internal and interface coordinates c) any forcing or base excitation data
% needed to solve a dynamic response problem. The program is ready to load the two
% data files into the work space

clear

    load data1.mat          % mast data

    K1=kb1, M1=mb1, O1=O, I1 = INT, R1=I1, F1 = f1

    load data2.mat          % antenna data

    K2=kb1, M2=mb1, O2=O, I2 = INT, R2=I2, F2 = f

flops(0)    reset the flops count to zero

% A .    Substructure 1

% Partition substructure 1 into internal and interface coordinates
```

```

Kool = K1(O1,O1);

Korl = K1(O1,R1);

K1=[K1(O1,O1) K1(O1,I1); K1(I1,O1) K1(I1,I1)];

M1=[M1(O1,O1) M1(O1,I1); M1(I1,O1) M1(I1,I1)];

% B. Calculate natural "free interface normal modes" for structure 1

[lam1,FRmodes1] = fmodes(K1,M1)

a1 = length(O1);

b1 = length(I1);

a = size(FRmodes1);

b = a(2);

for i=1

    lam1(i,1)=0; %make first three "zero" natural frequencies equal zero to

% correspond to R.B.

end;

% C. Prompt the user for the number of normal modes desired to be kept

% note: the number of total modes equals the sum of kept modes and deleted modes

c = input('enter the number of free interface normal modes desired to be kept for...

structure 1 ')

FRKmodes1 = [FRmodes1(:,b1+1:c)];% kept modes

FRDmodes1 = [FRmodes1(:,c+1:b)]; % deleted modes

lam1a=diag(lam1);

lamk1=lam1a(b1+1:c,b1+1:c);

```



```

lamd1=lam1a(c+1:b,c+1:b);

invlamk1=inv(lamk1);

invlamd1=inv(lamd1);

% D. Obtain the rigid body modes like constraint modes were calculated

RBmodes1 = [-inv(Koo1)*Kor1

              eye(length(R1))];

% unity mass normalize and orthogonalize the rigid body modes Note: since rigid
% body modes as calculated by matlab are not orthogonal wrt mass matrix, a "Gram
% Schmidt" procedure needs to be performed

[phrb] = rigid(M1,RBmodes1,b1)

RBmodes1 = phrb;

% E. Form the projection matrix [P] in support of the inertia relief solution

P1=[eye(a1+b1) - M1*RBmodes1*RBmodes1'];

GSTAR1 = inv(Koo1);

GBSTAR1 = zeros(a1+b1,a1+b1);

GBSTAR1(1:a1,1:a1) = GBSTAR1(1:a1,1:a1) + GSTAR1;

FA1 = [zeros(a1,b1);eye(b1,b1),];

% F. Obtain the inertia relief residual flexibility modes

GFLEX1 = P1'*GBSTAR1*P1;

% as calculated from kept normal modes

% IRAmodes1 = [GFLEX1 - FRKmodes1*invlamk1*FRKmodes1']*FA1;

% as calculated from deleted normal modes

```

```

%   IRAmodes1 = (FRDmodes1*invlamd1*FRDmodes1')*FA1;
%   Rmodes1A=IRAmodes1;
%   Note: because this code is tailored to rigid body for both structures an inertia
%   relief solution is being performed for both structures the following code would
%   apply if the first structure was fully restrained
%   Partition the normal modes into kept modes and deleted modes
%       FRKmodes1 = [FRmodes1(:,1:c)];
%       FRDmodes1 = [FRmodes1(:,c+1:b)];
%   Diagonalize and partition into kept and deleted natural frequencies
%       lam1a=diag(lam1);
%       lamk1=lam1a(1:c,1:c);
%       lamd1=lam1a(c+1:b,c+1:b);
%       invlamk1 = inv(lamk1);
%       invlamd1 = inv(lamd1);
%   D. Obtain the residual flexibility modes
%   Obtain the flexibility matrix
%       G1 = inv(K1);
%       FA1 = [zeros(a1,b1);eye(b1,b1)];
%   Obtain the residual flexibility modes from the kept modes
%       Rmodes = (G1 - FRKmodes1*invlamk1*FRKmodes1')*Fa;
%   from the deleted modes
%       Rmodes = (FRDmodes1*invlamd1*FRDmodes1')*FA1;

```

```

% E. Calculate the reduced mass and stiffness matrices for structure 1 transformation

%   matrix (SYSMODES1): [T]

%   SYSmodes1 = [FRKmodes1 Rmodes];

%   KSYS1 = SYSmodes1'*K1*SYSmodes1

%   MSYS1 = SYSmodes1'*M1*SYSmodes1

% II. Substructure 2

% A. Partition substructure one into internal and interface coordinates

      Koo2 = K2(O2,O2);

      Kor2 = K2(O2,R2);

      K2=[K2(O2,O2) K2(O2,R2); K2(R2,O2) K2(R2,R2)];

      M2=[M2(O2,O2) M2(O2,R2); M2(R2,O2) M2(R2,R2)];

% B. Calculate natural "free interface normal modes" for structure 1

      [lam2,FRmodes2] = fmodes(K2,M2)

      a2 = length(O2);

      b2 = length(I2)

      d = size(FRmodes2);

      e = d(2);

      for i=1:b2;

          lam2(i,1)=0;

      end;

```

% C. Prompt the user for the number of normal modes desired to be kept.

```
f = input('enter the number of free interface normal modes desired to be kept for  
structure 2 ');
```

```
FRKmodes2 = [FRmodes2(:,b2+1:f)];
```

```
FRDmodes2 = [FRmodes2(:,f+1:e)];
```

```
lam2a=diag(lam2);
```

```
lamk2=lam2a(b2+1:f,b2+1:f);
```

```
lamd2=lam2a(f+1:e,f+1:e);
```

```
invlamk2=inv(lamk2);
```

```
invlamd2=inv(lamd2);
```

% D. Obtain the rigid body modes as constraint modes would be obtained

```
RBmodes2 = [-inv(Koo2)*Kor2
```

```
eye(length(R2))];
```

% unity mass normalize and orthogonalize the rigid body modes

```
[phrb] = rigid(M2,RBmodes2,b2) % Gram-Schmidt
```

```
RBmodes2 = phrb;
```

% E. Form the projection matrix [p] in support of the inertia relief solution

```
P2=[eye(a2+b2) - M2*RBmodes2*RBmodes2'];
```

```
GSTAR2 = inv(Koo2);
```

```
GBSTAR2 = zeros(a2+b2,a2+b2);
```

```
GBSTAR2(1:a2,1:a2) = GBSTAR2(1:a2,1:a2) + GSTAR2;
```

```
FA2 = [zeros(a2,b2);eye(b2,b2),];
```

```

% F. Obtain the inertia relief residual flexibility modes...

GFLEX2 = P2'*GBSTAR2*P2;

% ...from the kept modes

%   IRAmodes2 = [GFLEX2 - FRKmodes2*invlamk2*FRKmodes2']*FA2;

%...or from the deleted modes

%   IRAmodes2 = (FRDmodes2*invlamd2*FRDmodes2')*FA2;

% G. Calculate the reduced mass and stiffness matrices for structure 1 transformation

%   matrix [T]

%   SYSmodes2 = [FRKmodes2 IRAmodes2];

%   XSYS2 = SYSmodes2'*K2*SYSmodes2

%   MSYS2= SYSmodes2'*M2*SYSmodes2

% H. Couple the two substructures.

    k1 = [IRAmodes1(a1+1:a1+b1,:) + IRAmodes2(a2+1:a2+b2,:)];

    k2=inv(k1);

    mdd1 = FRDmodes1(a1+1:a1+b1,:)*(invlamd1)^2*(FRDmodes1(a1+1:a1+b1,:))';

    mdd2 = FRDmodes2(a2+1:a2+b2,:)*(invlamd2)^2*(FRDmodes2(a2+1:a2+b2,:))';

    m1 = k2*(mdd1+mdd2)*k2;

% Rebuild the kept normal modes to include rigid body modes and elastic modes and

% kept natural frequencies

    FRKmodes1 = [RBmodes1 FRKmodes1];

    FRKmodes2 = [RBmodes2 FRKmodes2];

    lamk1=lam1a(1:c,1:c);

```

```

lamk2=lam2a(1:f,1:f);

% I. Build the system mass and stiffness matrices

MSYST = zeros(c+f,c+f);

MSYST(1:c,1:c) = MSYST(1:c,1:c) + eye(c,c)+...
    (FRKmodes1(a1+1:a1+b1,:))'*m1*FRKmodes1(a1+1:a1+b1,:);

MSYST(1:c,c+1:c+f) = MSYST(1:c,c+1:c+f) +...
    (-FRKmodes1(a1+1:a1+b1,:))'*m1*FRKmodes2(a2+1:a2+b2,:);

MSYST(c+1:c+f,1:c) = MSYST(1:c,c+1:c+f)';

MSYST(c+1:c+f,c+1:c+f) = MSYST(c+1:c+f,c+1:c+f)+eye(f,f)+...
    (FRKmodes2(a2+1:a2+b2,:))'*m1*FRKmodes2(a2+1:a2+b2,:);

KSYST = zeros(c+f,c+f);

KSYST(1:c,1:c) = KSYST(1:c,1:c) + lamk1 +
    (FRKmodes1(a1+1:a1+b1,:))'*k2*FRKmodes1(a1+1:a1+b1,:);

KSYST(1:c,c+1:c+f) = KSYST(1:c,c+1:c+f) +
    (-FRKmodes1(a1+1:a1+b1,:))'*k2*FRKmodes2(a2+1:a2+b2,:);

KSYST(c+1:c+f,1:c) = KSYST(1:c,c+1:c+f)';

KSYST(c+1:c+f,c+1:c+f) = KSYST(c+1:c+f,c+1:c+f) + lamk2 +
    (FRKmodes2(a2+1:a2+b2,:))'*k2*FRKmodes2(a2+1:a2+b2,:);

% J. DETERMINE THE CRAIG CHANG FORCE VECTOR

SYSmodes1 = [FRKmodes1 IRAmodes1];

SYSmodes2 = [FRKmodes2 IRAmodes2];

F1=[F1(O1,1);F1(I1,1)];

```

```

F2=[F2(O2,1);F2(I2,1)];

FCC1 = SYSmodes1'*F1;

FCC2 = SYSmodes2'*F2;

% Determine the second transformation matrix

% Note: since the final system mass and stiffness matrices partitions are known, this
% transformation matrix need not be used to build the system mass and stiffness matrices

T2 = [-k1*FRKmodes1(a1+1:a1+b1,1:c) k1*FRKmodes2(a2+1:a2+b2,1:f);
       k1*FRKmodes1(a1+1:a1+b1,1:c) -k1*FRKmodes2(a2+1:a2+b2,1:f);
       eye(c,c)                zeros(c,f);
       zeros(f,c)              eye(f,f)];

% determine the system Craig Chang force vector repartition the force vector

FCC1A=FCC1(c+1:c+b1,1);

FCC1B=FCC1(1:c,1);

FCC2A=FCC2(f+1:f+b2,1);

FCC2B=FCC2(1:f,1);

FCC1 =      [FCC1A;
              FCC2A;
              FCC1B;
              FCC2B];

FCC = T2'*FCC1;

% note: since the calculated system is not restrained, the following commands clean up
% the rigid body modes

```

```

P=[1:3];

F=[4:length(KSYST)];

KEX2=[KSYST(F,F) KSYST(F,P); KSYST(P,F) KSYST(P,P)];

MEX2=[MSYST(F,F) MSYST(F,P); MSYST(P,F) MSYST(P,P)];

KEX3=KSYST(F,F);

KEX4=KSYST(F,P);

Rbmodes=[-inv(KEX3)*(KEX4

            eye(length(P)))]];

[lamex,phiex]=fmodes(KEX2,MEX2);

    for i=1:3;

        lamex(i,1)=0;

    end;

    phiex(:,1:3)=Rbmodes;

    b2=3;

    [phrb]=rigid(MEX2,phiex,b2); %Gram-Schmidt

    phiex(:,1:3)=phrb;

    tu=phiex(:,1:3)'*MEX2*phiex(:,1:3),pause %orthogonality

    tk=phiex(:,1:3)'*KEX2*phiex(:,1:3),pause

    fc=size(FCC);

    fc1=fc(1,1);

    FCC= [FCC(4:fc1,1);

            FCC(1:3,1)];

```



```

KSYST=KEX2;

MSYST=MEX2;

lam_ccrf=lamex;

phi_ccrf=phiex;

omega_ccrf=sqrt(lam_ccrf)/(2*pi);

omega=omega_ccrf

flops    % determine total FLOPS

save data5.mat lam_ccrf phi_ccrf MSYST KSYST FCC SYSmodes1...

        SYSmodes2 T2 a1 a2 b1 b2 f c XBM

```

APPENDIX D

```
% LT Lynn James Petersen

% Naval Postgraduate School

% Mast-Antenna Survivability. Structural Dynamic Design Analysis by Component Mode
% Synthesis

% Program:Mrfrb2.m

% This program is written in accordance with the MacNeal residual flexibility method.

% The program loads two data files containing information from an FE generated
% substructure this information includes: a) the mass and stiffness matrices b) listing of
% internal and interface coordinates c) any forcing or base excitation data needed to solve
% a dynamic response problem. The program is ready to load the two data files into the
% work space

    load data1.mat          % mast data

    K1=kb1, M1=mb1, O1=O, I1 = INT, R1 = I1, F1=f1

    load data2.mat          % antennae data

    K2=kb1, M2=mb1, O2=O, I2 = INT, R2 = I2, F2=f

    flops(0); % zero out the FLOPS count

% I. Substructure 1

% A. Partition substructure one into internal and interface coordinates

    Kool=K1(O1,O1);
```

```

    Kor1=K1(O1,R1);

    K1=[K1(O1,O1) K1(O1,I1);K1(I1,O1) K1(I1,I1)];

    M1=[M1(O1,O1) M1(O1,I1);M1(I1,O1) M1(I1,I1)];

%   B. Calculate natural "free interface normal modes" for structure 1

    [lam1,FRmodes1] = fnodes(K1,M1);

    a1 = length(O1);

    b1 = length(I1);

    a = size(FRmodes1);

    b = a(2);

    for i=1:b1;

        lam1(i,1)=0;           % for rigid body modes only

    end;

%   C. Prompt the user for the number of normal modes desired to be kept.

    c = input('enter the number of free interface normal modes desired to be kept for...
              structure 1 ')

%   Partition the normal modes into kept modes and deleted modes

    FRKmodes1 = [FRmodes1(:,b1+1:c)];

    FRDmodes1 = [FRmodes1(:,c+1:b)];

    lam1a=diag(lam1);

    lamk1=lam1a(b1+1:c,b1+1:c);

    lamd1=lam1a(c+1:b,c+1:b);

    invlamk1=inv(lamk1);

```

```

    invlamd1=inv(lamd1);

% D. Obtain the rigid body modes as static constraint modes would be obtained

    RBmodes1 = [-inv(Kool)*Kor1
                eye(length(R1))];

% unity mass normalize and orthogonalize the rigid body modes

    [phrb] = rigid(M1,RBmodes1,b1);    %Gram-Schmidt
    RBmodes1 = phrb;

% E. Form the projection matrix [P] in support of the inertia relief solution

    P1=[eye(a1+b1) - M1*RBmodes1*RBmodes1'];

    GSTAR1 = inv(Kool);

    GBSTAR1 = zeros(a1+b1,a1+b1);

    GBSTAR1(1:a1,1:a1) = GBSTAR1(1:a1,1:a1) + GSTAR1;

    FA1 = [zeros(a1,b1);eye(b1,b1)];

% F. Obtain the residual flexibility modes...

    GFLEX1 = P1'*GBSTAR1*P1;

% ...from the kept modes

%   IRAmodes1 = [GFLEX1 - FRKmodes1*invlamk1*FRKmodes1']*FA1;

% ...from the deleted modes

%   IRAmodes1 = (FRDmodes1*invlamd1*FRDmodes1')*FA1;

% Note: this code is tailored to a synthesis of a free-free structure to a free-free structure
% (i.e. mast & antennae to support base acceleration formulation)

% the following code applies if the first structure was fully restrained

```

```

%      FRKmodes1 = [FRmodes1(:,1:c)];
%      FRDmodes1 = [FRmodes1(:,c+1:b)];
%      Diagonalize and partition into kept and deleted natural frequencies
%      lam1a=diag(lam1);
%      lamk1=lam1a(1:c,1:c);
%      lamd1=lam1a(c+1:b,c+1:b);
%      invlamk1 = inv(lamk1);
%      invlamd1 = inv(lamd1);
%      D. Obtain the residual flexibility modes...
%      Obtain the flexibility matrix
%      G1 = inv(K1);
%      FA1 = [zeros(a1,b1);eye(b1,b1)];
%      ...from the kept modes
%      Rmodes = (G1 - FRKmodes1*invlamk1*FRKmodes1')*Fa;
%      ...from the deleted modes
%      Rmodes = (FRDmodes1*invlamd1*FRDmodes1')*FA1;
%      E. Calculate the reduced mass and stiffness matrices for structure 1
%      Note: since the partitions of the system mass and stiffness matrices are known, the
%      following calculations need not be performed.
%      Transformation matrix (SYSMODES1): [T]
%      SYSmodes1 = [FRKmodes1 Rmodes];
%      KSYS1 = SYSmodes1'*K1*SYSmodes1;

```

```

%   MSYS1 = SYSmodes1'*M1*SYSmodes1;

% II. Substructure 2

%   A.   Partition substructure two into internal and interface coordinates

        Koo2 = K2(O2,O2);

        Kor2 = K2(O2,R2);

        K2=[K2(O2,O2) K2(O2,R2); K2(R2,O2) K2(R2,R2)];

        M2=[M2(O2,O2) M2(O2,R2); M2(R2,O2) M2(R2,R2)];

%   B. Calculate natural "free interface normal modes" for structure 2

        [lam2,FRmodes2] = fmodes(K2,M2)

        a2 = length(O2);

        b2 = length(I2);

        d = size(FRmodes2);

        e = d(2);

        for i=1:b2

            lam2(i,1)=0;   % rigid body modes only

        end;

%   C. Prompt the user for the number of normal modes desired to be kept

        f = input('enter the number of free interface normal modes desired to be kept for...

            structure 2 ')

        FRKmodes2 = [FRmodes2(:,b2+1:f)];

        FRDmodes2 = [FRmodes2(:,f+1:e)];

        lam2a=diag(lam2);

```

```

lamk2=lam2a(b2+1:f,b2+1:f);

lamd2=lam2a(f+1:e,f+1:e);

invlamk2=inv(lamk2);

invlamd2=inv(lamd2);

% D. Obtain the rigid body modes as constraint modes would be obtained

RBmodes2 = [-inv(Koo2)*Kor2
             eye(length(R2))];

% unity mass normalize and orthogonalize the rigid body modes

[phrb] = rigid(M2,RBmodes2,b2); % Gram-Schmidt

RBmodes2 = phrb;

% E. Form the projection matrix [P] in support of the inertia relief solution

P2=[eye(a2+b2) - M2*RBmodes2*RBmodes2'];

GSTAR2 = inv(Koo2);

GBSTAR2 = zeros(a2+b2,a2+b2);

GBSTAR2(1:a2,1:a2) = GBSTAR2(1:a2,1:a2) + GSTAR2;

FA2 = [zeros(a2,b2);eye(b2,b2)];

% F. Obtain the residual flexibility modes...

GFLEX2 = P2'*GBSTAR2*P2;

% ...from the kept modes

%      IRAmodes2 = [GFLEX2 - FRKmodes2*invlamk2*FRKmodes2']*FA2;

% ...from the deleted modes

%      IRAmodes2 = (FRDmodes2*invlamd2*FRDmodes2')*FA2;

```

```

% G. Calculate the reduced mass and stiffness matrices for structure 1 transformation
%     matrix [T]
%     SYSmodes2 = [FRKmodes2 IRAmodes2];
%     KSYS2 = SYSmodes2'*K2*SYSmodes2; % note: since final matrix is known,
%     these calculations are not required
%     MSYS2= SYSmodes2'*M2*SYSmodes2;
% H. Couple the two systems.
%
%     k1 = [IRAmodes1(a1+1:a1+b1,:) + IRAmodes2(a2+1:a2+b2,:)];
%
%     k2=inv(k1);
%
% Rebuild the kept normal modes to include rigid body modes and elastic modes and kept
% natural frequencies
%
%     FRKmodes1 = [RBmodes1 FRKmodes1];
%     FRKmodes2 = [RBmodes2 FRKmodes2];
%
%     lamk1=lam1a(1:c,1:c);
%     lamk2=lam2a(1:f,1:f);
% I. Build the system mass and stiffness matrices
%
%     MSYST = eye(c+f,c+f);
%     KSYST = zeros(c+f,c+f);
%     KSYST(1:c,1:c) = KSYST(1:c,1:c) + lamk1 +...
%
%         (FRKmodes1(a1+1:a1+b1,:))'*k2*FRKmodes1(a1+1:a1+b1,:);
%     KSYST(1:c,c+1:c+f) = KSYST(1:c,c+1:c+f) +...
%
%         (-FRKmodes1(a1+1:a1+b1,:))'*k2*FRKmodes2(a2+1:a2+b2,:);

```



```

KSYST(c+1:c+f,1:c) = KSYST(1:c,c+1:c+f)';

KSYST(c+1:c+f,c+1:c+f) = KSYST(c+1:c+f,c+1:c+f) + lamk2 +...

(FRKmodes2(a2+1:a2+b2,:))'*k2*FRKmodes2(a2+1:a2+b2,:);

% Build the transformation matrix for both substructures

SYSmodes1 = [FRKmodes1 IRAmodes1];

SYSmodes2 = [FRKmodes2 IRAmodes2];

% J. Determine the MacNeal force vector

% partition the force vector with internal forces followed by interface forces

F1=[F1(O1,1);F1(I1,1)];

F2=[F2(O2,1);F2(I2,1)];

% Premultiply the force vector by the first transformation matrix

FM1 = SYSmodes1'*F1;

FM2 = SYSmodes2'*F2;

% Determine the second transformation matrix

T2 = [-k1*FRKmodes1(a1+1:a1+b1,1:c) k1*FRKmodes2(a2+1:a2+b2,1:f);

k1*FRKmodes1(a1+1:a1+b1,1:c) -k1*FRKmodes2(a2+1:a2+b2,1:f);

eye(c,c) zeros(c,f);

zeros(f,c) eye(f,f)];

% determine the system MacNeal force vector

% repartition the force vector

FM1A=FM1(c+1:c+b1,1);

FM1B=FM1(1:c,1);

```

```

    FM2A=FM2(f+1:f+b2,1);

    FM2B=FM2(1:f,1);

    FM1 = [  FM1A;

            FM2A;

            FM1B;

            FM2B];

    FM = T2'*FM1;

% Partition the system mass and stiffness matrices to be suitable for base excitation
% problem (prescribed acceleration)

    P=[1:3];

    F=[4:length(KSYST)];

    KEX2=[KSYST(F,F) KSYST(F,P); KSYST(P,F) KSYST(P,P)];

    MEX2=[MSYST(F,F) MSYST(F,P); MSYST(P,F) MSYST(P,P)];

    KEX3=KSYST(F,F);

    KEX4=KSYST(F,P);

    Rbmodes= [-inv(KEX3)*(KEX4)

              eye(length(P))];

% calculate the system natural frequencies

    [lamex,phiex]=fmodes(KEX2,MEX2);

    for i=1:3;

        lamex(i,1)=0; % rigid body modes

    end;

```

```

% clean up the complex rigid body eigenvectors

    phiex(:,1:3)=Rbmodes;

    [phrb]=rigid(MEX2,phiex,b2);    %Gram-Schmidt

    phiex(:,1:3)=phrb;

% check orthogonality and diagonalization

    tu=phiex(:,1:3)'*MEX2*phiex(:,1:3),pause

    tk=phiex(:,1:3)'*KEX2*phiex(:,1:3),pause

% repartition the system force vector to correspond to mass and stiffness matrix

    fm=size(FM);

    fm1=fm(1,1);

    FM=[FM(4:fm1,1);

        FM(1:3,1)];

    KSYST=KEX2;

    MSYST=MEX2;

    lam_mrf=lamex;

    phi_mrf=phiex;

    omega_mrf=sqrt(lam_mrf)/(2*pi);

    save data6.mat    lam_mrf phi_mrf MSYST KSYST FM SYSmodes1 SYSmodes2

    T2 a1 a2 b1 b2 f c XBM

```

APPENDIX E

```
% LT Lynn J. Petersen

% Naval Postgraduate School

% Mast-Antenna Survivability: Structural Dynamic Design Analysis By Component

% Mode Synthesis

% Program: Basexda.m

% This program solves for the response of a system that is subject to base excitation.

% Structure is generated purely from FE modeling

load data3.mat

% A. Input the number of modes desired to be used

n = input('enter the number of modes desired: ');

phiex(:,n+1:length(phiex))=[];

% B. Place into modal coordinates

m1 = phiex'*mb1*phiex;

k1 = phiex'*kb1*phiex;

% C. Time and frequency parameters

dt = 0.001;

tmax = 0.4;

num_steps = tmax/dt;

t=0:dt:tmax;
```

```

    omegn=sqrt(lamex);

%   freq=8.9525 ;

%   freq=219.265;

    omega = freq*2*pi; %(rad/sec)

% D. Convert the force vector

    fl=f+ (omega)^2*FEX;

    fl=[fl(4:length(fl),1);

        fl(1:3,1)];

    F1=phiex'*fl;  %modal force vector

% E. Solving the differential equation

    for i=1:n;

        for j=1:num_steps+1;

            % for rigid body modes

                if i<=3;

                    c1=1/omega*F1(i,1)*cos(omega*t(j));

                    c2=0;

                    q(i,j)=-F1(i,1)/(omega^2)*sin(omega*t(j))+c1*t(j)+c2;

                else

                    q(i,j) =   -F1(i,1)*omega/(omegn(i)*(lamex(i)-...

omega^2))*sin(omegn(i)*t(j)) +F1(i,1)/(lamex(i)-omega^2)*sin(omega*t(j));

                end;

            end;

        end;

    end;

```

```

end;

% F. Converting back from modal to physical coordinates

x=phiex*q;

s=size(x)

x1=[x(s(1)-2:s(1),:);

    x(1:s(1)-3,:)];

x=x1;

save data6.mat x

```

APPENDIX F

```
% LT Lynn James Petersen

% Naval Postgraduate School

% Mast-Antenna Survivability: Structural Dynamic Design Analysis by Component Mode

% Synthesis

% Program Basexcb.m

% This program solves for the response of a system that is subject to base excitation

% using the Craig -Bampton formulation

    load data10.mat

% A. Input the number of modes desired

    n = input('enter the number of modes desired: ')

    phi_cpl(:,n+1:length(phi_cpl))=[];

% B. Place into modal coordinates

    m1 = phi_cpl'*M_cpl*phi_cpl;

    k1 = phi_cpl'*K_cpl*phi_cpl;

    F1 = phi_cpl'*FCB;

% C. Time and frequency parameters
```

```

dt = 0.001;

tmax=0.4;

num_steps = tmax/dt;

t = 0:dt:tmax;

omegn = sqrt(lam_cpl);

%   freq=8.9525;

%   freq=219.265;

omega = freq*2*pi; %(rad/sec)

% D. Solving the differential equation

for i=1:n;

    for j = 1:num_steps+1;

% for rigid body modes

        if i<=3;    %3 rigid body modes

            c1=1/omega*F1(i,1)*cos(omega*t(j));

            c2=0;

            q(i,j)=-F1(i,1)/(omega^2)*sin(omega*t(j))+c1*t(j)+c2;

        else

            q(i,j) = F1(i,1)*omega/(omegn(i)*(lam_cpl(i)*omega^2))*sin(omegn(i)*t(j))

                + F1(i,1)/(lam_cpl(i,1)-omega^2)*sin(omega*t(j));

        end;

    end;

end;

```



```

end;

% E. Converting from modal (phys,modal) to Craig-Bampton coordinates

x=phi_cpl*q;

% F. Converting back from Craig-Bampton coordinates to physical

x3=[x(1:y,:);x(y+s+1:y+s+a,:)];

x1l=NC_MODES1*x3;

x4=[x(y+1:y+s,:);x(y+s+1:y+s+a,:)];

x2l=NC_MODES2*x4;

x2la=[x2l(e+1:e+b,:);x2l(1:e,:)];

save data11.mat x1l x2la

```

APPENDIX G

```
% LT Lynn James Petersen
% Naval Postgraduate School
% Mast-Antenna Survivability: Structural Dynamic Design Analysis by Component Mode
% Synthesis
% Program: Basexrf.m
% This program solves for the response of a system that is subjected to base excitation
% using the Craig-Chang and MacNeal formulations
% the following input prompts the user as to what method will be used in the base
% excitation problem

type=input('enter type of residual flexibility method, 1 if Craig-Chang, 2 if Macneal')

    if type==1

        load data5.mat

    else

        load data6.mat

    end;

% A. Input the number of modes desired

    n = input('enter the number of modes desired: ')

    if type==1
```

```

        phi_ccrf(:,n+1:length(phi_ccrf))=[];
    else
        phi_mrf(:,n+1:length(phi_mrf))=[];
    end;

% B. Place into modal coordinates
if type==1
    m1 = phi_ccrf*MSYST*phi_ccrf;
    k1 = phi_ccrf*KSYST*phi_ccrf;
    F1 = phi_ccrf*FCC;
else
    m1 = phi_mrf*MSYST*phi_mrf;
    k1 = phi_mrf*KSYST*phi_mrf;
    F1 = phi_mrf*FM;
end;

% C. Time and frequency parameters
dt = 0.001;

tmax = 0.4;

num_steps = tmax/dt;

t = 0:dt:tmax;

if type==1
    omegn = sqrt(lam_ccrf);

```

```

else

    omegn = sqrt(lam_mrf);

end;

%   freq=8.9525;

%   freq=219.265;

omega = freq*2*pi; %(rad/sec)

% D. Solving the differential equation

if type==1

    for i=1:n;

        for j = 1:num_steps+1;

%   for rigid body modes

            if i<=3;

                c1=1/omega*F1(i,1)*cos(omega*t(j));

                c2=0;

                q(i,j)=-F1(i,1)/(omega^2)*sin(omega*t(j))+c1*t(j)+c2;

            else

                q(i,j) =    -F1(i,1)*omega/(omegn(i)*(lam_ccrf(i)-

omega^2))*sin(omegn(i)*t(j)) + F1(i,1)/(lam_ccrf(i,1)-omega^2)*sin(omega*t(j));

            end;

        end;

    end;

end;

```

```

else;

    for i=1:n;

        for j = 1:num_steps+1;

% for rigid body modes

            if i<=3;

                c1=1/omega*F1(i,1)*cos(omega*t(j));

                c2=0;

                q(i,j)=-F1(i,1)/(omega^2)*sin(omega*t(j))+c1*t(j)+c2;

            else

                q(i,j) = -F1(i,1)*omega/(omegn(i)*(lam_mrf(i)-
omega^2))*sin(omegn(i)*t(j)) + F1(i,1)/(lam_mrf(i,1)-omega^2)*sin(omega*t(j));

            end;

        end;

    end;

end;

% E. Converting from modal(phys,modal) to Craig-Chang or MacNeal coordinates

if type==1

    x=phi_ccrf*q;

else

    x=phi_mrf*q;

end;

```

% F. Converting back from Craig-Chang/MacNeal coordinates to physical

% first convert back to the individual substructures

sz=size(x);

sz1=sz(1);

x= [x(sz1-2:sz1,:);

x(1:sz1-3,:)];

x1 = T2*x;

x2 = [x1(b1+b2+1:b1+b2+c,:);x1(1:b1,:)];

x3 = [x1(b1+b2+c+1:b1+b2+c+f,:);x1(b1+1:b1+b2,:)];

xstr1 = SYSmodes1*x2;

xstr2 = SYSmodes2*x3;

xstr2=[xstr2(a2+1:a2+b2,:);xstr2(1:a2,:)];

if type==1

save data7.mat xstr1 xstr2

else

save data8.mat xstr1 xstr2

end;

APPENDIX H

% LT Lynn James Petersen
% Naval Postgraduate School
% Mast-Antenna Survivability Structural Dynamic Design Analysis by Component Mode
% Synthesis
% This appendix contains an alphabetical listing of the auxillary functions that support
% the main programs that are listed in appendices A-G

% Function: El3mk.m

function [ke,me] = el3mk(l,gamma,I,E,r,c,s)

% This function is called to build the elemental and global mass and stiffness matrices for
% a 3 DOF/node "FE" problem.
% A. Element stiffness matrice:

ke(1,1)=l/r*l/r*c*c + 12*s*s;

ke(1,2)=l/r*l/r*c*s - 12*c*s;

ke(1,3)=-6*l*s;

ke(1,4)=-l/r*l/r*c*c - 12*s*s;

ke(1,5)=-l/r*l/r*c*s + 12*c*s;

ke(1,6)=-6*l*s;

$$ke(2,1)=l/r*l/r*c*s - 12*c*s;$$

$$ke(2,2)=l/r*l/r*s*s + 12*c*c;$$

$$ke(2,3)=6*l*c;$$

$$ke(2,4)=-l/r*l/r*c*s + 12*c*s;$$

$$ke(2,5)=-l/r*l/r*s*s - 12*c*c;$$

$$ke(2,6)=6*l*c;$$

$$ke(3,1)=-6*l*s;$$

$$ke(3,2)=6*l*c;$$

$$ke(3,3)=4*l*l;$$

$$ke(3,4)=6*l*s;$$

$$ke(3,5)=-6*l*c;$$

$$ke(3,6)=2*l*l;$$

$$ke(4,1)=-l/r*l/r*c*c - 12*s*s;$$

$$ke(4,2)=-l/r*l/r*c*s + 12*c*s;$$

$$ke(4,3)=6*l*s;$$

$$ke(4,4)=l/r*l/r*c*c + 12*s*s;$$

$$ke(4,5)=l/r*l/r*c*s - 12*c*s;$$

$$ke(4,6)=6*l*s;$$

$$ke(5,1)=-l/r*l/r*c*s + 12*c*s;$$

$$ke(5,2)=-l/r*l/r*s*s - 12*c*c;$$

$$ke(5,3) = -6*l*c;$$


```

ke(5,4)=l/r*l/r*c*s - 12*c*s;
ke(5,5)=l/r*l/r*s*s + 12*c*c;
ke(5,6)=-6*l*c;
ke(6,1)=-6*l*s;
ke(6,2)=6*l*c;
ke(6,3)=2*l*l;
ke(6,4)=6*l*s;
ke(6,5)=-6*l*c;
ke(6,6)=4*l*l;
ke=E*l/l^3*ke;
g=386.09;

```

% B. Element mass matrix

```

me(1,1)=140*c*c + 156*s*s;
me(1,2)=-16*c*s;
me(1,3)=-22*l*s;
me(1,4)=70*c*c + 54*s*s;
me(1,5)=16*c*s;
me(1,6)=13*l*s;
me(2,1)=-16*c*s;
me(2,2)=156*c*c + 140*s*s;

```

$me(2,3)=22*l*c;$
 $me(2,4)=16*c*s;$
 $me(2,5)=54*c*c + 70*s*s;$
 $me(2,6)=-13*l*c;$
 $me(3,1)=-22*l*s;$
 $me(3,2)=22*l*c;$
 $me(3,3)=4*l*l;$
 $me(3,4)=-13*l*s;$
 $me(3,5)=13*l*c;$
 $me(3,6)=-3*l*l;$
 $me(4,1)=70*c*c + 54*s*s;$
 $me(4,2)=16*c*s;$
 $me(4,3)=-13*l*s;$
 $me(4,4)=140*c*c + 156*s*s;$
 $me(4,5)=-16*c*s;$
 $me(4,6)=22*l*s;$
 $me(5,1)=16*c*s;$
 $me(5,2)=54*c*c + 70*s*s;$
 $me(5,3)=13*l*c;$
 $me(5,4)=-16*c*s;$
 $me(5,5)=156*c*c + 140*s*s;$

```

me(5,6)=-22*l*c;

me(6,1)=13*l*s;

me(6,2)=-13*l*c;

me(6,3)=-3*l*l;

me(6,4)=22*l*s;

me(6,5)=-22*l*c;

me(6,6)=4*l*l;

me = gamma*l/(420)*me;

```

```

% Function: Fmanor

```

```

% function[phi_normal,orth]=fmanor(phi,mass)

```

```

% this function mass normalizes a modal matrix.

```

```

a = size(phi);

```

```

nummodes=a(1,2);

```

```

phi_normal=zeros(a);

```

```

%

```

```

for ii=1:nummodes;

```

```

    modalmass(ii)=phi(:,ii)'*mass*phi(:,ii);

```

```

    if modalmass(ii)~=0,

```

```

        phi_normal(:,ii)=(1/sqrt(modalmass(ii)))*phi(:,ii);

```

```

    else

```

```

        phi_normal(:,ii)=phi(:,ii);

    end;

end;

% do the ortho calc:

%

    orth=phi_normal'*mass*phi_normal*100;

% Function: Fmodes.m

% this function returns a vector containing mode freqs (rad/sec)^2 and a matrix
% containing the mass
% normalized mode shapes. The mode information is sorted by frequency in ascending
% order.

% [omega,phi]=fmodes(k,m)

function [omega,phi]=fmodes(k,m)

    a=length(m);

    [v,d]=eig(m\k);

    [omga,index]=sort(diag(d));

    omega=zeros(a,a);

    for i=1:a;

        omega(i,i)=omga(i);

    end;

```

%

```
for i=1:a;  
    phitemp(:,i)=v(:,index(i));  
end;  
omega=diag(omega);  
[phi,orth]=fmanor(phitemp,m);
```

% Function: Kmbe.m

```
function [KEX,MEX,FEX]=kmbe(kb1,mb1,INT,BS,XBM)
```

% A. Partitioning of the mass and stiffness matrices according to internal and base coordinates

```
MII = mb1(INT,INT);
```

```
MIB = mb1(INT,BS);
```

```
MBI = mb1(BS,INT);
```

```
MBB = mb1(BS,BS);
```

```
KII = kb1(INT,INT);
```

```
KIB = kb1(INT,BS);
```

```
KBI = kb1(BS,INT);
```

```
KBB = kb1(BS,BS);
```

% B. Form the ex-mass and ex-stiffness matrices

MEX = (MII - KIB*inv(KBB)*MBI);

KEX = (KII - KIB*inv(KBB)*KBI);

% C. Form the ex-force vector

FEX = (MIB-KIB*inv(KBB)*MBB)*XBM;

% Function: Rigid.m

function [phrb] = rigid(mb1,phi,b2)

% This function obtains orthogonality of 3 linearly independent but not orthogonal

% vectors using the Gram-Schmidt procedure

if b2==3; % 3 rigid body modes

% 1. Obtain "v" vectors

V1 = phi(:,1);

V2 = phi(:,2);

V3 = phi(:,3);

% 2. solve for alpha

alpha = (V2'*mb1*V1)/(V1'*mb1*V1);

V2T = V2 - alpha*V1;

% 3. solve for beta and gamma

c(1,1) = V3'*mb1*V1;

c(2,1) = V3'*mb1*V2T;

a(1,1) = V2T'*mb1*V1;

```

a(1,2) = V1'*mb1*V1;

a(2,1) = V2T'*mb1*V2T;

a(2,2) = V1'*mb1*V2T;

x = inv(a)*c;

beta = x(1,1);

gamma = x(2,1);

V3T = V3 - beta*V2T - gamma*V1;

phrb = [V1 V2T V3T];

% 4. unity mass normalize the phrb shapes

[phi_normal,orth]=finanor(phrb,mb1);

phrb = phi_normal;

else      %2-DOF/NODE

\% 1. Obtain "v" vectors

V1 = phi(:,1);

V2 = phi(:,2);

% 2. solve for alpha

alpha = (V2'*mb1*V1)/(V1'*mb1*V1);

V2T = V2 - alpha*V1;

% 3. reassign the rigid body modes

phrb = [V1 V2T];

```

```

% 4.  unity mass normalize the phrb shapes

    [phi_normal,orth]=fmanor(phrb,mb1);

    phrb = phi_normal;

end;


% Function: ForcEDA.m

function(sh,mo)=forcEDA(type)

% this program calculates the maximum shear and moment to a basex problem

if type==1 % finite element

    load data6.mat

    load data3a.mat

    load data3.mat

    datdabe

elseif type ==2 % Craig-Bampton

    load data 11.mat

    load data1.mat

    load data1a.mat

elseif type ==3 % Craig-Chang

    load data 6.mat

    load data1.mat

```



```

load data1a.mat

else          % MacNeal

load data 7.mat

load data1.mat

load data1a.mat

% input location where shear and moment are desired

if    type == 1

    sm = input('enter the element where the sheer and moment are desired')

    g=size(x);

    h=g(1,2);

elseif type==2

    str = input('enter which structure is desired for analysis')

    if str ==1

        load data_mst.mat

        x=x11

    else

        load data_ant.mat

        x=x21a

    end;

    sm = input('enter the element where the sheer and moment are desired')

    g=size(x);

```

```

    h=g(1,2);
elseif type == 3

    str = input('enter which structure is desired for analysis')

    if str == 1

        load data_mst.mat

        x=xstr1

    else

        load data_ant.mat

        x=xstr2

    end;

sm = input('enter the element where the sheer and moment are desired')

g=size(x);

h=g(1,2);

else

    str = input('enter which structure is desired for analysis')

    if str == 1

        load data_mst.mat

        x=xstr1

    else

        load data_ant.mat

```

```

x=xstr2

end;

sm = input('enter the element where the sheer and moment are desired')

g=size(x);

h=g(1,2);

[ke2,me2]=el3mk(l(sm),gamma(sm),I(sm),E(sm),r(sm),c1(sm),s1(sm));

t2=[c1(sm) s1(sm) 0 0 0 0;

    -s1(sm) c1(sm) 0 0 0 0;

    0 0 1 0 0 0;

    0 0 0 c1(sm) s1(sm) 0;

    0 0 0 -s1(sm) c1(sm) 0;

    0 0 0 0 0 1];

% t2=eye(6);

if type == 1

    y3=abs( [x(3*con(sm,1)-5,:);x(3*con(sm,1)-4,:);x(3*con(sm,1)-3,:);x(3*con(sm,2)...

    ... -5,:);x(3*con(sm,2)-4,:);x(3*con(sm,2)-3,:)] );

    for j=1:h;

        y4=ke2*t2*y3;

    end;

n1 = input ('enter 1 if first node is desired or 2 if second node is desired')

```

```

if n1 == 1

    sh=max(y4(2,:))

    mo=max(y4(3,:))

else

    sh=max(y4(5,:))

    mo=max(y4(6,:))

end;

elseif type <=4

    if str=1

        y3=abs( [x(3*con(sm,1)-5,:);x(3*con(sm,1)-4,:);x(3*con(sm,1)-
3,:);x(3*con(sm,2)...
-5,:);x(3*con(sm,2)-4,:);x(3*con(sm,2)-3,:)] );

        for j=1:h;

            y4=ke2*t2*y3;

        end;

        n1 = input ('enter 1 if first node is desired or 2 if second node is desired')

        if n1 == 1

            sh=max(y4(2,:))

            mo=max(y4(3,:))

        else

            sh=max(y4(5,:))

```

```

        mo=max(y4(6,:))
    end;
else
    y3=abs( [x(3*con(sm,1)-2,:);x(3*con(sm,1)-1,:);x(3*con(sm,1),:);x(3*con(sm,2)...
        -2,:);x(3*con(sm,2)-1,:);x(3*con(sm,2),:)] );
    for j=1:h;
        y4=ke2*t2*y3;
    end;
    n1 = input ('enter 1 if first node is desired or 2 if second node is desired')
    if  n1 == 1
        sh=max(y4(2,:))
        mo=max(y4(3,:))
    else
        sh=max(y4(5,:))
        mo=max(y4(6,:))
    end;
end;
end;
end;

```

```

% Function: Trig.m

function [c,s]      = trig(theta,n)

% This function is written in order to minimize on truncation error in calculating the
% angle between beam elements of finite element code

    for j=1:n

        if theta(1,j) < 0.02 & theta(1,j) > 6.25

            c(1,j)=1;

            s(1,j)=0;

        elseif theta(1,j) < 1.58 & theta(1,j) > 1.56

            c(1,j) = 0;

            s(1,j) = 1;

        elseif theta(1,j) > 3.11 & theta(1,j) < 3.17

            c(1,j) = -1;

            s(1,j) = 0;

        elseif theta(1,j) > 4.68 & theta(1,j) < 4.74

            c(1,j) = 0;

            s(1,j) = -1

        else

            c(1,j)=cos(theta(1,j));

            s(1,j)=sin(theta(1,j));

        end;

    end;

```

LIST OF REFERENCES

1. Corbell, R.D., *Shock Qualification of Combat Systems Equipment Using Tuned Mounting Fixtures on the U.S. Navy Mediumweight Shock Machine*, Master's Thesis, Naval Postgraduate School, Monterey, California, June 1992.
2. NKF Report 8969-AEA/1, *Modal Test and Shock Response Analysis of the LHD-1 Foremast and the SPA-72 Antenna and Platform*, by NKF Engineering, April, 1993.
3. Colub, G.H., and Van Loan, C.F., *Matrix Computations*, pp. 231, Johns Hopkins, 1983.
4. Kolman, B., *Elementary Linear Algebra*, pp. 165, Macmillan Publishing Co., Inc. 1982.
5. Hurty, W.C., *Dynamic Analysis of Structural Systems Using Component Modes*, AIAA J., v. 3, pp. 678-685, 1965.
6. Jet Propulsion Laboratory Tech Memo, *A Modal Combination Program for Dynamic Analysis of Structures*, by R.M. Bamford, pp. 33-290, 1967.
7. Craig, R.R., and Bampton, M.C., *Coupling of Substructures for Dynamic Analysis*, AIAA J., v. 6, pp. 1313-1319, 1968.
8. Goldman, R.L., *Vibration Analysis by Dynamic Partitioning*, AIAA J., v. 7, pp. 1152-1154, 1969.
9. Hou, S., *Review of Modal Synthesis Techniques and a New Approach*, Shock and Vibration Bulletin, no. 40, pp. 25-39, Naval Research Laboratory, Washington, D.C., 1969.
10. MacNeal, R.H., *A Hybrid Method of Component Mode Synthesis*, Journal of Computers and Structures, v. 1, pp. 581-601, 1971.
11. Chang, C.J., *A General Procedure for Substructure Coupling in Dynamic Analysis*, Ph.D. Dissertation, University of Texas at Austin, Austin, Texas, 1977.
12. Craig, R.R., *Structural Dynamics, An Introduction to Computer Methods*, John Wiley and Sons, 1981.

INITIAL DISTRIBUTION LIST

	No. Copies
1. Defense Technical Information Center Cameron Station Alexandria, VA 22304-6145	2
2. Library, Code 52 Naval Postgraduate School Monterey, CA 93943	2
3. Professor J.H. Gordis, Code ME/Go Department of Mechanical Engineering Naval Postgraduate School Monterey, CA 93943	3
4. Professor Y.S. Shin, Code ME/Sg Department of Mechanical Engineering Naval Postgraduate School Monterey, CA 93943	2
5. Department Chairman, Code ME Department of Mechanical Engineering Naval Postgraduate School Monterey, CA 93943	1
6. Naval Engineering, Code 34 Naval Postgraduate School Monterey, CA 93943	1
7. LT. Lynn James Petersen USN 5306 Yermo Toledo, OH 43613	1